

**CRUSTAL STRUCTURE OF THE SALTON TROUGH: CONSTRAINTS FROM
GRAVITY MODELING**

A Thesis

Presented to

The Faculty of the Department of Earth and Atmospheric Science

University of Houston

In Partial Fulfillment

of the Requirements for the Degree

Master of Science

By

Uchenna Ikediobi

August 2013

Crustal structure of the Salton Trough: Constraints from gravity modeling

Uchenna Ikediobi

APPROVED:

Dr. Jolante van Wijk

Dr. Dale Bird (Member)

Dr. Michael Murphy (Member)

Dr. Guoquan Wang (Member)

Dean, College of Natural Sciences and Mathematics

ACKNOWLEDGEMENTS

Special thanks to my advisor, Professor Jolante van Wijk, for her input and guidance throughout the duration of this study. I also want to thank my other committee members, Dr. Dale Bird, Dr. Michael Murphy, and Dr. Guoquan Wang for their feedback and very helpful critical comments.

I am grateful to the institutions that were generous enough to provide me with necessary data and most of all, to my family for their moral support.

**CRUSTAL STRUCTURE OF THE SALTON TROUGH: CONSTRAINTS FROM
GRAVITY MODELING**

An Abstract of a Thesis

Presented to

the Faculty of the Department of Earth and Atmospheric Science

University of Houston

In Partial Fulfillment

of the Requirements for the Degree

Master of Science

By

Uchenna Ikediobi

August 2013

ABSTRACT

The Salton Trough (ST) in the southwestern U.S. is the northward extension of the Gulf of California extensional province. It consists of a series of deep, complex pull-apart structures that formed at different stages of rift evolution. The ST formed as a result of strike-slip motion between the Pacific and North-American plates after Farallon plate subduction ceased and the San Andreas Fault system developed. Pull-apart basins formed at step-overs along the strike-slip faults. Further south, the pull-apart basins evolved into short seafloor spreading segments in the Gulf of California. Different basins within the ST and further south in the Gulf of California are at different stages of evolution. The nature of the underlying crust depends on the stage of evolution of the basin. There is debate on the nature of the crust below the Salton Trough; models range from oceanic crust to highly extended continental crust.

This study uses gravity and magnetic anomaly data to better understand the type of rock that underlies the ST area. These data, in conjunction with supplementary data such as Moho depth from refraction studies, sediment thickness, depth to the lithosphere-asthenosphere boundary, and other geologic data are used to produce 2D gravity models. Moho depth in the study area ranges from 22 – 43 km. The sedimentary layers were modeled with densities of 2.4-2.5 kg/m³ and 2.57-2.9 kg/m³ for other crustal layers, to produce models that reveal a thick sedimentary package (3-5 km) in the Salton Trough area, as well as basaltic igneous intrusions with density 3.0 kg/m³ in the crust.

The models matched for oceanic, continental, and transitional crustal types. However, I propose that the thick sediment package in the basin, the basin's structure, and the presence of basaltic intrusions indicate that the crust underneath the pull-apart basins of the Salton Trough is of transitional type. Continental rupture has not evolved into a mature spreading ridge.

TABLE OF CONTENTS

Acknowledgements	iii
Abstract	v
Table of Contents	vii
List of Figures	ix
Chapter 1: Introduction	1
Chapter 2: Strike-slip faults, pull-apart basins, crustal types, and sheared margins	6
2.1: Strike-slip fault discontinuities	6
2.2: Pull-apart basins	10
2.2.1: Development of pull-apart basins	11
2.2.2: Characteristics of pull-apart basins	14
2.3: Pull-apart basins around the world.	16
2.3.1: Dead Sea Basin	16
2.3.2: Erzincan Basin	19
2.3.3: Death Valley	20
2.3.4: Cayman Trough	23
2.4: Crustal evolution during rifting : continental, oceanic, and heavily intruded continental crust.	24
Chapter 3: Regional tectonic setting of south western California border and evolution of the Salton Trough.	30
3.1: Regional tectonic setting	30
3.2: Tectonic evolution of the Salton Trough	33
3.3: Basins and major faults of the Salton Trough area	36
3.3.1: The San Andreas Fault	36

3.3.2: Brawley Fault, Imperial Fault, Cerro Prieto Fault	38
3.3.3: San Jacinto and Elsinore Fault	38
3.3.4: Salton Sea	39
3.3.5: Imperial Valley and Brawley Seismic Zone	39
3.3.6: Mesquite Basin	40
3.3.7: Cerro Prieto Basin and Mexicali Valley	41
3.3.4: Altar Basin	42
3.3.5: Laguna Salada Basin	42
3.3.6: Wagner Basin	43
Chapter 4: Data and methodology	45
4.1: Objective	45
4.2: Gravity and magnetic modeling	45
4.3: Gravity and magnetic characteristics of the region	56
4.4: Data collection and processing	57
4.5: Supplementary data	58
4.6: Previous gravity and other studies of the Salton Trough	65
Chapter 5: 2D models and interpretation	69
5.1: 2-D gravity models	69
5.2: Model results	73
Oceanic crust test	74
Continental crust test	83
Intruded continental crust test	88
Chapter 6: Nature of the crust beneath the Salton Trough	93
Chapter 7: Conclusions	96
References	98

LIST OF FIGURES

Figure 1: Map of study area.	5
Figure 2: Simplified schematic figure of a strike-slip fault discontinuity.	7
Figure 3: Three-D geometry of an idealized pull-apart basin.	8
Figure 4: Smaller fracture types within the strike-slip system.	10
Figure 5: Different stages in pull-apart basin development.	13
Figure 6: The Dead Sea Basin.	17
Figure 7: The Erzincan Basin.	20
Figure 8: The Death Valley Basin.	21
Figure 9: The Cayman Trough.	24
Figure 10: Rifting mechanism and process from crustal thinning to new ocean basin.	29
Figure 11: Regional Tectonic Setting of the Salton Trough and the Gulf of California.	32
Figure 12: Two-stage evolutionary model for the Salton Trough.	34
Figure 13: Present-day model of the Salton Trough.	35
Figure 14: Bouguer gravity anomaly map of the study area.	51
Figure 15: Free-Air anomaly map of the study area.	52
Figure 16: Magnetic anomaly map of the study area.	53
Figure 17: Residual Bouguer gravity anomaly map of the study area.	55
Figure 18: Topography/Elevation map of the study area.	60
Figure 19: Offshore topography map of the study area.	61
Figure 20: Basement topography map of the study area.	62
Figure 21: Geologic map of the study area.	63
Figure 22: Gravity anomaly map of the area with profile lines and refraction stations.	64

Figure 23: Previous gravity model across the Imperial Valley region of the Salton Trough by Fuis et al. (1984).	66
Figure 24: Gravity model study across the Salton Trough area by Hussein (2007).	67
Figure 25: Profile lines for 2-D models across the study area.	67
Figure 26: Profile line 1 model for oceanic crust.	75
Figure 27: Profile line 2 model for oceanic crust.	76
Figure 28: Profile line 3 model for oceanic crust.	78
Figure 29: Shallow Asthenosphere test for line 1.	80
Figure 30: Shallow Asthenosphere test for line 2.	81
Figure 31: Shallow Asthenosphere test for line 3.	82
Figure 32: Profile line 1 model for continental crust.	85
Figure 33: Profile line 2 model for continental crust.	86
Figure 34: Profile line 3 model for continental crust.	87
Figure 35: Profile line 1 model for intruded continental crust	89
Figure 36: Profile line 2 model for intruded continental crust.	90
Figure 37: Profile line 3 model for intruded continental crust.	91

CHAPTER 1: INTRODUCTION

The Salton Trough in southern California, western U.S.A., is an elongate basin consisting of a series of deep (~10-16 km thick sediment package), sedimentary basins extending from Palm Springs in California to the head of the Gulf of California (Figure 1). The Salton Trough is geographically divided into 3 regions: the Mexicali Valley in the south, the Imperial Valley and the Salton Sea in the middle and the Coachella Valley in the north. The Salton Trough tectonic province represents the transition (i.e., the transitional link) between the oblique divergent seafloor spreading system in the southern Gulf of California and the San Andreas Fault system transform boundary to the north (Yunker et al., 1982). In the Salton Trough, this link is manifested by a system of stepped faults and (pull-apart) basins.

The Miocene-Pliocene Salton Trough was formed as a result of transtensional motion between the Pacific and North American plates (Elders et al., 1972; Elders and Sass, 1988; Axen and Fletcher, 1998; Brothers et al., 2009; Dorsey and Umhoefer, 2011; and others). Rifting has been described as multi-staged (Herzig and Jacobs, 1994; Dorsey, 2006); the Miocene phase of continental rifting resulted in crustal thinning and lithosphere weakening producing alkali basalts, while Pliocene subalkalic basalts that erupted along the axis of the Salton Trough would indicate transitional crust or oceanic spreading since ~4 Ma (Herzig and Jacobs, 1994; Dorsey, 2006). A major tectonic reorganization in the region around 1.4 Ma resulted in the formation of the San Jacinto, Elsinore, and Laguna Salada strike-slip faults (Figure, 1), and changed the topography of the area by uplifts and basin inversion (Dorsey, 2006; Dorsey and Umhoefer, 2012). A

series of pull-apart basins developed between the strike-slip fault segments (the Cerro Prieto Fault, Imperial Fault, and San Andreas Fault, Figure 1), forming the Salton Trough. The northern part of the Trough is bound by the San Andreas and San Jacinto faults (Sylvester, 1999, Figure 1).

Dorsey (2006) described the Miocene to Pleistocene evolution of the Salton Trough in 3 stages. From Early to Late Miocene, continental rifting resulted in the formation of a non-marine rift and alkali volcanism (Herzig and Jacobs, 1994). This was followed by Pliocene to early Pleistocene extension and transtension, and formation of a large basin initially filled with marine sediments and later with terrestrial sediments. Most recently, the initiation of strike-slip faulting and related folding in the region of the San Jacinto and Elsinore fault zones caused uplift and erosion of older deposits from Pleistocene to present time.

In the southern Gulf of California, sea-floor spreading began around 2-6 Ma forming a system of short spreading ridges linked by transform faults (Umhoefer, 2011). The long term northwestern plate motion of the Pacific Plate relative to the North American Plate caused transtensional deformation and in the southern Gulf of California, the total rupture of the lithosphere, leaving behind a series of sediment-starved ocean spreading centers in the south and shallow marine to non marine sediment-filled basins in the northern, landward Salton Trough (Dorsey, 2010; Lizarralde et al., 2007). Today, the Colorado River provides most of the sediments that are deposited in the Salton Trough (Dorsey, 2006).

The nature of the crust in the northern Gulf of California and Salton Trough is debated. Thick packages of sediments overlie the crust, making it difficult to ascertain the exact nature (oceanic, continental, or transitional) of the crust. One end-member model suggests that the crust below the Salton Trough is gabbroic in composition, resulting from continental rapture in the early Pliocene (Herzig and Jacobs, 1994; Hussein, 2007; Fuis and Kohler, 1984). In this model, the Brawley Seismic Zone (or Brawley Basin, Figure 1) is an active spreading center covered by several kilometers of sediments. Brothers et al. (2009), however, suggested that the structure of the Salton Sea region resembles a pull-apart basin in the earlier stages of development underlain by continental crust. Other studies suggest that the Salton Trough has remained in a transitional stage, with heavily intruded lower crust overlain by a thick package of metasedimentary rocks (Axen and Fletcher, 1998; Lekic et al., 2011).

A recent receiver function study by Lekic et al. (2011) showed that the depth of the lithosphere-asthenosphere boundary and seismic wave velocities in the upper mantle below the Salton Trough are consistent with both an advanced continental rift stage of the Salton Trough and a rapture stage in which continental lithosphere has been replaced by new oceanic lithosphere. Fuis et al. (1984) and Fuis and Kohler (1984) used refraction and gravity data to show that Bouguer gravity anomalies in the Salton Trough region can be modeled by a lower crust that is equivalent in composition as the oceanic middle crust. These results were confirmed by Hussein (2007) and Hussein et al. (2011), who used two-dimensional forward gravity models to show that the gravity data are consistent with a gabbroic lower crust of the Salton Trough. Axen and Fletcher (1998) suggested that the

crust below the Trough is transitional, made up of mafic intrusions, sedimentary strata, and meta-sedimentary rocks.

In this study, I use gravity data to model the Salton Trough. The new information on the Moho depth and lithosphere-asthenosphere boundary below the Trough (Lekic et al., 2011), and constraints from a recent seismic experiment in the Salton Sea (Brothers et al., 2009) that were not available in previous gravity studies, may provide new insights on the nature of the Salton Trough crust and its structure.

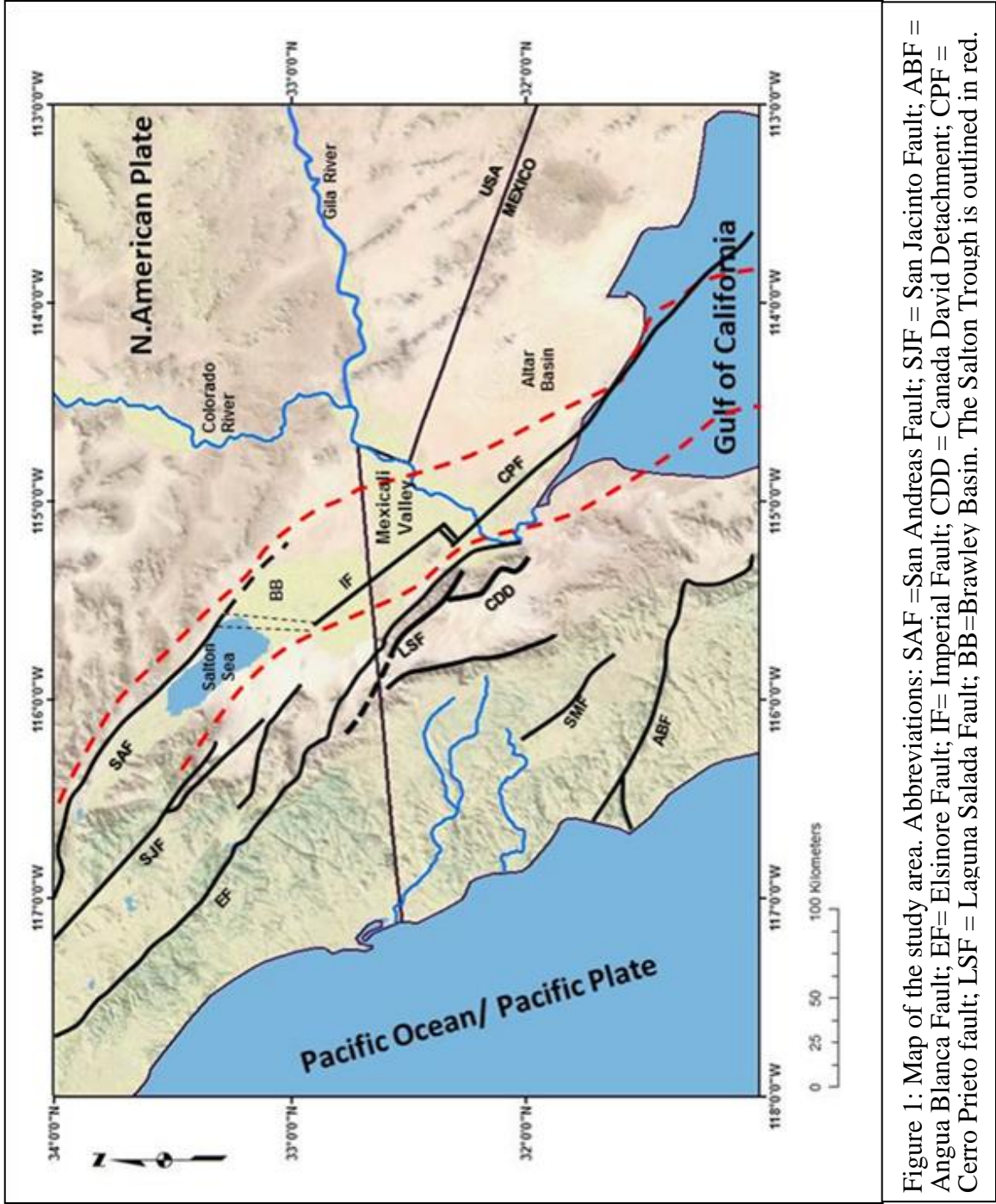


Figure 1: Map of the study area. Abbreviations: SAF =San Andreas Fault; SJF = San Jacinto Fault; ABF = Angua Blanca Fault; EF= Elsinore Fault; IF= Imperial Fault; CDD = Canada David Detachment; CPF = Cerro Prieto fault; LSF = Laguna Salada Fault; BB=Brawley Basin. The Salton Trough is outlined in red.

CHAPTER 2: STRIKE-SLIP FAULT DISCONTINUITIES, PULL-APART BASINS, AND SHEARED MARGINS

2.1 Strike-slip fault discontinuities

Strike slip faults are vertical (or nearly vertical) fractures along which crustal blocks move mostly horizontally and parallel to the strike of the fault (Bates and Jackson, 1987). Strike-slip faults are discontinuous on many scales, and discontinuities include bends and step-overs. Bends are curved parts of a continuous fault trace that connect two non-planar segments of a fault and represent the difference in strike of two contiguous fault segments (Bilham and King, 1989). Stepovers are regions where one fault ends and another one of the same orientation begins (Twiss, 2007). Offsets occur in fault zones when two adjoining parallel fault segments do not line along the same straight line (Bilham and King, 1989).

At fault discontinuities (bends or step-overs), pull-apart basins may form if fault segments are right-stepping with dextral shear or if they are left-stepping with sinistral shear (Atmaoui et al., 2006). When plate motion is not entirely parallel to the strike-slip fault segments, transpressional or transtensional deformation may occur. Transpression is the simultaneous combination of strike-slip motion along a structure and compression perpendicular to it; it occurs where the strike-slip motion is under compression. Bends that accommodate contraction in these areas of local compression or convergent deformation are called restraining bends (Crowell, 1974; Christie-Blick and Biddle, 1985). Transtension is the simultaneous combination or occurrence of strike-slip motion along a structure and extension perpendicular to it, such fault bends that accommodate

local extension in areas of extensional deformation are called releasing bends (Crowell, 1974; Christie-Blick and Biddle 1985). Releasing and restraining bends do not occur singly but instead, are usually huddled up in arrays of multiple en-échelon faults. These segments may link up under increased strike-slip displacement to form alternating zones of convergence and divergence oriented in a consistent pattern along the strike-slip fault system (Tchalenko, 1970; Crowell, 1974, Christie-Bick and Biddle, 1985; Allen and Allen, 2005).

In southern California, the strike-slip faults are arcuate, sub-parallel, and have an eastward convex shape which is more pronounced in the region of the Transverse Ranges restraining bend north of the Salton Trough, with its releasing bend pair running from the Salton Trough into the Gulf of California (Cunningham and Mann, 2007). The wide low-lying regions of the Imperial Valley, northern Mexico, and the Gulf of California are characterized by en-échelon pull-apart basins (Cunningham and Mann, 2007) which developed at releasing bend step-overs of the strike-slip faults in the area.

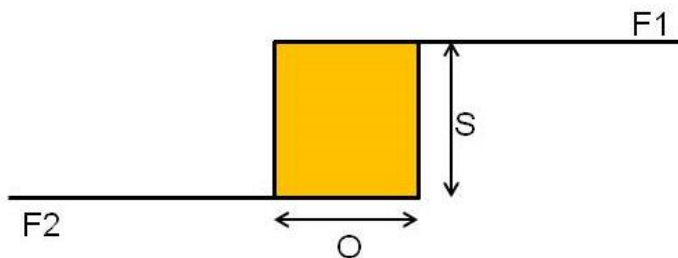


Figure 2: Simplified, schematic figure of a strike-slip fault discontinuity showing the master faults F1 and F2, the offset, O of the master strike-slip faults and the separation, S between the faults.

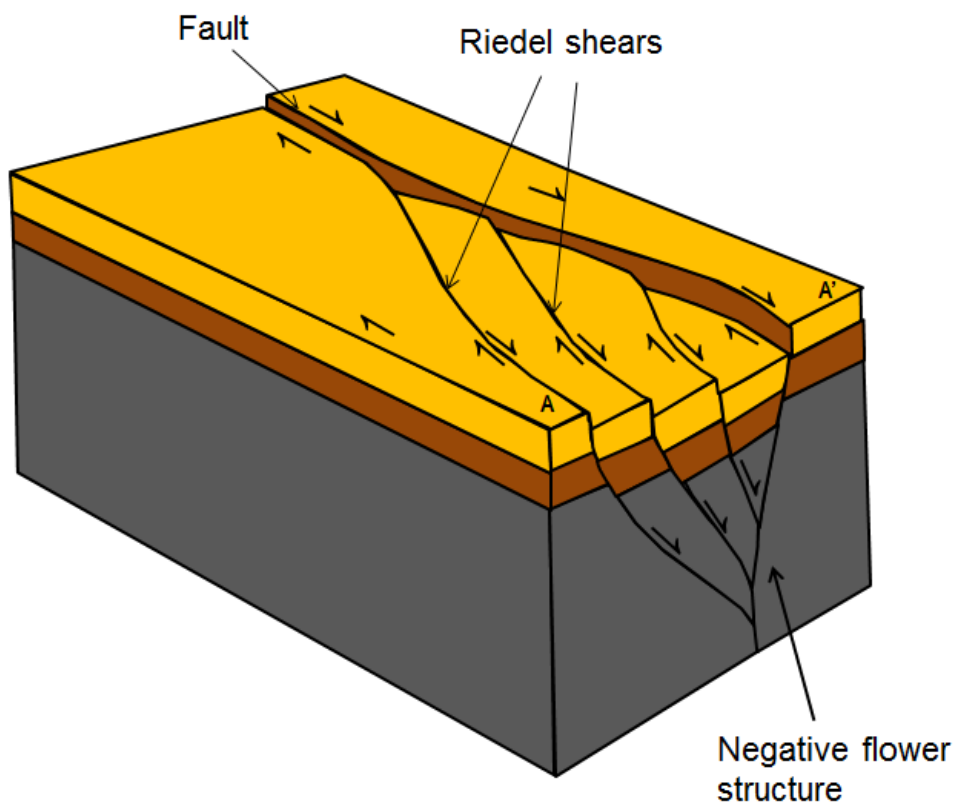
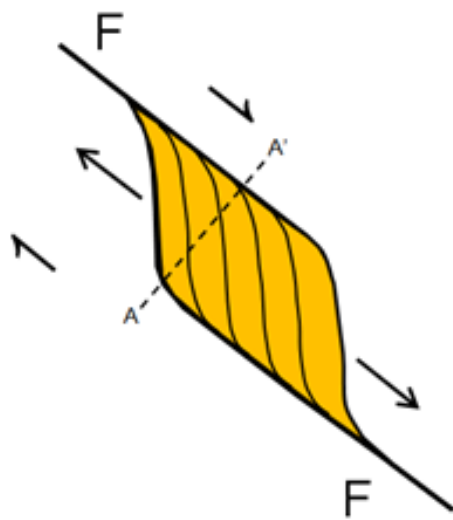


Figure 3: 3-D geometry of an idealized pull-apart basin

Large strike-slip faults are usually not exactly continuous or straight but consist of numerous smaller fractures and branches that result in kinks and offsets. There are various fracture types associated with shear displacement (Figure 3, 4) and they are commonly found within strike-slip systems in the Riedel shear zones (Davis et al., 2000) which evolve as a sequence of linked displacement surfaces (Tchalenko, 1970). Riedel (R) shears are an overstepping array of synthetic strike-slip faults developed and oriented at small angles ($\sim \pm 15^\circ$) (Rahe et al., 1998; Davis et al., 2000) to the regional strike-slip shear couple and their sense of offset is the same as that of the principal displacement zone (Figure 3). Conjugate Riedel (R') shears are antithetic shear fractures that form at higher angles, striking $\sim \pm 75^\circ$ to the main displacement zones or regional strike-slip shear couple (Rahe et al., 1998; Davis et al., 2000) and their sense of offset is opposite to bulk movement. Both Riedel shears and conjugate Riedel shears can be found in pull-apart basins (Figure 3) and the Salton Trough region.

Other deformation structures related to pull-apart basin systems include P-shears, which are secondary en-échelon arrays of synthetic faults with a sense of offset similar to that of the main displacement direction (Figure 4). They form with the progressive development of the Riedel systems and also strike $\sim \pm 15^\circ$ (- for dextral and + for sinistral) to the trace of the strike-slip shear zones (Rahe et al., 1998; Davis et al., 2000). Tension fractures are related to extension in the strain ellipse and form at $\sim \pm 45^\circ$ to the trace of the shears. Y-shears are faults that are sub-parallel to the principal displacement zone and trace of the shear zone (Figure 4).

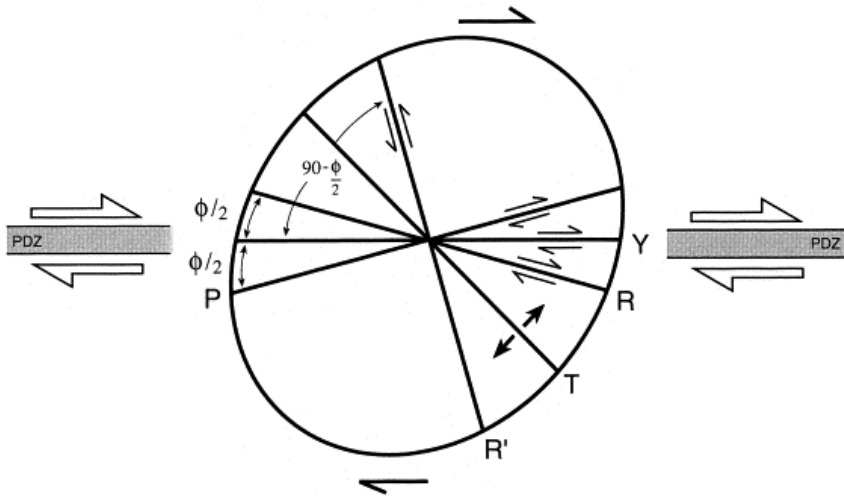


Figure 4: Smaller fault types within the strike-slip system (after Davis et al., 2000).

2.2 Pull-apart basins

Pull-apart basins (Figure 3) are structural depressions which develop at releasing bends along a strike-slip fault (Rahe et al., 1998). Gurbüz (2010) defined pull-apart basins as depressions bound on their sides by 2 or more strike-slip faults and on their ends by diagonal transfer faults. They are generated at the releasing bend of transform faults and their evolution starts off from a small spindle-shaped initial stage (Figure 5) through a 'lazy-S' and rhomboidal basin to a more mature elongate trough stage (Mann et al., 1983; Einsele, 2000; Cunningham and Mann, 2007).

2.2.1 Development of pull-apart basins

The evolution of pull-apart basins has been described in four stages (Figure 5, after Mann et al., (1983). During stage 1, pull-apart basins nucleate at a strike-slip fault discontinuity with 'releasing bend' geometry (Figures 5a & b). Examples of pull-apart basins in their earliest phase of development are the Mesquite Basin between the dextral San Andreas and Imperial Fault zones in the Salton Trough (Mann et al., 1983) and the Glynn Wye Lake Basin between two non-parallel, non-overlapping strands of the dextral Hope Fault Zone in New Zealand (Mann et al., 1983; Freund, 1971). After nucleation of pull-aparts at releasing bends, continued slip along the master faults produces basins shaped as 'lazy-S' (Figure 5c) if the master faults are left-lateral or sinistral; or 'lazy-Z' if the master faults are right-lateral or dextral (Mann et al., 1983) . An example of a basin in this stage of development that shows a strong 'lazy-Z' shape is the Niksar Basin, a young sigmoidal pull-apart basin formed along the eastern segment of the North Anatolian Fault Zone in Turkey (Tatar et al., 2007) and the Death Valley in California, in the southwestern U.S. Lazy Z-shaped basins are bounded by Y-faults at the transform boundary and R faults at the corner of the step-over (Basile and Brun, 1998). Pull-apart basins at this stage tend to show more pronounced topography than basins in the previous stage. The depressions are deeper and sedimentation is enhanced by the creation of more accommodation space.

During the third stage of pull-apart basin formation, the S- or Z- shaped basins 'mature' through continued lengthening and increasing master fault offset. The basin assumes a rhomboidal shape (Figure 5d) (Mann et al., 1983). At this stage, the high angle

R' faults replace the lower angle R faults and produce a rhomb-shaped graben (Basile and Brun, 1998). Because the faults' offset, O (which defines the basin length) increases and the fault separation, S (Figure 2) (which defines the width of the basin) remains constant, the length to width ratio of the basin tends to increase at this stage of development (Mann et al., 1983). The anoxic Cariaco Basin between the Moron and El Pilar Fault Zones in central-eastern Venezuelan continental borderland is an example of a rhomb-shaped pull-apart basin (Schubert, 1982).

During the last stage of pull-apart basin development (stage 4), the rhomboidal pull-apart basins continue to lengthen and they eventually become narrow ocean basins with seafloor spreading centers (Figure 5e) (Mann et al., 1983). The Cayman Trough in the Caribbean is a good example of a pull-apart basin at this stage of sea-floor spreading with the Mid-Cayman Rise as the axis of spreading (Holcombe et al., 1973).



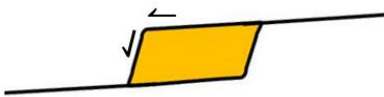
a: Initial fault geometry



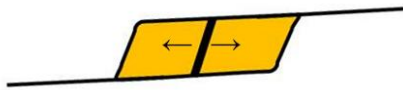
b: Spindle-shaped basin of the nucleation stage



c: "Lazy-S" shaped basin



d: Rhomboidal basin



e: Extreme stage of development: a seafloor spreading center develops

Figure 5: Different stages in pull-apart basin development after Mann et al., (1983).

Pull-apart basins may develop in a range of different tectonic settings. They may form along long strike-slip boundary zones between continental plates where they occur as a series of basins on a segment of the principal displaced fault oblique to the direction of regional interplate slip (Mann et al., 1983). The Salton Trough for example, is formed along the Pacific-North America plate boundary zone. Pull-apart basins also form along strike-slip fault systems in active arc settings (Mann et al., 1983). An example of this is the Andaman Sea where the overriding Southeast Asian plate converges with the subducting Australian plate at a high oblique angle. This basin has been described as a complex back-arc extensional basin (Curry, 2005) and in some cases, as a pull-apart rather than a typical back-arc-extensional basin (Kayal, 2008). In convergent zones formed by collision or development of strike-slip restraining bend, buoyancy of the continental lithosphere keeps the crustal blocks from sinking but instead they move laterally away from the point of contact of both continents. These zones are known as 'zones of tectonic escape' (Sengör et al., 1985). The North Anatolian fault zone in Turkey along which several pull-apart basins are aligned is a good example of strike-slip faults and pull-apart basins in these settings (Gürbüz, 2010).

2.2.2 Characteristics of Pull-Apart Basins

Pull-apart basins are often characterized by high heat flow and volcanic activity (Cunningham and Mann, 2007). High surface heat flow results from localized crustal stretching and lithospheric extension; heat flow increases with lithospheric thinning.

Decompression melting below the thinned lithosphere results in volcanic activity in the pull-apart basin. In the Salton Trough for example, basalts erupted along the rift axis (Herzig and Jacobs, 1994). Theoretical and field studies have revealed that pull-apart basins lose heat rapidly during the extension process, in part, through lateral conduction (Cochran, 1983; Pitman and Andrews, 1985; Xie and Heller, 2009).

Pull-apart basins are typically narrow, less than 50 km wide rifts (Einsele, 2000), and smaller than those produced by regional (orthogonal) extension (Xie and Heller, 2009). They usually have steep basin-bounding faults and cross-basin fault zones that dissect the basin floor into segments (Dooley and McClay, 1997). The pull-apart basin size depends mainly on the separation between the two master faults and their overlap (Einsele, 2000). The width of the basin depends on the separation of the faults and the overlap of the master faults determines the length of the basin (Aydin and Nur, 1982). The depth of a pull-apart is to some extent controlled by the amount of stretching; short basins tend to be shallow and long basins on the other hand tend to be very deep (Einsele, 2000; Hempton and Dunne, 1984).

Pull-apart basins subside more rapidly than the wider continental rifts because the heat from upwelling asthenosphere under the stretched lithosphere is lost laterally very rapidly and fault-controlled subsidence is localized and effective (Einsele, 2000). Subsidence curves of strike-slip basins may occur at irregular intervals and end abruptly and subsidence is rapid (around several hundreds of meters per m.y.) and short-lived (Xie and Heller, 2009). The basin fill of pull-apart basins is asymmetric in both longitudinal and lateral sections showing downfaulting on the side of the dominant fault

and less subsidence on the opposite side. This is due to the steepness of the fault scarp on the margin of the basin bounded by a strike-slip fault (Einsele, 2000).

2.3 Pull-Apart Basins around the World

2.3.1 Dead Sea Basin

The Dead Sea transform fault is about 1000 km long and joins the divergent plate boundary along the Red Sea/Gulf of Aqaba seafloor spreading with the zone of plate convergence along the Alpine orogenic belt, the Neo-Tethyan collision in Turkey (Brew et al., 2001; Garfunkel and Ben-Avraham, 1996). The thickness of the crust is 30-35 km on the basin walls and around the transform system, thinning towards the margin of the Eastern Mediterranean basin (Garfunkel and Ben-Avraham, 1996). The transform formed in the mid-Cenozoic as a result of the breakaway of Arabia from Africa; it represents the active boundary between the Sinai and Arabian plates and connects the incipient mid-oceanic ridge of the Red Sea to the collision and subduction belt in the southern part of Turkey (ten Brink and Ben-Avraham, 1989). The southern part of the transform (Dead Sea Basin) is characterized by a transform valley 5-15 km wide and an internal structure dominated by left-stepping en-echelon strike-slip faults which produce deep pull-apart basins (Garfunkel and Ben-Avraham, 1996). The Dead Sea basin (Figure 6) is one of the largest pull-apart basins located along the intra-continental Dead Sea left-lateral transform. The longitudinal over-stepping strike-slip faults bound the deep, symmetrically subsiding basin (ten Brink and Ben-Avraham, 1989).

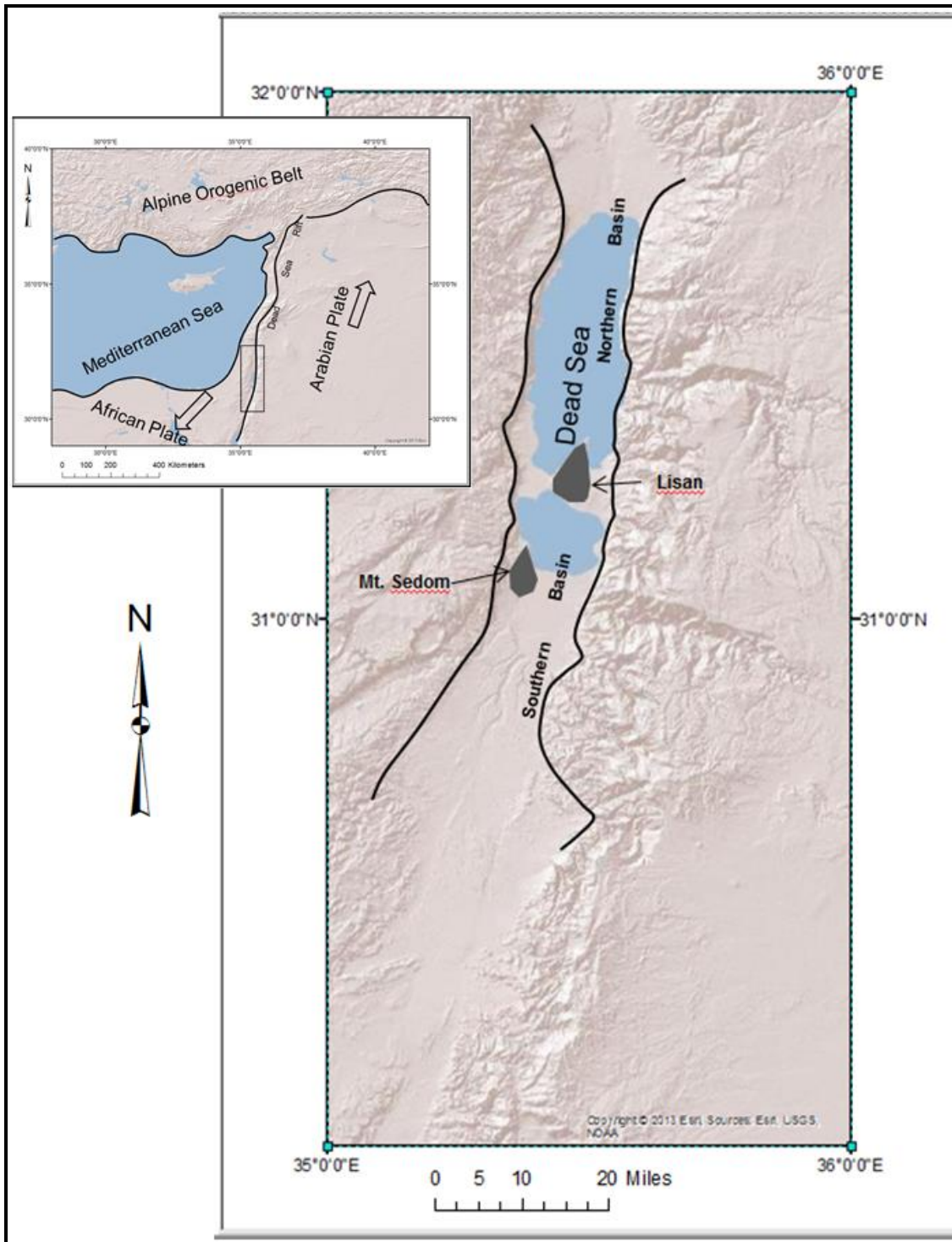


Figure 6: Dead Sea Basin after ten Brink and Ben-Avraham (1989).

The Dead Sea Basin is about 150 km long and 8-15 km wide (Garfunkel and Ben-Avraham, 1996). The east and west sides of the basin are highlands while the northern and southern parts in-between the highlands have no topographic expression (Figure 6). The northern part is occupied by the Dead Sea, a saline lake and the subaerial southern part is generally flat with two hilly areas over two salt domes, the Mount Sedom and Lisan (Figure 6) (Garfunkel and Ben-Avraham, 1996; ten Brink and Ben-Avraham, 1989).

The thick sediment fill in the basin gives rise to a strong negative gravity anomaly which changes gradually towards the south as the basin fill thins. Magnetic anomalies across the basin show the magnetic basement at a depth of ~10 km and a WNW-ESE trending magnetic gradient represents a fault in the basement which divides the basin into two segments (Garfunkel and Ben-Avraham, 1996).

Heat flow in the western part of the basin is low and may be higher in areas where hot waters rise along faults. Heat flow may also be higher in the lake due to conduction by the salt diapirs but may be much lower in the areas of thicker sediment packages (Ben-Avraham, 1996).

2.3.2 Erzincan Basin

The Erzincan Basin (Figure 7) is one of several active pull-apart basins that lie along the North Anatolian Fault (Hempton and Dunne, 1984). The North Anatolian fault zone is about 1600 km long and 100 km wide running approximately E-W across northern Turkey from Karhova in eastern Turkey to Gulf of Saros north of the Aegean Sea (Gürbüz and Gürerb, 2008). The fault zone separates the Eurasian plate in the north from the southern Anatolian plate (Gurbüz, 2010). The North Anatolian Fault consists of a series of long discontinuous right-stepping faults strands with slightly different strikes and pull-apart basins form between these fault offsets (Hempton and Dunne, 1984; Hempton and Linneman, 1984). The Erzincan basin is about 2.9 km deep (Aktar et al., 2004; Gurbüz, 2010), about 50 km long and less than 15 km wide.

Rhyolite domes within the basin (Figure 7) and at its northern border have been dated between 0.25 and 3.1 Ma (Hempton and Linneman, 1984). The Erzincan Basin is suggested to be of Pliocene age (Barka and Gülen, 1989).

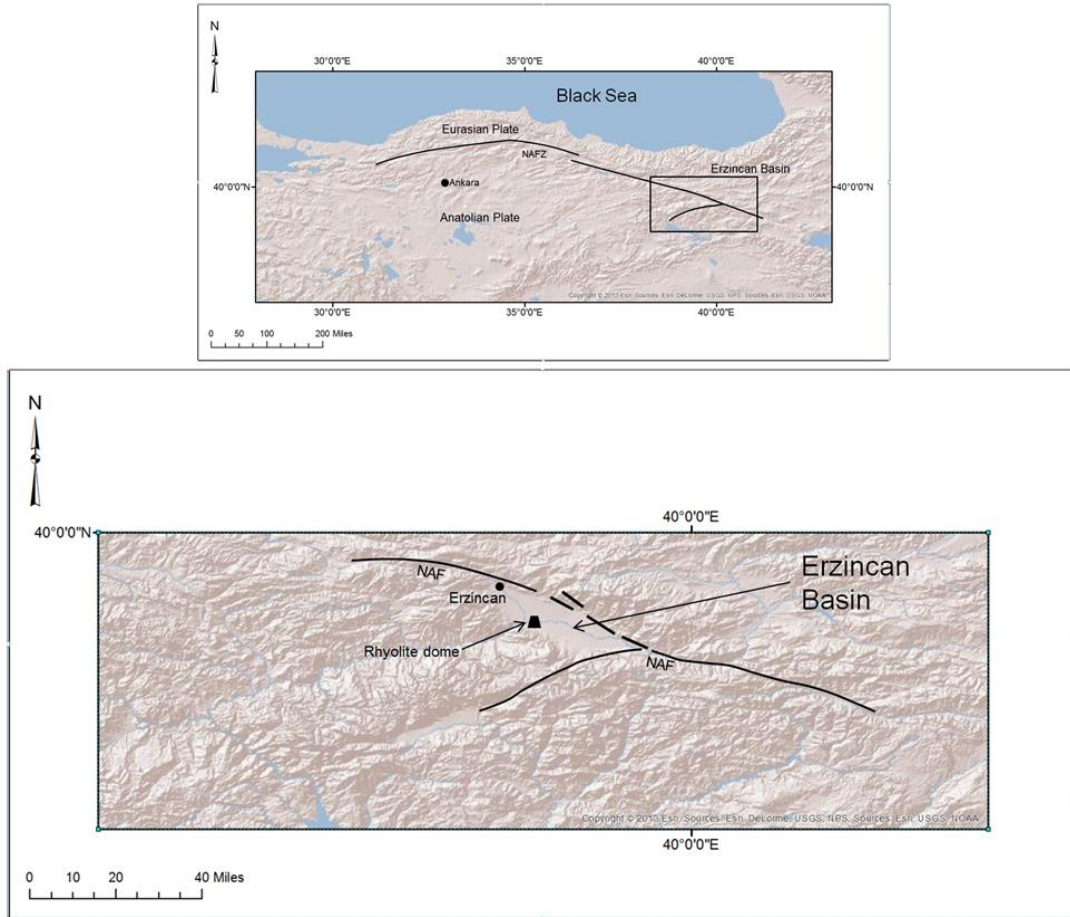


Figure 7: The Erzincan pull-apart basin, modified from Gürbüz and Gürerb (2008). NAF= North Anatolian Fault.

2.3.3 Death Valley Pull-apart

The Death Valley is a structural depression in the southwestern part of the Basin and Range geologic province in the southwestern United States (Hill and Troxel, 1966). It is a long, narrow and continuous valley which trends about 200 km in a north-northwest direction (Blakely et al., 1999; Burchfiel and Stewart, 1966). It is bound on the west by the Panamint Range and on the east by the Black Mountains (Blakely et al., 1999).

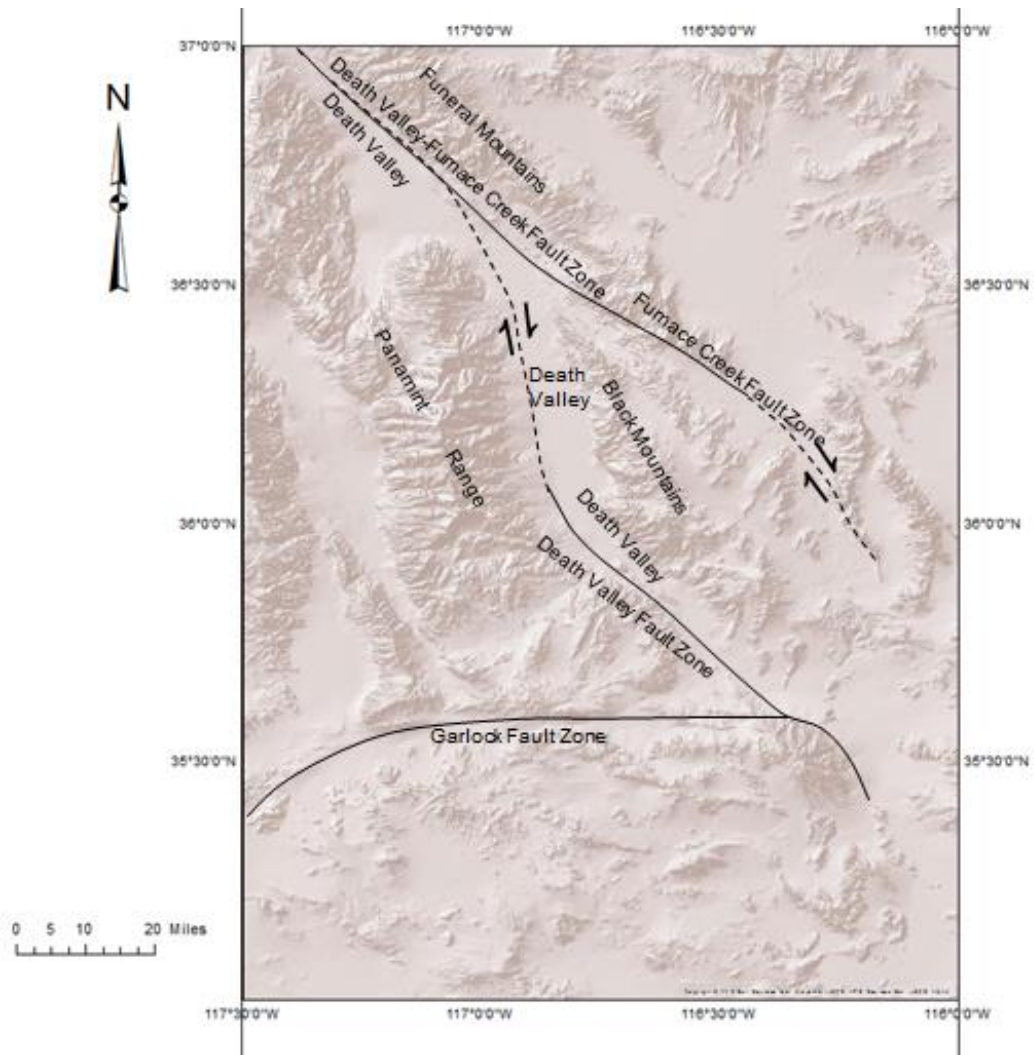


Figure 8: Death Valley Pull-Apart Basin showing the lazy-Z outline is prominent.

The Death Valley pull-apart system (Figure 8) is divided into northern, central and southern parts. The northern segment is about 88 km long and the southern segment is about 40 km long and they both trend in a northwest direction while the central segment trends north and is about 72 km long (Burchfiel and Stewart, 1966). The central part of Death Valley was formed in late Miocene through Holocene time (Christie-Blick and Biddle, 1985), along a segment of a strike-slip fault where tensional forces are slightly oblique to the main trend of the fault (Burchfiel and Stewart, 1966). It developed as an east-tilted half graben bound by northwest-striking dextral strike-slip faults (Christie-Blick and Biddle, 1985).

The Death Valley fault zone and the Furnace Creek fault zone represent the main strike-slip faults in the Death Valley area (Hill and Troxel, 1966) and these fault zones merge in the northern part of the Death Valley (Burchfiel and Stewart, 1966). Right-lateral slip on the northern Death Valley-Furnace Creek and southern Death Valley faults systems is translated into oblique extension across the Death Valley pull-apart basin (Keener et al., 1993). Bouguer gravity anomalies in the Death Valley area are series of NE-SW-trending highs and lows. Gravity highs over the Black Mountain may be due to large mafic intrusions or high density Precambrian rocks in the subsurface. The relative high magnetic anomalies are due to exposed mafic intrusions and shallow buried magnetic bodies (Mickus et al., 1989).

2.3.4 Cayman Trough

The Cayman Trough is a pull-apart basin that has reached the stage of extreme development where an axis of sea-floor spreading, the Mid-Cayman Rise has formed (Figure 9). It has gone from a stage of stretched and rifted continental crust to extreme thinning and eventually to a stage of very slow spreading and formation of new oceanic crust (ten Brink et al, 2002). The Cayman Trough is about 1200 km long, 100 km wide and 5 km deep (ten Brink et al., 2002). It is located between the Cayman Ridge on the north and the Nicaraguan rise on the south (Bowin, 1968). A slow-spreading ridge, about 100 km long is active between two offset transform faults; the Swans Island transform fault and the Oriente transform fault (Holcombe et al., 1973). The rift in the Cayman Trough is at the center and at an equal distance from both ends of the trough indicating that spreading has been symmetric from the Mid-Cayman Rise (Holcombe et al., 1973). Crustal thickness increases in both west and east directions away from the spreading center reaching about 7-8 km at the ends of the trough. Basement depth on the other hand, becomes shallower as we move away from the spreading center (ten Brink et al., 2002). The Oriente fracture zone to the north and the Swan fracture zone to the south formed from the master strike-slip faults along the north and south walls of the Cayman Trough (Holcombe et al., 1973).

The Cayman Trough represents the area in the Caribbean Sea with the shallowest depth to the mantle, and gravity and seismic refraction studies indicate the presence of very thin crust which further suggest that the trough was formed by slow extension and upwelling of mantle material to shallower depths (Bowin, 1968). Magnetic data

interpretations by Leroy et al. (2000) suggest that the Cayman Trough opened up in early Eocene time.

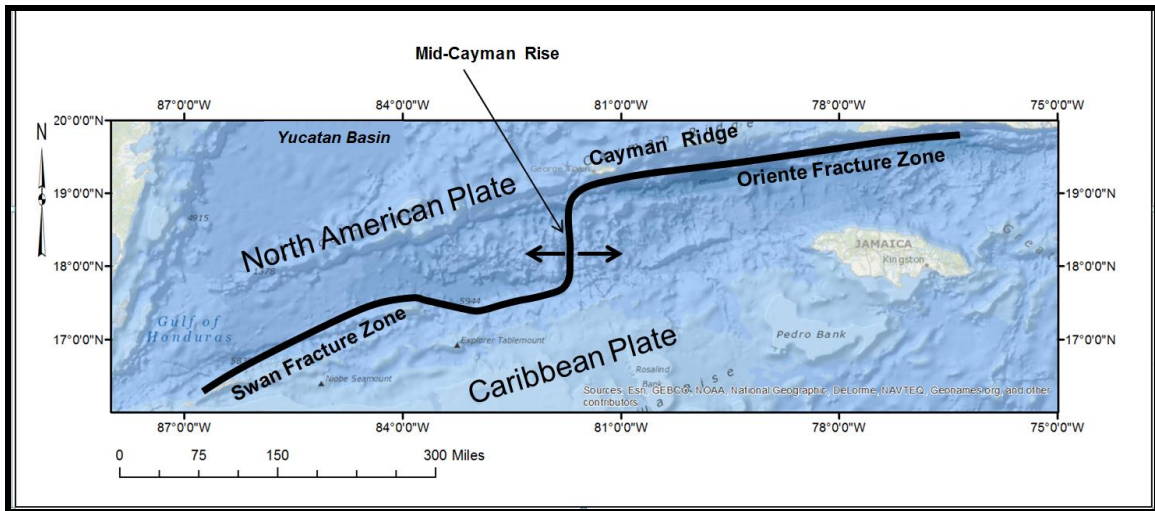


Figure 9: The Cayman Trough with the Mid-Cayman Rise spreading center and the Swan and Oriente Fracture Zones.

2.4 Crustal evolution during rifting: continental, transitional, and oceanic crust

The crust is the outermost layer of the earth; the upper rigid part of the lithosphere whose base is defined by the Moho seismic discontinuity. It extends vertically from the Earth's surface to the Moho. The crust-mantle boundary represented by the Moho is marked by a jump in compressional wave velocity from approximately 7 km/s to approximately 8km/s and in some regions; the boundary may be a transitional region rather than an abrupt contact (Rudnick and Gao, 2003).

Vertically, the crust is compositionally stratified and studies have shown that it becomes more mafic with depth (Rudnick and Gao, 2003). Depending on whether it lies

underneath the ocean or continental area, the crust differs in composition and thickness and is classified into 3 types on the basis of seismic experiments carried out on land and in the ocean (Rezanov, 1983): continental, transitional, and oceanic.

Rifting is the process by which lithospheric plates rupture. The process of continental plate break-up starts with lithospheric extension and thinning. When rifting progresses, magmatic intrusions become increasingly important in accommodating extension. As a result the lithosphere weakens, and may eventual break-up by formation of new oceanic crust and a seafloor spreading center.

Continental rifts are fault-bounded basins produced by extension of the continental crust. Continental extension can result in either narrow rifts which may show large lateral gradients in crustal thickness and topography, or wide rifts characterized by more subtle lateral gradients (Buck, 1991). Narrow rifting occurs in cratonic regions while wide rifts are formed in warm lithosphere when extensional deformation spreads to adjacent unextended areas and rifting can no longer continue in the original location (Buck, 1991). Buck (1991) also identified metamorphic core complexes as another form of rifting in which high-grade metamorphic rocks from the middle to lower crust are exposed at the surface.

Depending on the mechanism of rifting, rifts have traditionally been classified into 2 categories: active rifts and passive rifts. Active rifts are produced by mantle plumes (Olsen, 1982) through doming of the lithosphere, where doming results from rising mantle plumes (Olsen and Morgan, 1995). Active rifts contain relatively large volumes of

volcanic rock and are characterized by early regional uplift. Uplift extends for hundreds of kilometers beyond the rift zone proper. The zone of thinning is several times wider than the rift width (Thompson and Gibson, 1994). The East African Rift zone has been mentioned as an example of an active rift (Burke and Dewey, 1973).

In passive rifting, the lithosphere is thinned in response to far-field tensional forces (Olsen and Morgan, 1995). These are produced by stresses in moving lithospheric plates or drag at the base of the lithosphere. In passive rifts, immature clastic sediments exceed volcanics in abundance (Olsen, 1982). Uplift in passive rifts extends beyond the faulted near-surface region and beyond the shoulder of the rift zone, and also lithospheric thinning extends beyond the width of the rift zone (Thompson and Gibson, 1994). As a result of lithosphere thinning, the asthenosphere rises passively (Morgan and Baker, 1983) (Figure 10). The tensional forces that cause rifting are attributable to a mechanism outside the rift region rather than of local origin (Bott, 1995) and this stress may be generated at plate margins (Turcotte and Emerman, 1983).

The Salton Trough is an example of a passive rift. Extensional stresses result from the relative movements of the North American and Pacific plates.

During the continental rift phase, continental crust is stretched, thinned, and intruded magmatically. The pre-stretched continental crust is approximately 40 km thick (but may be as thick as 70 km), and is composed of rocks of highly diverse lithologies (Rudnick and Gao, 2003). Continental crust lithologies are mostly metamorphic and felsic igneous rocks with an average density of 2.75 g/cm^3 . During extension in continental rifts the lower crustal layer is thinned to about 4-14 km thick, reflecting its ductile behavior.

As stretching and thinning of the continental lithosphere progresses, mantle asthenosphere moves into the space created by the thinned lithosphere, and eventually rises close to the surface (Figure 10c). At rifted margins, the change from thinned continental crust to oceanic crust does not occur abruptly at a sharp boundary but rather changes over a transitional zone. The transitional crust has velocity values characteristic of neither continental nor oceanic crust (Whitmarsh et al., 1993). This is the point of transition from continental rifting to seafloor spreading and the transitional crust here is significantly different from normal continental and oceanic crusts. This transitional crust is heavily intruded. Transitional crust may either form as highly stretched continental crust (quasicontinental) or as a mixture of sediments and basaltic intrusions (quasioceanic). This is possible where sedimentation occurs simultaneously with volcanism within a rift basin, resulting in a complex mixture of sedimentary and igneous components, producing a crustal complex of sediments, dykes, sills and lava with oceanic characteristics but unusual thickness (Dickinson, 1974). The crust below the Salton Trough has been described as transitional crust.

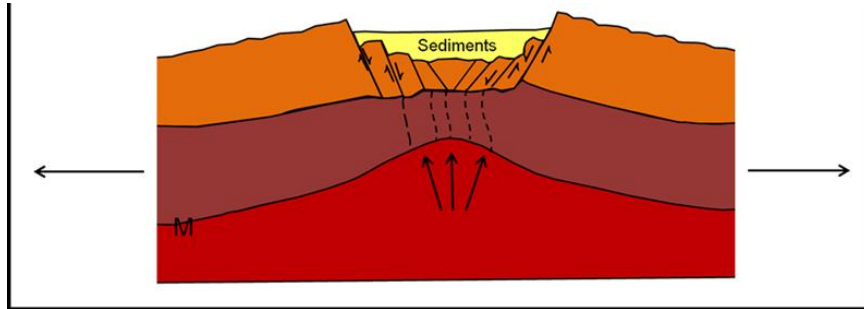
Thinning and metasomatism of the mantle lithosphere occurs in mature rifts which are close to initiation of seafloor spreading (Figure 10d). When extension of spreading centers causes continental blocks to be rifted apart, new igneous oceanic crust is created adjacent to thick continental crust through submarine volcanism and intrusions. At spreading centers along the crest of a mid-oceanic ridge, new oceanic crust is continually being formed (Dickinson, 1974). Oceanic crust is thinner than continental crust with thickness typically ranging from 3-15 km and an average of 7 km; it is composed of

relatively dense mafic igneous rock types such as basalts and gabbros and is relatively young ($\leq 200\text{Ma}$ old) (Rudnick and Gao, 2003) with an average density of 3.0 g/cm^3 .

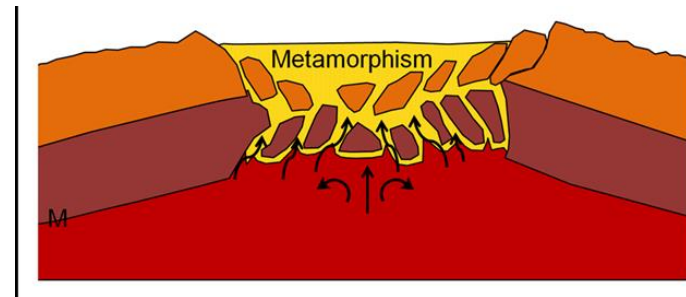
Complete rupture of a continent requires a progression from early severe lithospheric thinning, through rifting and to eventual continental break-up that forms oceanic spreading centers. Whether a rift progresses and develops to this stage depends mainly on the thermal structure, crustal thickness and crustal strength of the lithosphere, and tensional stresses (Umhoefer, 2011). Depending on the tectonic setting of the rift, continental rupture may produce either large ocean basins or small narrow marginal seas; these are two 'end-member' results of continental rifting. Large oceans commonly form in old, cold continental lithosphere or within former large collisional belts while narrow marginal seas commonly form along active continental margins. The Gulf of California is an example of a marginal sea formed along an active continental margin from pull-apart basins (Umhoefer, 2011).



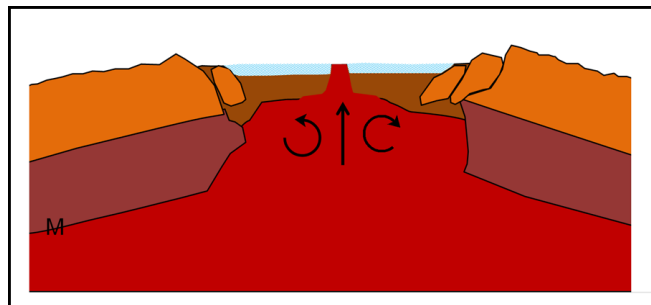
(a) Initial stage with 2 crustal layers above a hot mantle layer. M=Moho.



(b) Stage of lithospheric stretching and subsequent thinning.



(c) Stage of extreme thinning of the lithosphere with basaltic magma intrusions.



(d) Stage of extreme thinning and seafloor spreading with creation of new crust and opening of new ocean basin.

Figure 10: Rifting process from thinning to formation of a new ocean basin.

CHAPTER 3: Regional tectonic setting of South western California and evolution of the Salton Trough

3.1 Regional Tectonic Setting

The tectonic evolution of the California continental margin is to a large extent a result of the process of microplate capture, basically driven by the ending of Farallon subduction. This was followed by formation of the San Andreas Fault system, and other strike-slip faults toward the south. At discontinuities of this strike-slip fault system, pull-apart basins started to develop evolving to sediment-filled basins in the Salton Trough and sediment-starved basins characterized by seafloor spreading in the southern Gulf of California.

Prior to 29 Ma, the East Pacific Rise was an offshore spreading center between the Pacific and Farallon plates, and the Farallon plate was subducting under the North American Plate (Stock and Hodges, 1989). As the East Pacific Rise approached the trench, the subducting Farallon plate broke up into numerous microplates.

As the zone of subduction swallowed up the Pacific-Farallon spreading center, subduction slowed down and eventually ceased, and the boundary was converted from a slightly oblique subduction to a transtensional dextral transform boundary (Mammerickx and Klitgord, 1982; Nicholson et al., 1994) leading to the formation of faults of the San Andreas Fault system. The lateral relative motion between the Pacific and North American plates generated shear stresses resulting in prominent strike-slip faults in the

San Andreas Fault system, a complex system of mostly strike-slip faults including the San Andreas Fault itself.

Approximately around 12-15 Ma, rifting started in the Gulf of California. At around 5 million years ago the East Pacific Rise finally split the Baja Peninsula from the mainland of Mexico forming a series of transform faults separated by short spreading ridges (Bischoff and Henyey, 1974). Since then, the Baja Peninsula has been moved about 162 miles north-westwards from mainland North America.

Details of the formation of the Gulf between ~12 and 6 Ma are still debated. Two end-member models describe Gulf of California development during this time. They differ mainly in explaining Gulf formation as a result of strain partitioning (orthogonal or east-west extension in the proto-Gulf, and strike-slip motion along the Tosco-Abreojos fault) followed by shear since about 5-6 Ma, or by shearing in the proto-Gulf since about 12 Ma (Stock and Hodges, 1989; Oskin and Stock, 2003; Fletcher et al., 2007; Umhoefer, 2011). In the second model, the southern Gulf of California spreading segments have developed from pull-apart basins in the proto-Gulf since ~12 Ma. This model would be similar to what is observed in the Salton Trough evolution.

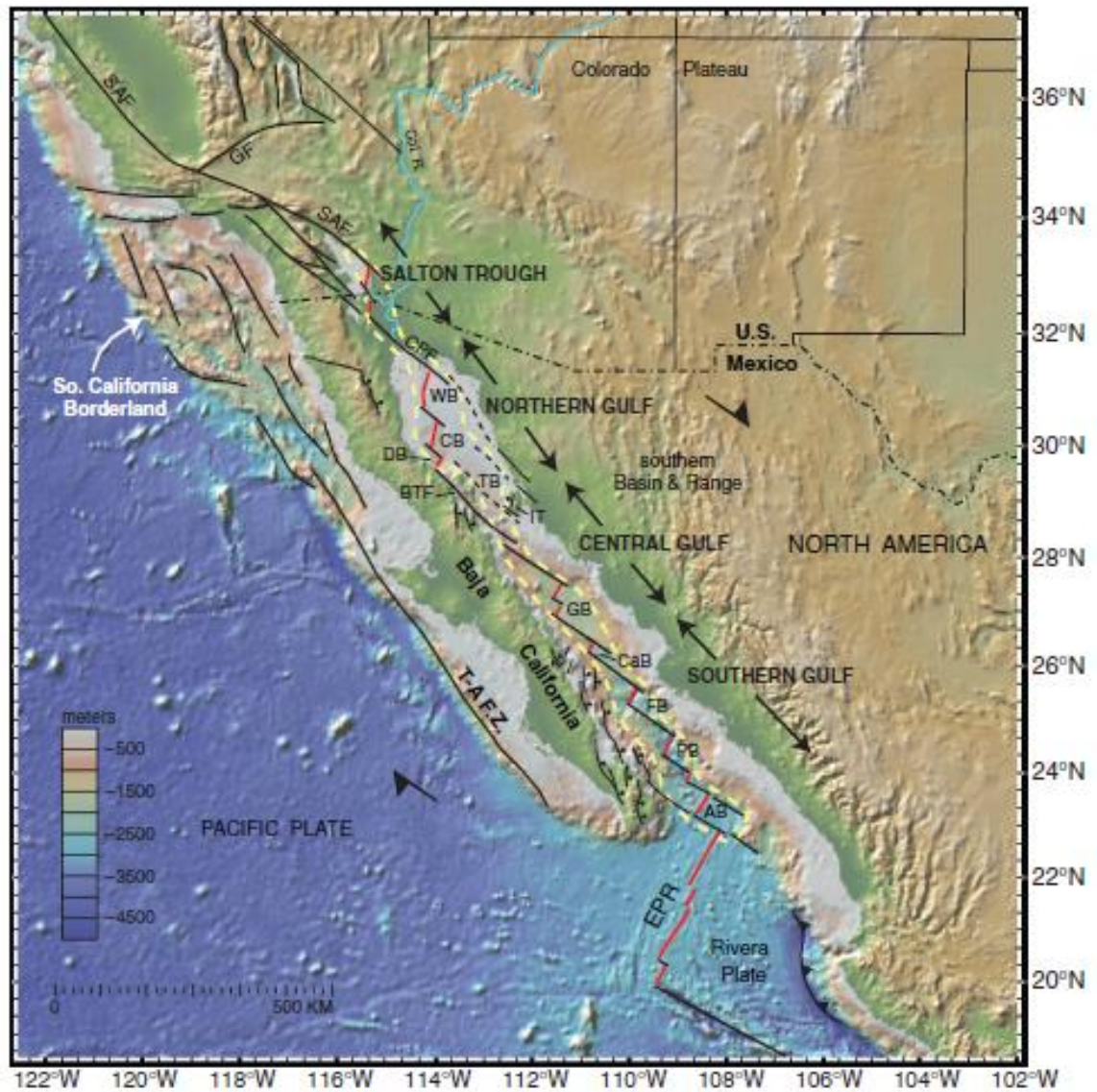


Figure 11: Regional Tectonic Setting of the Salton Trough and Gulf of California after Dorsey and Umhoefer (2011). SAF= San Andreas Fault, GF = Garlock fault, CPF = Cerro Prieto Fault, GB=Guaymas Basin, FB= Farallon Basin, PB= Pescadero Basin, AB= Alarcon Basin, BTF=Ballena transform fault, CaB= Carmen basin, CB=Consag Basin, EPR=East Pacific Rise, T.A.F.Z = Tosco-Abreojos fault zone, WB = Wagner Basin, TB = Tiburón Basin, IT = Isla Tiburón.

3.2 Tectonic evolution of the Salton Trough

The Salton Trough is an elongated basin considered to be the northward, landward extension of the Gulf of California (Sylvester and Smith, 1976). It represents the transition zone between crustal spreading in the Gulf of California and right-lateral transform motion along the San Andreas Fault system (Larsen and Reilinger, 1991). The formation of the Trough is the result of the northward progression of opening of the Gulf of California (Elders et al., 1972) which widens from the northwesterly drift of Baja California away from the North American continent. The Trough is demarcated from the Gulf by a sub-aerial delta built by sediments from the Colorado River (Meriam and Bandy, 1965; Winker, 1987; Dorsey and Umhoefer, 2011). Sediments from the Colorado River deposited in the Trough are rapidly buried and undergo metamorphism by magmatism and high heat flow at shallow depth (Elders and Sass, 1988; Dorsey and Umhoefer, 2011).

Brothers et al. (2009) proposed a 2-stage evolutionary process for the formation of the Salton Trough. According to their model, the tectonic evolution of the trough started with transpression between the San Andreas and San Jacinto faults with clockwise rotating blocks bound by north-east striking sinistral faults accommodating the strain between the faults (Figure 12a). Extension then started as the San Andreas - Imperial fault step-over formed and the cross faults started to accommodate normal slip (Figure 12b).

Different crustal models by different workers (Fuis et al., 1984) suggest that most of the southern part of the Salton Trough is underlain and intruded by younger mafic

material and volcanism in the southern edge of the Salton Sea has been attributed to result from the presence of a buried spreading center between the San Andreas and Imperial faults (Elders et al., 1972; Fuis et al., 1984).

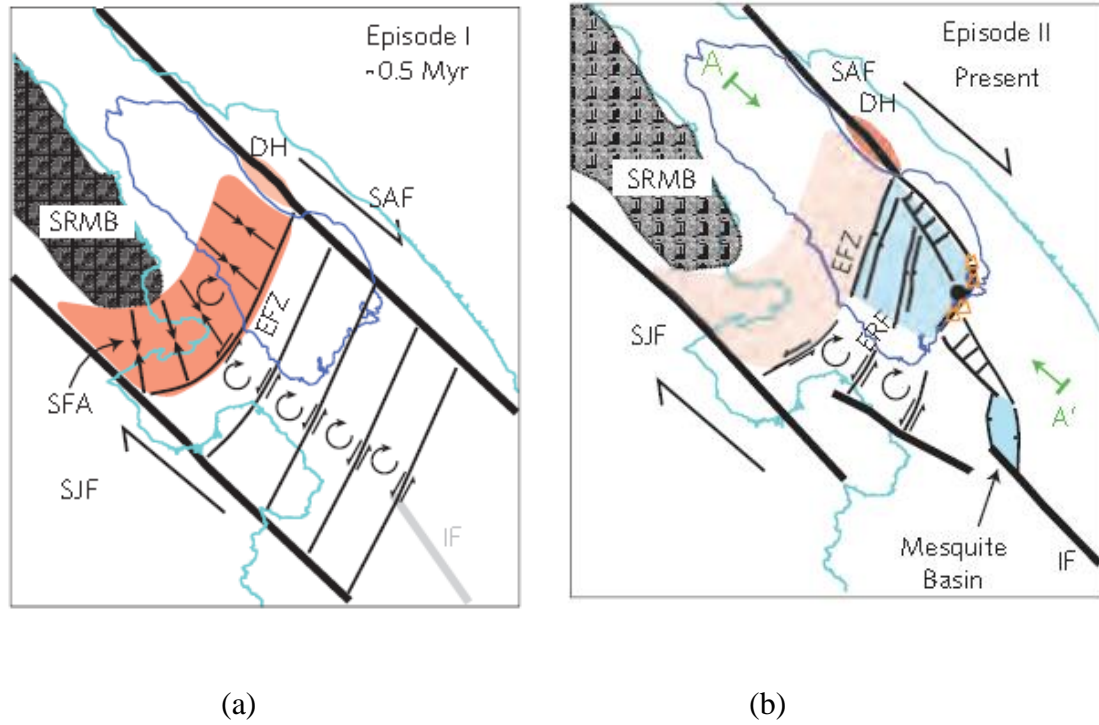


Figure 12. Two-stage evolutionary model for the Salton Trough by Brothers et al. (2009).

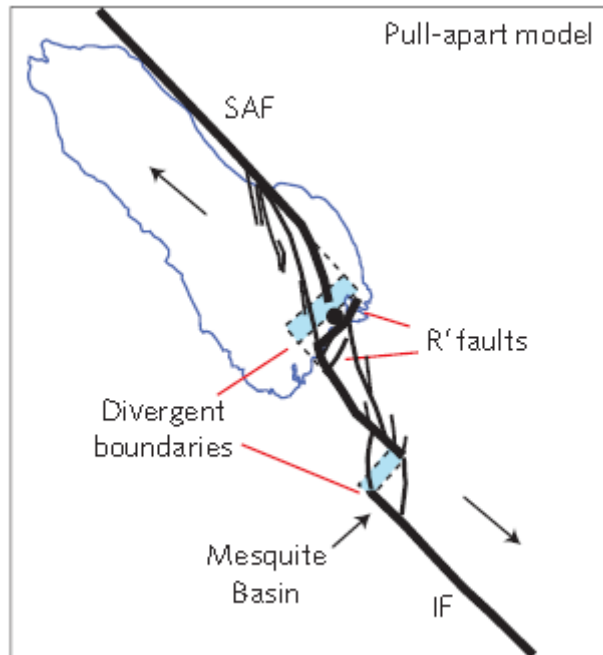


Figure 13: Present-day model of the Salton Trough from Brothers et al. (2009).

IF=Imperial Fault, SAF= San Andreas Fault.

The pull-apart basins of the Salton Trough formed in the same way as described for general pull-apart basins; a combination of tensional and right-lateral strike-slip movements associated with the opening and widening of the Gulf (Elders et al., 1972). The main strike-slip faults are the San Andreas and San Jacinto fault in the northern part of the Trough and Imperial fault in the southern part (Figure 12). The San Andreas and San Jacinto Faults bound the Salton Trough as a right-shear couple with left-slip cross faults in between them. The cross-faults bound thin crustal blocks that rotate clockwise on the captured Farallon plate that now moves in a northwesterly direction with the

Pacific plate (Sylvester, 1999). Oblique extension across these faults causes subsidence and pull-apart basins development at fault discontinuities.

3.3 Basins and major faults of the Salton Trough and its environs

The San Andreas Fault system is a network of predominantly right-lateral strike-slip faults that accommodate most of the relative motion between the Pacific and North American plates (Wallace, 1990). Numerous pull-apart basins develop at step overs between the different sub-parallel faults in the Salton Trough. The San Andreas, Imperial, Cerro Prieto and Brawley faults form a series of east-stepping, right lateral transforms linked by pull-apart basins. Some of the basins include the Brawley Basin between the Brawley Fault and the southern end of the San Andreas Fault; the Mesquite Basin between the Brawley and Imperial Faults; the Cerro-Prieto Basin between the Imperial and Cerro Prieto Fault, and the Salton Buttes spreading center (Elders et al., 1972).

3.3.1 The San Andreas Fault

The San Andreas Fault is a right-lateral transform fault, which means that if you stand on either side of the fault and look across to the opposite side, the objects or features on the opposite side appear to be moving to the right. It is a continental transform fault with a complex structural and sedimentary regime (Brew et al., 2001). The origin of the San Andreas Fault system is directly related to the collision between North America and the Pacific-Farallon ridge following the cessation of subduction.

The San Andreas Fault extends from the Mendocino fracture zone off the Northern coast of California to the tip of Baja California. In much of northern and central

California, the San Andreas trends in a southeast direction as a boundary between the Salinian block of granitic and metamorphic rocks on the west and the Franciscan assemblage and overlying strata of the great valley sequence on the east (Wallace, 1990). The San Andreas strike-slip zone which runs in a northwesterly direction from the Mendocino fracture zone, makes a sharp eastward bend (the big bend) across the top of the Western Transverse Ranges and then splays out into a series of sub-parallel strike-slip faults that extend to the head of the Gulf of California (Figure 11). At discontinuities of this series of strike slip faults, pull-apart basin structures have formed, such as those that form the Salton Trough.

The east of the Salton Trough is formed by the San Andreas Fault, where it consists of Precambrian rocks and Mesozoic plutons. The western side consists of Cretaceous plutonic rocks of the Southern California Batholith and their metamorphic host rocks (Wallace, 1990). The Gulf of California segment of the San Andreas Fault is a series of long transform faults that connect very short spreading ridges in the Gulf of California. The continental crust under the northern Gulf of California has thinned and the ocean floor is shallow.

Rocks on either side of the San Andreas fault are basically sitting on different plates and deformation is produced as the North American plate slips relatively southwards past the portion of continental crust captured by the Pacific plate (Atwater, 1998).

3.3.2 Brawley Fault, Imperial Fault, Cerro Prieto Fault

The Imperial Fault (Figure 1) is a northwest-southeast trending dextral fault. It is about 60 km long extending southeast into Baja California (Segall and Pollard, 1980); along the northern extension of the Imperial Fault, it bends and trends north (Larsen and Reilinger, 1991). The Brawley Fault is located 6 km east of, and trends parallel to, the northern extension of the Imperial Fault (Larsen and Reilinger, 1991) (Figure 1). The Cerro Prieto Fault is a right-lateral strike-slip fault (Pacheco-Romero et al., 2006) which strikes northwest and runs from the Mexicali Valley into the Gulf of California (González-Escobar et al., 2009).

3.3.3 San Jacinto and Elsinore Faults

The San Jacinto Fault is a seismically active fault that diverged away from the San Andreas Fault northwest of Cajon Canyon and extends for 215 km in an almost straight line ending on the southwest side of the Salton Trough (Brown, 1990). The San Jacinto Fault zone is relatively straight and continuous from the San Bernardino Valley across the northeastern Peninsular Ranges to the Imperial Valley (Sharp, 1967).

The Elsinore Fault is located about 35 km to the southwest of the San Jacinto fault (Brown, 1990), Figure 1. It is the major dextral shear system which parallels the southern part of the San Andreas Fault and accommodates about 5 mm/yr of the Pacific-North American plate boundary slip (Hull and Nicholson, 1992). Lowman (1980) suggests that structural and lithologic continuity across the faults in the Elsinore fault zone implies that

they have undergone little or no strike-slip movement and the Elsinore Fault is a dip-slip fault at least along its southern portion.

3.3.4 Salton Sea

The Salton Sea is a lake that lies between the Coachella and Imperial Valleys in the Salton Trough with its base at approximately 90 m below mean sea level (Bilham and King, 1989), Figure 1. It is separated from the waters of the Gulf of California by the subaerial delta built by the Colorado River and geologic records indicate that alternate flooding and desiccation episodes have occurred in the Salton Sea since the Miocene time (Helgeson, 1968). The present-day Salton Sea and its lacustrine deposits were formed after the Colorado River delta separated the Salton Trough from waters of the Gulf of California (Axen and Fletcher, 2010).

The Salton Sea geothermal field occupies the southeastern shore of the Salton Sea in the vicinity of five small volcanic buttes (Helgeson, 1968). In the Salton Sea geothermal system, there is a continuous transition from sediments through hardened sedimentary rocks to low-grade metamorphic rocks of the greenschist facies (Muffler and White, 1968).

3.3.5 Imperial Valley and Brawley Seismic Zone

The Imperial Valley is that part of the Salton Trough that is north of the US-Mexico border and south of the Salton Sea. It is one of the most seismically active areas in California (Larsen and Reilinger, 1991), Figure 1. In the Imperial Valley, sediment thickness is about 6-7 km (Fuis et al., 1984) and the basement floor is relatively flat

(Elders et al., 1972). The basement complex beneath the valley is composed of pre-Tertiary metamorphic rocks with granitic intrusions (Tarbet, 1951). Despite the thick sediment package in the valley it is characterized by a high gravity anomaly relative to its surrounding areas, indicating that the crust under the Imperial Valley is either very thin or is of higher density than normal continental crust and surrounding areas. The Imperial Valley is one of the most seismically active regions of California and the bulk of this seismicity occurs within the Brawley seismic zone.

The Brawley seismic zone is a region located at the southern end of the Salton Sea characterized by swarms of earthquake activity (Johnson and Hill, 1982), high heat flow and recent volcanism (Lachenbrauch et al., 1985). The zone is about 50 km long and approximately 10 km wide and has been described as the northernmost spreading center belonging to a series of spreading centers that exist further south in the Gulf of California (Lomintz et al., 1970), Figure 1. Geodetic data suggest that the Brawley Seismic zone is marked by *en-échelon* northwest-trending right-lateral faults linked by conjugate left-lateral structures; the Brawley fault has extended about 30 km to the northwest and the southern part of the San Andreas Fault has moved in about the same direction (Johnson and Hadley, 1976), leaving behind a fossil transform or linear alignment of earthquakes referred to as the Sand Hills Seismicity Lineament (Larsen and Reilinger, 1991).

3.3.6 Mesquite Basin

The Mesquite Basin is a pull-apart basin formed at, and occupying a right-step between the Brawley and Imperial Faults in southern California (Segall and Pollard, 1980). The Mesquite Lake is a topographic depression with approximately 10 m of relief

located within the right step. The basin is bound by the north-striking end of the Brawley Fault on the east and by the Imperial Fault on the southwest; the northwest edge of the basin is bound by north-striking branches at the end of the Imperial Fault (Segall and Pollard, 1980).

The lack of offset between the Brawley and northern part of the Imperial faults suggests that the region of the Mesquite basin is still in its early stage of tectonic development (Larsen and Reilinger, 1991). Geodetic measurements of surface deformation and measurement of vertical slip along the Imperial and Brawley Faults suggest that the Mesquite Basin is still actively subsiding (Larsen and Reilinger, 1991).

3.3.7 Cerro Prieto Basin and Mexicali Valley

The Mexicali Valley is the part of the Salton Trough just south of the US-Mexico border (Figure 1). It is characterized by a system of grabens resulting from crustal extension associated with strike-slip transform movement along the Cerro Prieto and Imperial Faults (Albores et al., 1980). The Mexicali Seismic zone is the area located at the stepover between the Imperial and Cerro Prieto right-lateral strike-slip faults (Frez and González, 1991). The zone is characterized by high heat flow, active seismicity, and volcanism (Glowacka et al., 1999). Elders and Sass (1988) and Lomintz et al. (1970) proposed the Mexicali Seismic zone to be a spreading center. The Cerro Prieto geothermal field is situated in a pull-apart basin in the Mexicali Valley (Glowacka et al., 1999); and the heat source is probably a magmatic body at a depth of 5-6 km below the surface (Elders et al., 1984).

The interior of the Cerro Prieto graben is subjected to tension in a NW-SE direction, as indicated by the presence of oblique fractures with some normal faulting. Also, the crust in the graben is broken into a series of blocks bounded by fracture planes aligned parallel to the Imperial-Cerro Prieto fault system (Puente and De la Pefia, 1979).

3.3.8 Altar Basin

The Altar Basin is a part of the Salton Trough tectonic province (González-Escobar et al., 2013) located in northwestern Sonora, Mexico. It is a subsidiary basin which makes up an inactive part of the Colorado River Delta and lies east of the active modern delta; the basin became inactive as the Colorado River realigned its course and the focus of tectonic activity moved westward from the Altar fault to the Cerro Prieto fault (Pacheco-Romero et al., 2006).

The basin is bounded by the Cerro Prieto and Altar faults and is separated from other basins in the Salton Trough by the Colorado River Delta (Pacheco-Romero et al., 2006).

The magnetic and gravity anomalies within and around the Altar Basin trend in a northwest direction and seem to imply that the basin structure is controlled by northwest-trending faults (Pacheco-Romero et al., 2006).

3.3.9 Laguna Salada Basin

The Laguna Salada Basin is an active transtensional basin (Dorsey and Martin-Barajas, 1999) in northern Baja California. It is an elongate basin, about 100 km long, 20 km wide and trends in a NNW direction (Garcia-Abdeslem et al., 2001). The basin is bounded on the west by the Sierra Juárez and on the east by the Sierras El Mayor and

Cucapá (Garcia-Abdeslem et al., 2001). The eastern boundary of the Sierra Juárez is the Gulf Escarpment which consists of a discontinuous series of high-angle, northwest-striking faults that dip steeply to the east and west (Axen and Fletcher, 1998). On the east of the Laguna Salada Basin, the Laguna Salada Basin is bound by the Sierra El Mayor and Sierra Cucapá. In the Sierra El Mayor, plutonic rocks intrude metasedimentary rocks (Siem, 1992). The Sierra Cucapá range is made up of Upper Cretaceous granite which has intruded and metamorphosed the Cretaceous and/or Paleozoic sediments (Punte and De la Pena, 1979).

The Sierras El Mayor and Cucapá trend northwest and are bounded on their west side by the Laguna Salada Fault and the Canada David detachment fault. Within the basin, sediment thickness increases eastwards and reaches a maximum of about 3 km (Garcia-Abdeslem et al., 2001).

3.3.10 Wagner Basin

The Wagner Basin is the northernmost spreading center in the Gulf of California (Figure 11). It is at the incipient stage and is located along the Pacific-North America plate boundary. Sediments from the Colorado River accumulate and fill up the basin. The Cerro Prieto strike-slip fault extends offshore into the Wagner basin and together with the Consag and Wagner normal faults, comprises the most important structural features of the basin (González-Escobar et al., 2009).

The Wagner Basin is an elongate trough, 60 km long and 27 km wide, bound by the Cerro Prieto fault on the east, the Wagner fault on the northwest side, and the Consag

fault on the western part of the basin. The basement underneath the basin is about 7 km deep (González-Escobar, et al., 2009).

CHAPTER 4: DATA AND METHODOLOGY

4.1 Objective

The complex tectonic history of the area gave rise to a complex tectonic structure with many outstanding questions. One of the open questions relates to the nature of the crust beneath the Salton Trough: is it new oceanic crust, heavily intruded continental crust, or just much thinned continental crust? The objective of this study is to model the crustal structure of the Salton Trough using gravity data, and integrating other geologic and geophysical data to find out whether it is oceanic, normal continental, or intruded continental crust.

4.2 Gravity and Magnetic modeling

Gravity and magnetic modeling is based on the principle that responses can be directly related to physical properties of rocks such as density and magnetic susceptibility, and can therefore be correlated with different rock types. Gravity studies aim to locate and describe subsurface structures from the gravity effects arising from their anomalous densities (Lowie, 2007).

Gravity data acquisition entails measurement of raw gravity values for locations of interest. These readings are affected by different external influences and processing raw gravity data involves making corrections to account for these external effects.

Some of the corrections usually made on gravity data are:

1. Drift Correction: The effect of instrumental drift from changes in thermal elastic and other physical properties of the measuring instrument's spring. This may be partly induced by thermal changes and is corrected by repeated measurements at different time intervals of the day, with the assumption that drift is linear between repeated measurements and then subtracting the linear drift from all other readings. This process is known as drift correction (Blakely, 1995; Lowrie, 2007).
2. Tidal Correction: Gravity measurements on earth are also affected by tidal attractions from the sun and the moon which results in elevation variations on the Earth's surface. This gravity attraction depends on latitude and also varies over different time intervals. It is corrected by applying tidal corrections to the measured gravity values (Blakely, 1995; Lowrie, 2007).
3. Topographic or Terrain Correction: The presence of hills or valleys in the immediate vicinity of the gravimeter also affects measurements. This can be corrected by making a terrain or topographic correction to remove the effect of topography around a gravity station on the measured gravity value. This correction is added to the measured gravity value (Lowrie, 2007).
4. Elevation Correction: Because the Earth's gravitational field decreases with increasing elevation, measured gravity is again affected by the elevation of the gravity station above the ellipsoid. This can be compensated for by a Free Air and Bouguer correction for the station elevation. The correction will be added to the measured gravity (Lowrie, 2007).
5. Bouguer plate Correction: On land, there is usually some material (Bouguer plate) between the base of the station and sea level or the reference ellipsoid, a

mathematical surface that corresponds to mean sea level. So even after correction for elevation, the effect of the Bouguer plate on measured gravity has to be taken into account (Lowrie, 2007). The simple Bouguer correction approximates all mass above sea level to be a homogenous, infinitely extended slab whose thickness is same as the height of the observation point above sea level (Blakely, 1995). Bouguer plate correction is made to remove the effect of this flat layer seated between the gravity station and this correction is subtracted from the measured gravity (Lowrie, 2007).

6. Latitude Correction: Gravitational attraction varies with latitude, being stronger at the flatter poles than at the bulging equators and this affects the value of our measured gravity. Variations due to changes in latitude on the Earth's surface are corrected by calculating the appropriate value for g from the International Gravity Formula (IGF) and subtracting it from the observed value.
7. Spatial corrections are also made on marine and airborne data to account for variations due to the motion of the ship or aircraft.
8. In a similar fashion, the Eötvös correction is applied to data recorded from a vehicle moving along a path that is parallel to the Earth's surface and creating a centrifugal acceleration in the process. The correction removes the influence of this acceleration (Blakely, 1995; Lowrie, 2007).

If the interior of the Earth were homogenous with uniform distribution of density, the value of measured gravity would be the same as the theoretical gravity calculated from the normal gravity formula. Non-homogeneity of the interior of the Earth and

variations in density give rise to differences or anomalies. An anomaly arises when there is a difference between an observation and a norm or reference (Wolfgang and Smilde, 2009; Lowrie, 2007).

The difference in density of the body with respect to the surrounding rocks is called density contrast. A body has a positive density contrast if it has a higher density than its host or surrounding rocks and density contrast is negative if the density of the body is lower than that of its surrounding host rocks. A gravity anomaly is the difference between the corrected value of measured gravity and the theoretical gravity (Lowrie, 2007).

There are two common types of gravity anomalies:

1. Bouguer gravity anomaly
2. Free-Air gravity anomaly

Bouguer gravity anomaly (Δg_B) is the gravity anomaly from measured data that has been corrected for Free-Air, Bouguer plate, terrain, and tidal effects. It is shown by the simple equation below:

$$\Delta g_B = g_{\text{obs}} + (\Delta g_{\text{FA}} - \Delta g_{\text{BP}} + \Delta g_{\text{T}} + \Delta g_{\text{tide}}) - g_n.$$

The Free-Air anomaly (Δg_F) is the gravity anomaly from measured data that has been corrected for Free-Air, terrain, and latitude (Lowrie, 2007):

$$\Delta g_F = g_{\text{obs}} + (\Delta g_{\text{FA}} + \Delta g_{\text{T}} + \Delta g_{\text{tide}}) - g_n.$$

where g_{obs} is the observed gravity value, the value obtained from field measurement; Δg_{FA} is the free air correction; Δg_{BP} is the Bouguer plate correction; Δg_{T} is the correction for terrain effects; Δg_{tide} is the tidal correction, and g_{n} is the normal gravity value which is the gravity value observed from the surface of the reference ellipsoid.

Gravity data are generally used to define basin geometry and magnetic data are often used to define the spatial extent and depth of basement structures. Gravity and magnetic data can be combined to create models that represent the overall shape of the basin and identify predominant basement fabrics and structural trends. From these models we can determine the type of crust; continental, oceanic, or transitional, that underlies the basin and the extent of geological units in the study area.

Faults produce steep gradients on gravity and magnetic anomaly curves; the shallower the fault is, the steeper the gravity anomaly gradient. Magnetic anomalies also exhibit steep gradients when the basement or a magnetic sedimentary layer is faulted and the amplitude of the anomaly will depend on both depth and magnetic susceptibility. Dipping beds also produce steep gradient anomalies, but in this case, the anomaly gradient and magnitude increase as the bed nears the surface (Prieto, 1996).

Gravity anomalies are indicative of the presence of bodies or structures with anomalous densities; the strength depends on the thickness or size and depth of the anomalous body. It may be positive or negative depending on the density contrast which is the difference between the density of the anomalous body and its surrounding material. It is positive for bodies that are denser than their surroundings and negative for bodies

that are less dense than the surrounding rocks. Generally, gravity anomaly highs are related to structural highs and anomaly lows are related to structural lows except for very long wavelengths. Short magnetic wavelengths are related to shallow sources and long wavelengths are related to deep sources (Bird, D.; personal communication).

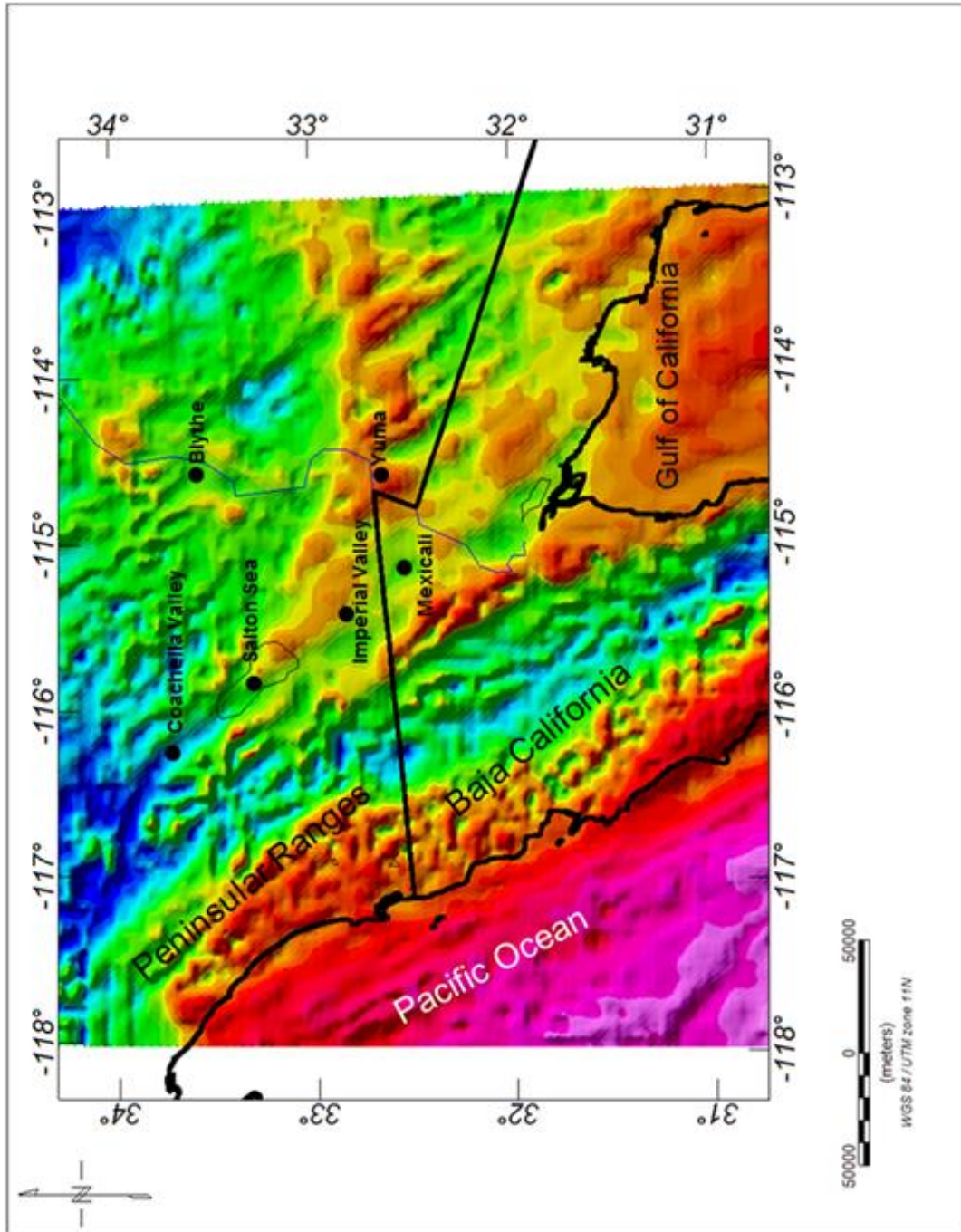


Figure 14: Bouguer gravity anomaly map of the study area.

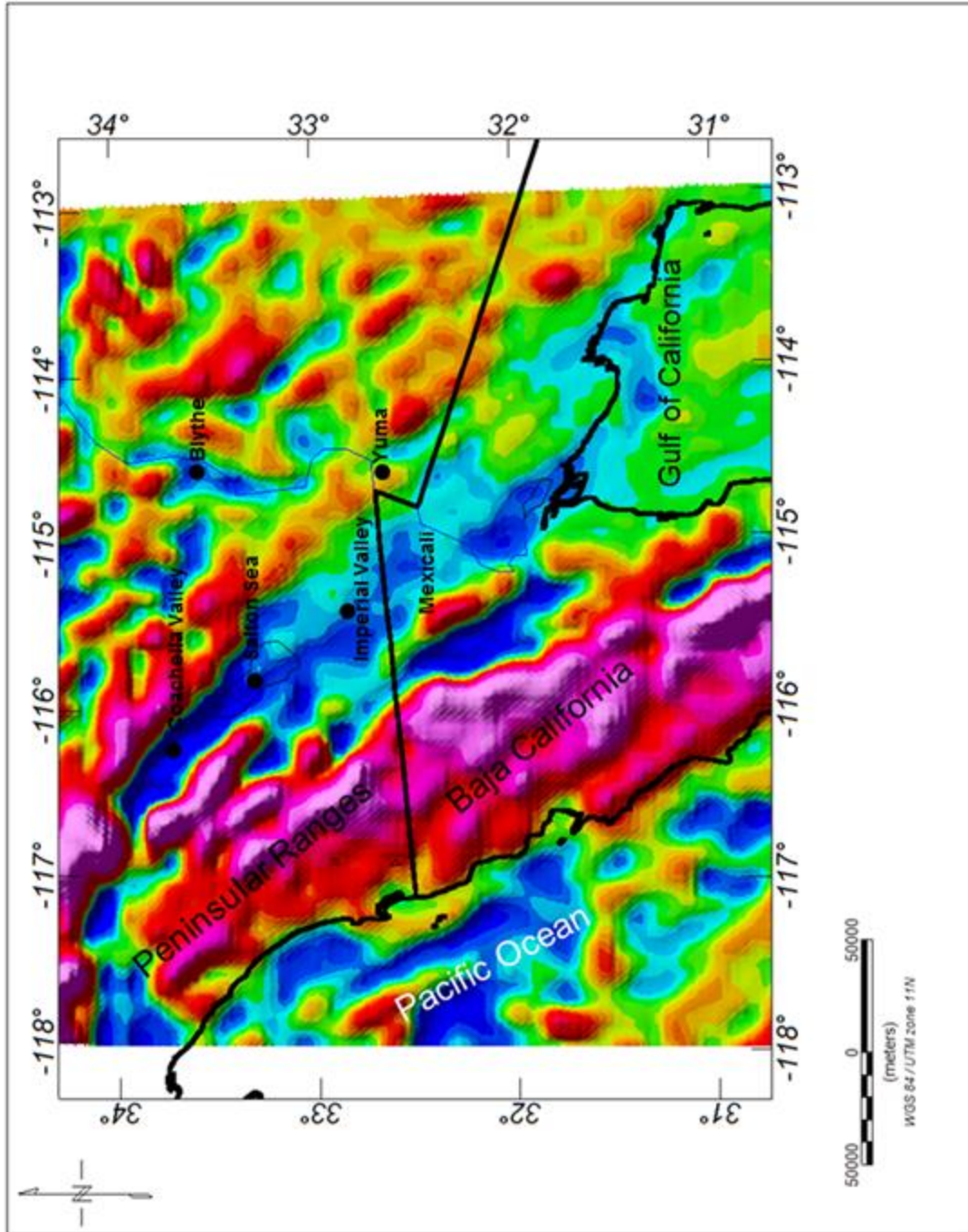


Figure 15: Free Air gravity anomaly map of the study area.

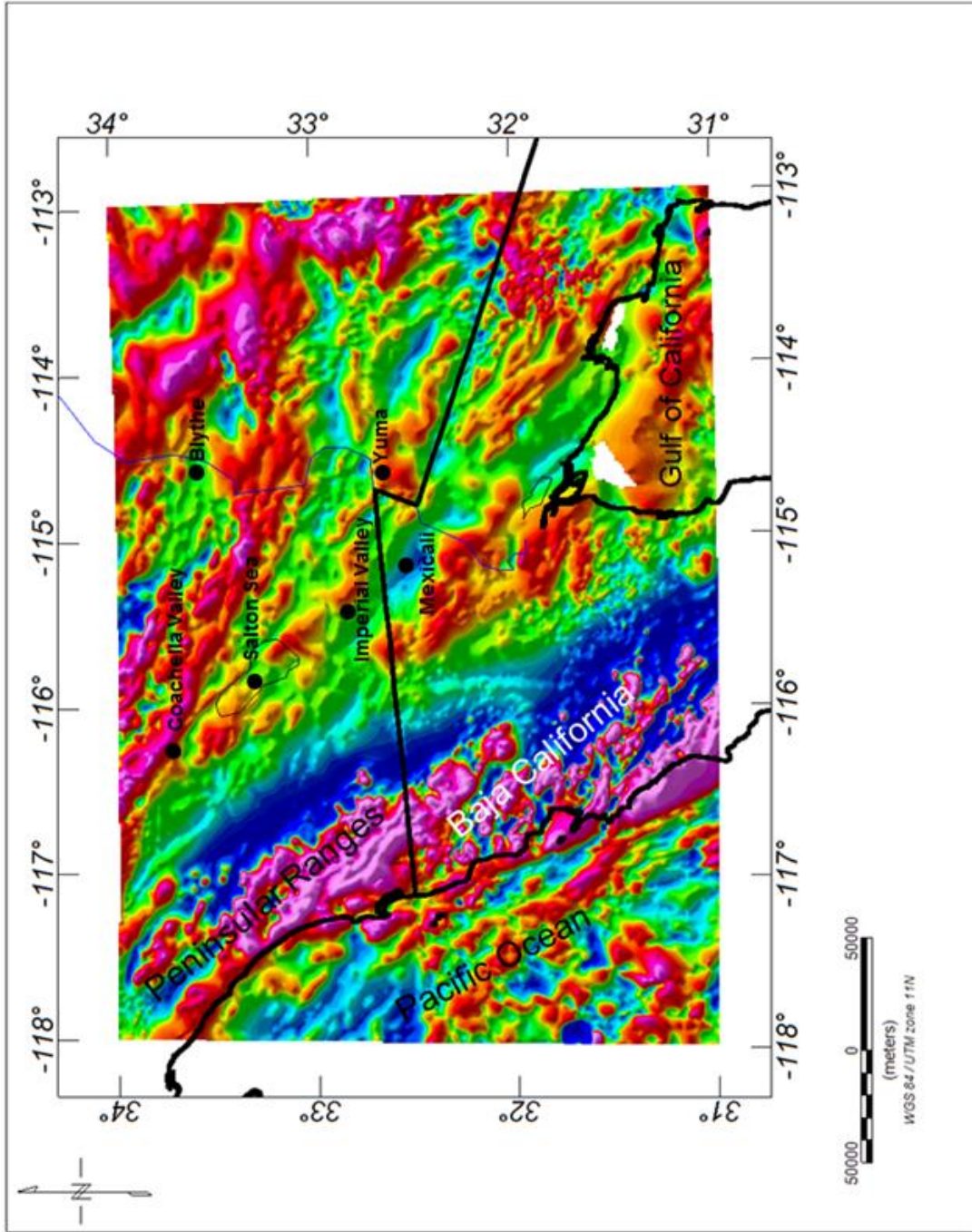


Figure 16: Magnetic anomaly map of the study area.

The wavelength of an anomaly is its horizontal extent and is related to the burial depth of the anomalous mass. Deeply buried large bodies produce long wavelength, low amplitude anomalies called regional anomalies, and small shallow bodies cause short-wavelength anomalies called residual anomalies.

Various gravity and magnetic data enhancements techniques are used to separate regional and residual anomalies to draw attention to particular features in the gravity or magnetic by filtering and enhancements to produce series of shaded relief images that define or emphasize interesting features and structural trends. Enhanced maps emphasize the gravity anomalies in the area some of which can be correlated to the geologic features on the geologic map (Figure 17). Enhanced Bouguer gravity maps are by far smoother than the regular anomaly maps because after filtering, the short wavelength anomalies which are more representative of the surface geology of the area remain.

There are different methods of filtering depending on the features of interest. Using the ‘upward continued’ technique for an elevation of 15 km, I produced an enhanced gravity anomaly grid of the area which I subtracted from the original Bouguer gravity anomaly grid to yield a Bouguer residual grid (Figure 17). This technique increases the elevation at which measurement was taken (that is, distance from the point of measurement to the source) and the end result is a map with short wavelength features smoothed out relative to the longer wavelength anomalies.

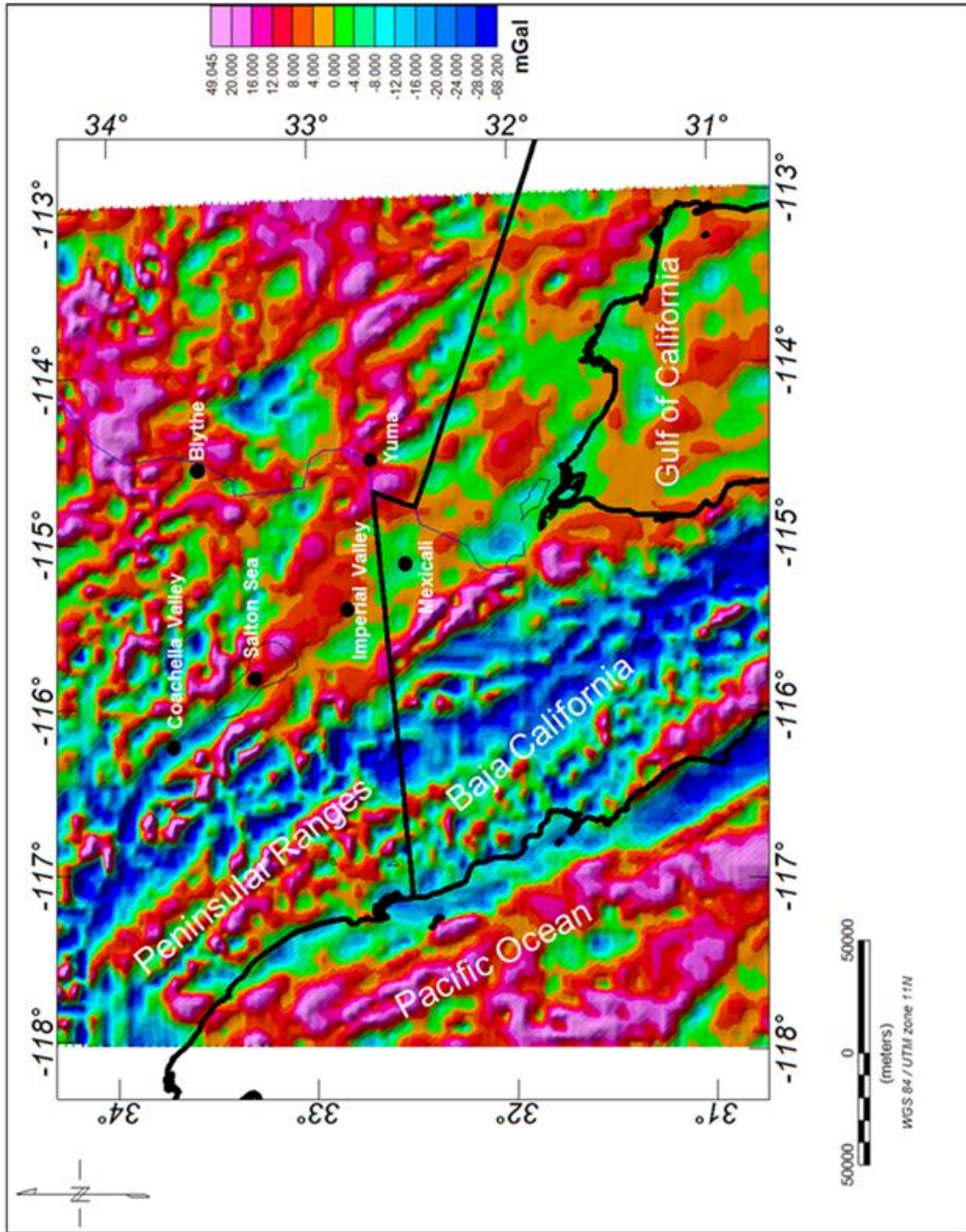


Figure 17: Residual Bouguer gravity anomaly map of the study area after 15 km upward continuation.

4.3 Gravity and magnetic characteristics of the region

Gravity anomalies over the San Andreas Fault system are linear highs and lows that trend sub-parallel to the major faults in the area in a NW-SE direction. Bouguer gravity anomalies in the study area are high along the coastal areas and reduce towards the northeast reflecting a gradual transition from thin oceanic crust to much thicker continental crust (Griscom and Jachens, 1990). Some of the deep lows as seen in the Salton Sea and Salton Trough area are caused by thick accumulations of Cenozoic sediment deposits that fill the tectonic basins adjacent to the faults (Griscom and Jachens, 1990).

Magnetic anomalies in the vicinity of the San Andreas Fault system are typically caused by ophiolitic rocks and tabular serpentinite bodies associated with the Franciscan assemblage, mafic plutonic rocks such as those exposed in the western peninsular ranges and some sedimentary rocks that may contain detrital serpentinite (Griscom and Jachens, 1990). Several magnetic anomalies in the area reflect remnant magnetization in the ocean crust which is primarily basaltic volcanic rock (Wallace, 1990).

Across the Peninsular Range, gravity anomalies are high and low, almost representing two extremes on our data range. The western part shows high Bouguer gravity and magnetic anomalies, possibly indicating the presence of mafic material while the eastern part of the Range reads low Bouguer gravity and magnetic anomalies indicating felsic composition of the subsurface material. On the eastern part of the Peninsular Range, the Moho topography does not correlate with surface topography

suggesting that the highest elevations are not supported by a local Airy crustal root, support here may be achieved through a combination of flexure and lateral variation in crustal or upper mantle density (Lewis et al., 2001).

Along the axis of the Salton Trough, the anomalies are generally low with a few isolated localized high anomalies. Just south of the US-Mexico border, in the Laguna Salada basin region, Bouguer gravity anomaly is low in the Sierra Juárez region, indicating the presence of a topographic root. The transition from the eastern margin of the Sierra Juárez towards the Laguna Salada Basin shows a smooth horizontal gravity gradient suggesting that the rocks have similar densities without much structural features (Siem, 1992). The Sierra Cucapá and Sierra El Mayor form the eastern boundary of the Laguna Salada Basin (Axen and Fletcher, 1998) and the gravity gradient over their western margin is steeper and may be due to structural disruptions and sharp changes in density across the Laguna Salada Fault and Canada David Detachment fault (Siem, 1992).

In the Altar basin, the magnetic anomaly map shows a magnetic low with much higher anomaly readings in the eastern and northwestern parts of the basin. Along the Cerro Prieto Fault, high northwest-trending magnetic anomalies suggest the presence of basaltic intrusions along the fault (Goldstein et al., 1984).

4.4 Data collection and processing

We obtained the gravity anomaly dataset from the International Gravimetric Bureau (BGI) website; the dataset contains 17,279 points of Bouguer Gravity Anomaly,

Free-Air Anomaly, and Elevation data. Magnetic data were downloaded from the website of The University of Texas El Paso <http://irpsrvgis00.utep.edu/repositorywebsite/> and contains 84,586 points. Both dataset cover an area of about 191,212 km². I constructed 2-D crustal models using the GM-SYS application on Geosoft's Oasis Montaj software. Bouguer, Free-Air, and Magnetic data maps of the study area are show in Figures 14, 15 and 16.

Interpretation of the gravity data involved iterative forward modeling which is a process of making inferences about the density and shapes of subsurface bodies from processed observed anomaly values until we can approximately match the calculated gravity anomaly curve to the observed anomaly curve. The calculated gravity anomaly resulting from a model is computed to be the sum of the contributions of individual bodies each with a given density and volume.

Supplementary data

The gravity and magnetic dataset were supplemented with tomographic images, refraction data and various geological datasets. These datasets provided control parameters that constrained the models. Supplementary data include:

1. Topography (onshore and offshore): Topography data serve to constrain the topographic and bathymetric extents. We used a combination of onshore topography data (gtopo30) and offshore terrain base data from Bird Geophysical website, <ftp://ftp.birdgeo.com/> for this.

2. Refraction data for depth to the Moho: Moho depth is directly related to the tectonic evolution of an area and is important for characterizing the overall structure of the crust. Data for depth to the Moho were obtained from different seismic refraction experiments carried out in the area (Nava and Brune, 1982; Hearn, 1984; Hussein et al., 2011; Zhu and Kanamori, 2000; Hamilton, 1970; McCarthy et al., 1991; Steinhart and Meyer, 1961; Philips, 1964; www.gps.caltech.edu) and results reveal rapidly changing and widely varying Moho topography as seen in the models. The refraction stations are shown on a gravity anomaly map of the area in figure 22 and the depths to the Moho at the various stations are shown in table 1.
3. Sediment thickness and depth to the basement: Sediment thickness and depth to the basement data serve as an important control as it further reduces the unknown crustal parameters. Data were obtained from previous work and experiments carried out in the area (Fuis et al., 1984; Axen and Fletcher, 1998; González-Escobar et al., 2009; Chávez et al., 1999; Shor et al., 1976; Garcia-Abdeslem et al., 2001).
4. Geologic and Basement map. This gives us an idea of the surface geology. Basement topography data was obtained from the Basement Map of North America by the American Association of Petroleum Geologists and the United States Geological Survey, 1967 (Figure 20). The geologic map (Figure 21) was created using ArcGIS and shapefiles obtained from <http://ngmdb.usgs.gov/gmna/>.

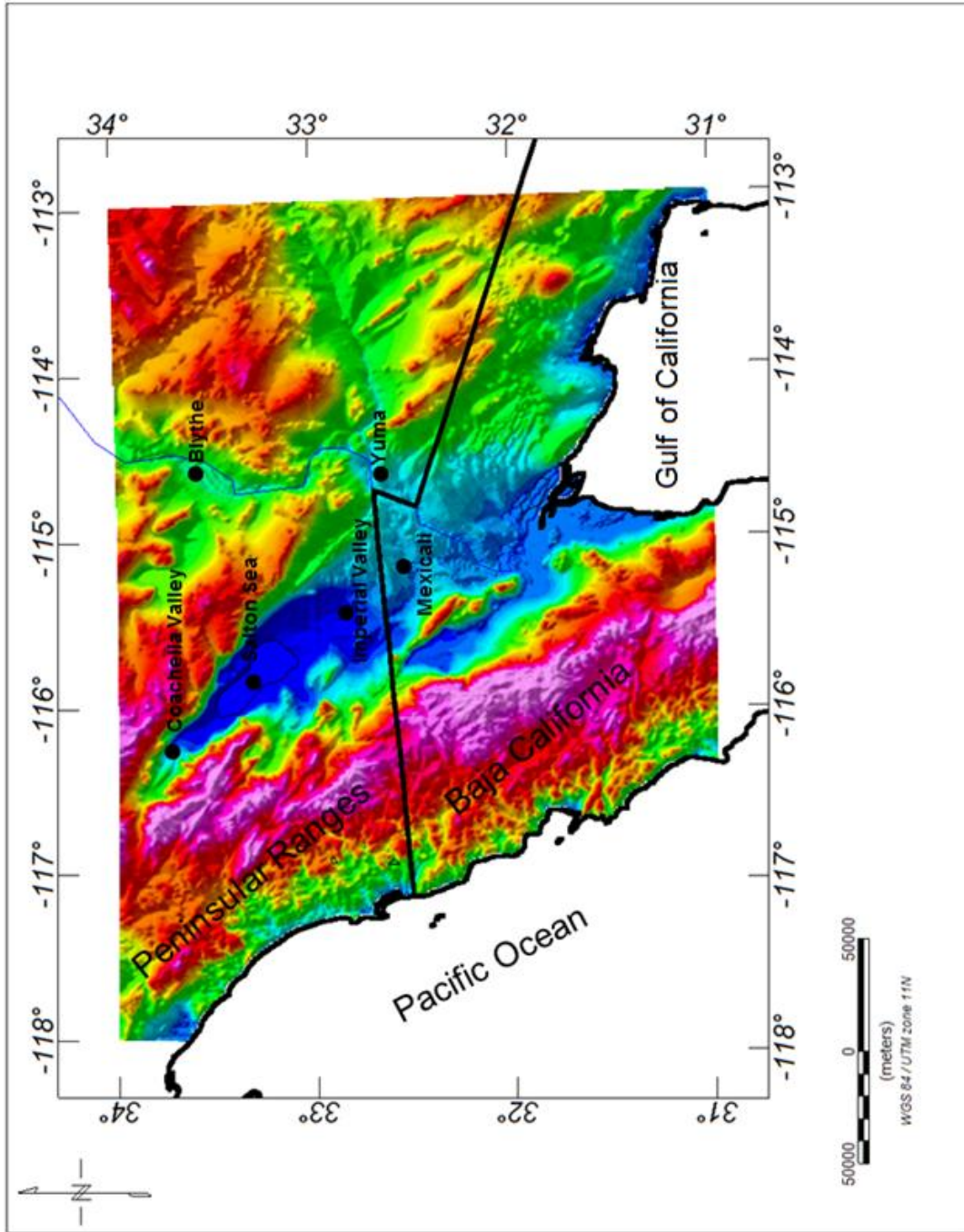


Figure 18: Topography/Elevation map of the study area.

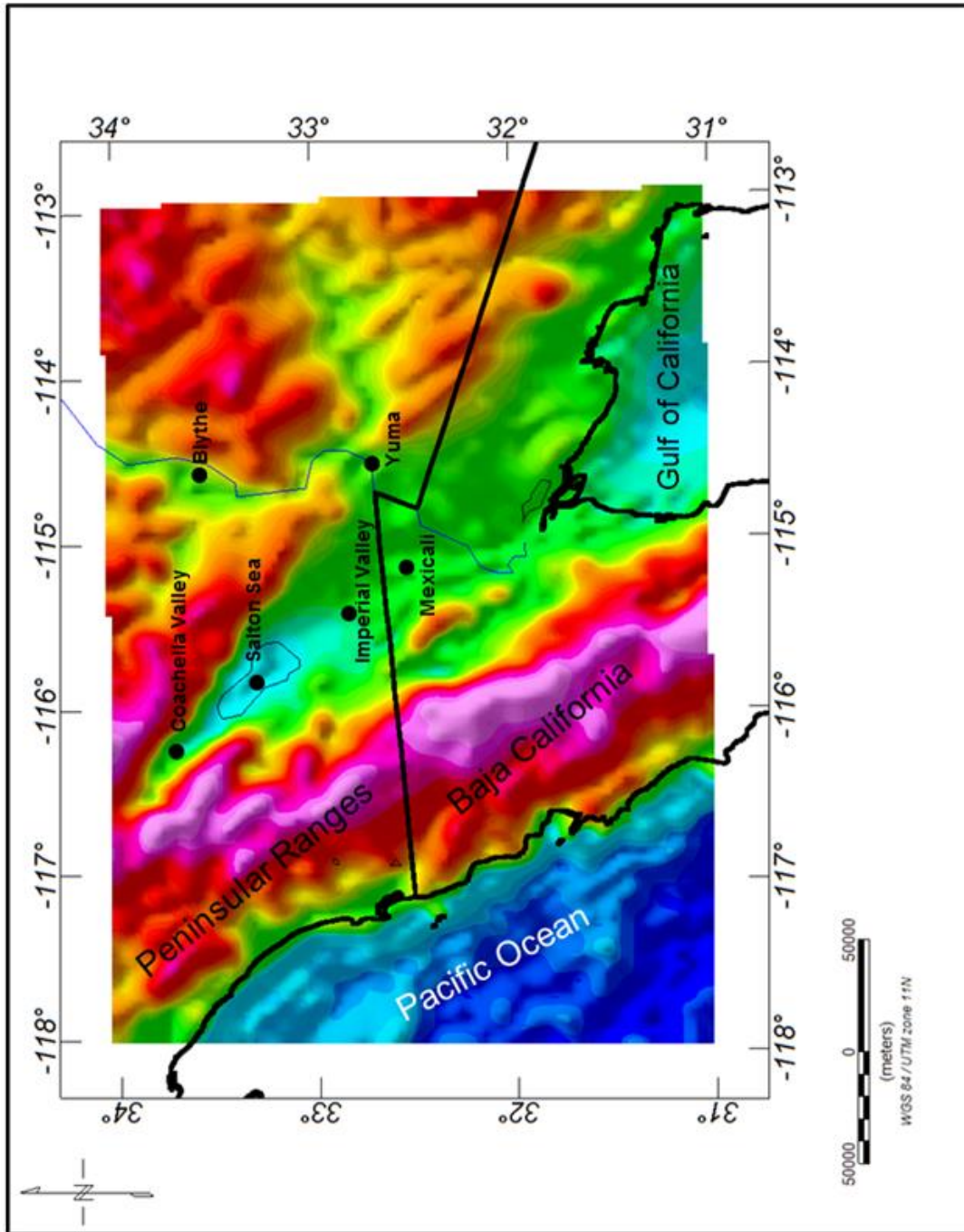


Figure 19: Offshore topography map of the study area.

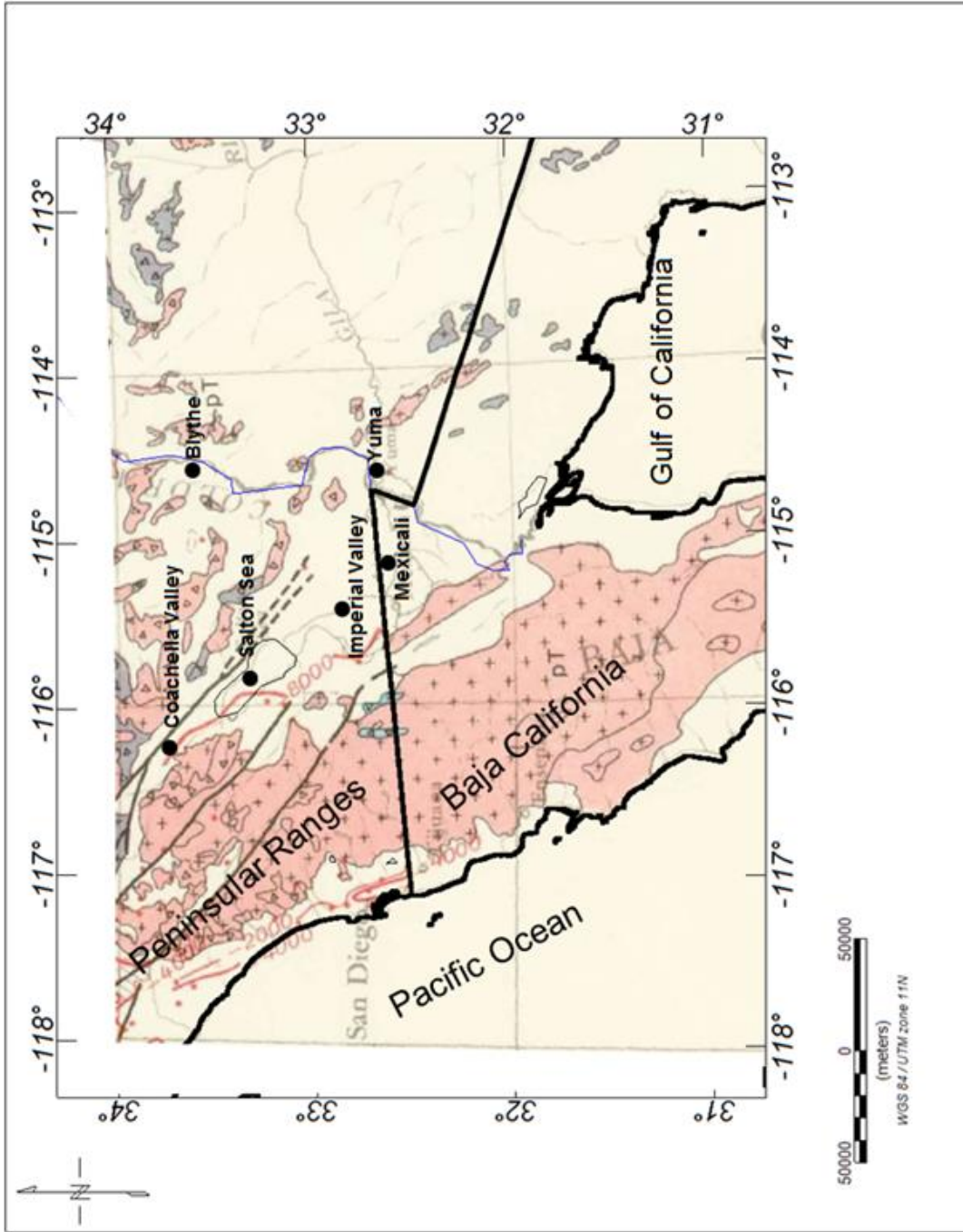


Figure 20: Basement topography map of the study area. Modified from the basement map of North America by the American Association of Petroleum Geologists and the United States Geological Survey, 1967.

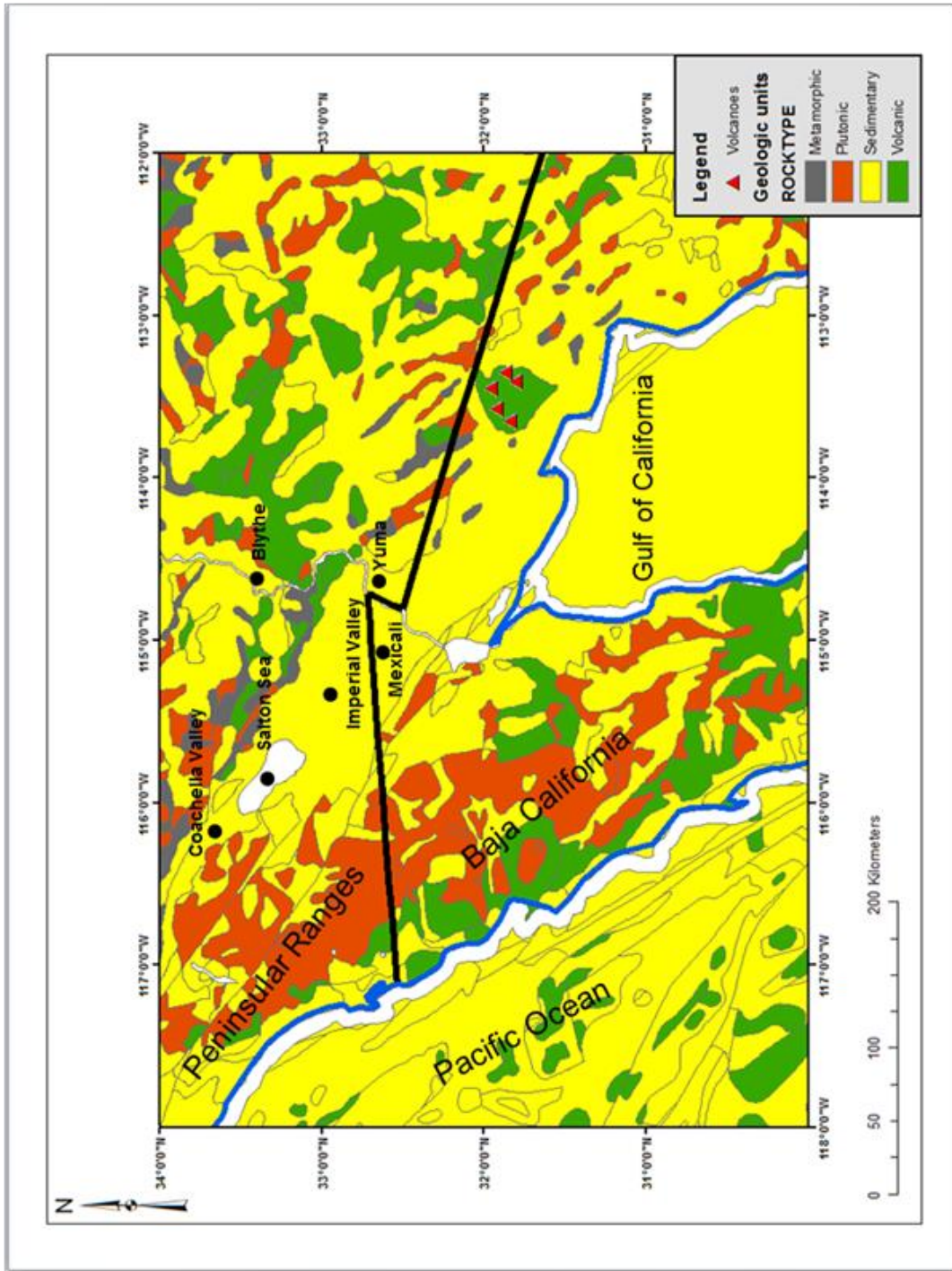


Figure 21: Geologic map of the study area.

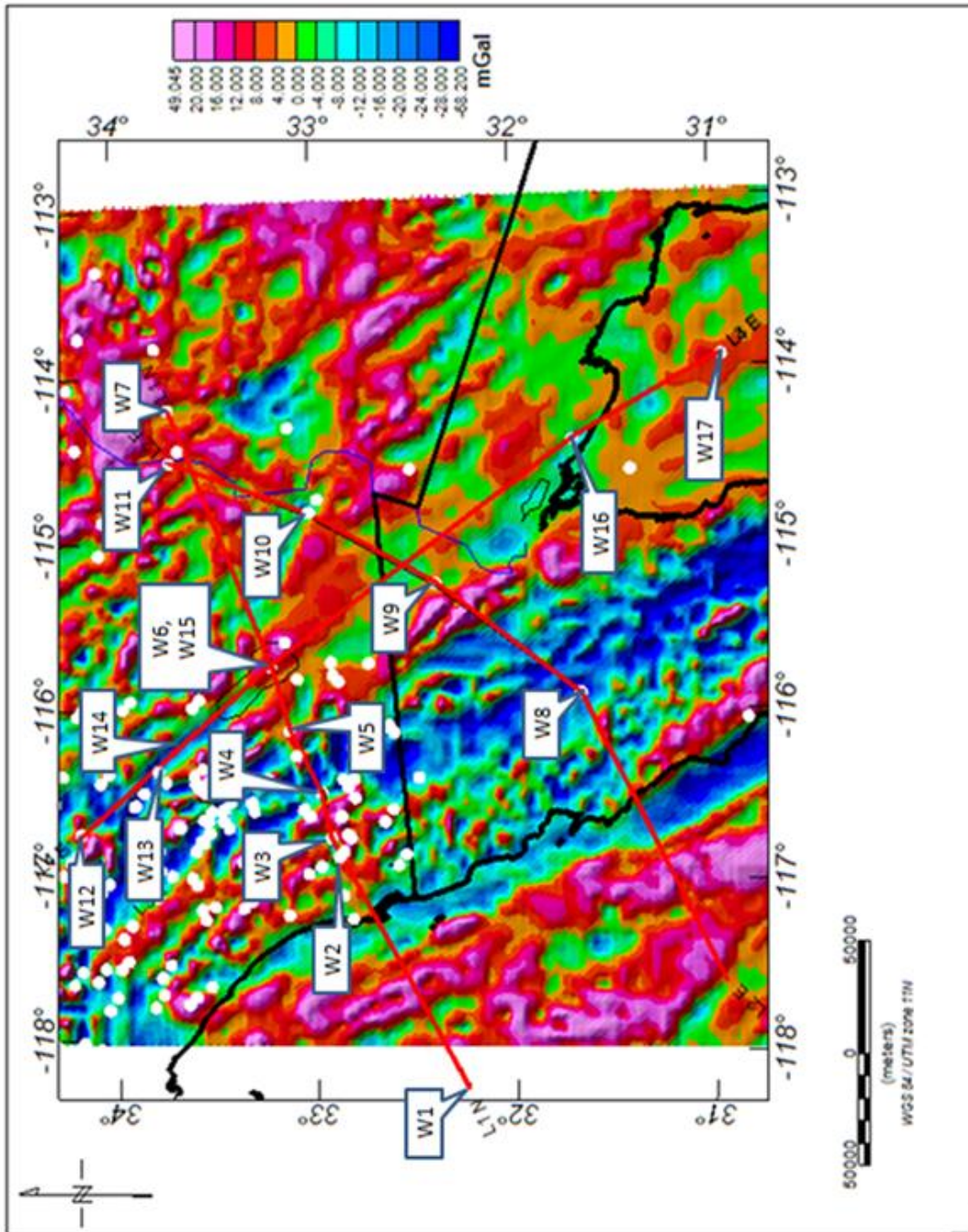


Figure 22: Gravity anomaly map of the area showing the profile lines and refraction stations.

Line	Well	Moho Depth (km)	Reference
1	W1	26	Hearn, 1984
1	W2	38	Zhu & Kanamori, 2000
1	W3	41.8	Nava & Brune, 1982
1	W4	28	Hearn, 1984
1	W5	25	Hamilton, 1970
1	W6	22	Hearn, 1984
1	W7	27.2	McCarthy et al., 1991
2	W8	32.5	Hussein et al., 2011
2	W9	25.5	Hussein et al., 2011
2	W10	27	Hussein et al., 2011
2	W11	33.49	Hussein et al., 2011
3	W12	40	Steinhart, 1961
3	W13	33	Zhu & Kanamori, 2000
3	W14	22.9	Persaud, 2007
3	W15	22	Hearn, 1984
3	W16	24	Phillips, 1964
3	W17	18.3	Phillips, 1964

Table 1 : Moho depth values for refraction stations along the profiles.

5. Depth to the Lithosphere-Asthenosphere Boundary (LAB depth): Data on the depth to the Lithosphere-Asthenosphere Boundary from seismic experiments (Lekic et al., 2011) were used to constrain the models.

Previous gravity studies of the Salton Trough

The previous gravity study by Fuis et al. (1984) involved seismic refraction data, modeling a gravity profile across the region, and inferring rock compositions from their velocity-depth functions. They analyzed five profiles and produced a model for the

Imperial Valley region of the Salton Trough. Figure 23 shows a West to Southeast cross-section from La Jolla to the Chocolate Mountains from Fuis et al. (1984). The profile suggests that the Imperial Valley region of the Salton Trough consists of a sedimentary layer, a transition zone, a basement and sub-basement layer. The subbasement is thought to be oceanic crustal type mafic intrusion due to its high velocity and the presence of basaltic intrusions in the sedimentary section. Fuis et al. (1984) concluded that new crust was being formed in the Salton Trough with sedimentation filling it in from above and mafic intrusive rocks filling it from below as the rift opens.

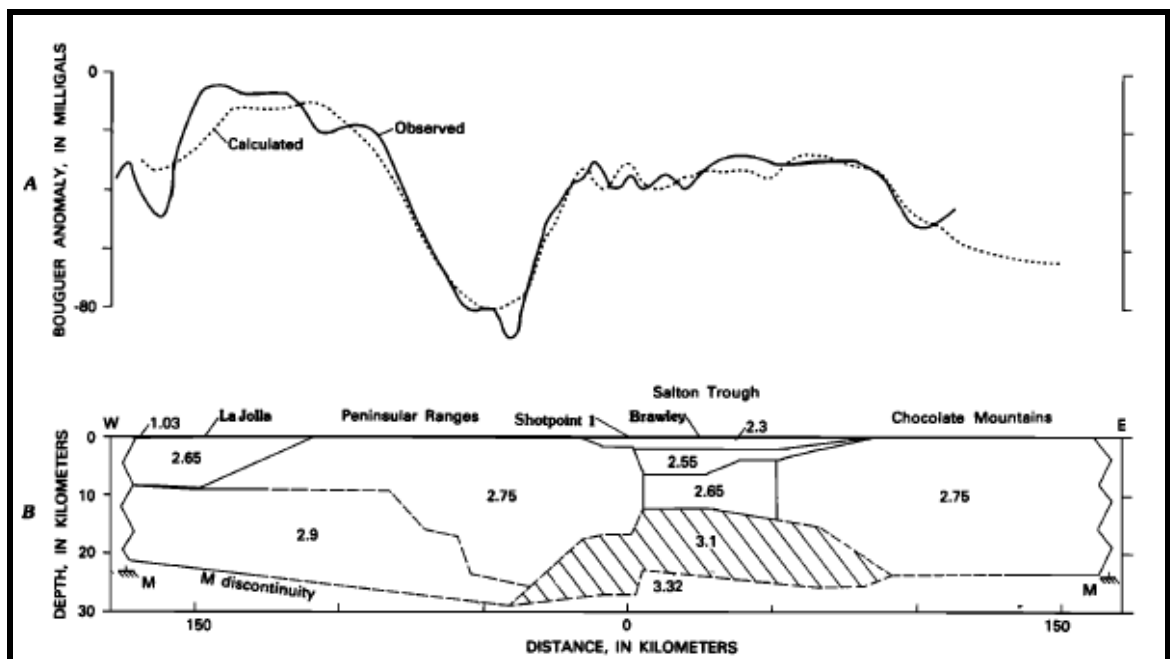


Figure 23: Previous gravity model across the Imperial Valley region of the Salton Trough by Fuis et al. (1984).

Hussein (2007) modeled the Salton Trough by integrating receiver function, gravity, and magnetic data. Depth to the Moho was determined from receiver function data and densities of upper and lower crust were inferred from velocities determined from

the seismic profile of Fuis et al. (1984). The 2-D crustal models (Figure 24) created indicate that the lower crust of the Salton Trough is more oceanic/gabbroic in composition (density 2950-2800 kg/m³) and the upper crust density ranges from 2650-2300 kg/m³. Hussein (2007) concluded that the large density variation between the upper and lower crust suggests magmatism in the lower crust and sedimentation in the upper crust which seems to agree with the findings of Fuis et al. (1984).

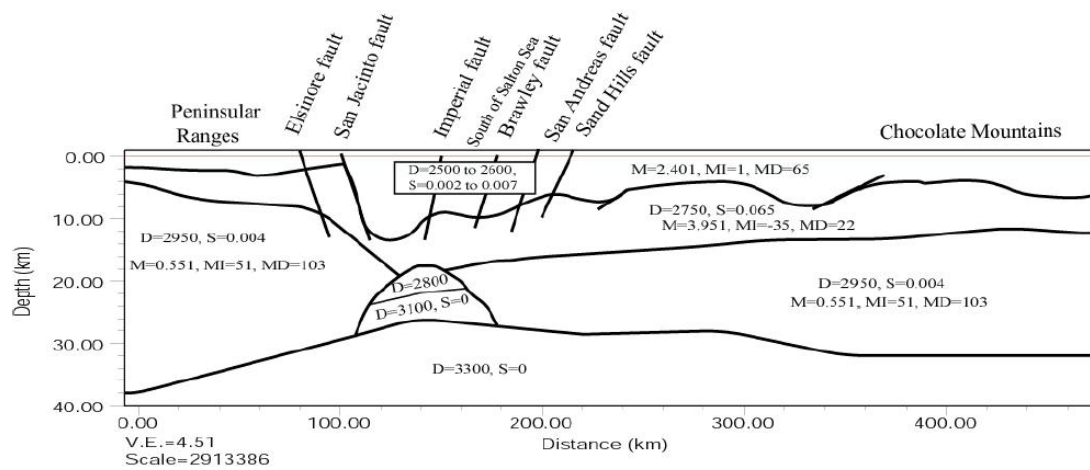


Figure 24. Gravity model from Hussein et al. (2011) along a profile crossing the central region of the Salton Trough. A gabbroic body is interpreted below the Salton Trough. D= density (kg/m³), S=susceptibility, M= magnetization (A/m), MI= magnetic inclination (degree), MD= magnetic declination (degree).

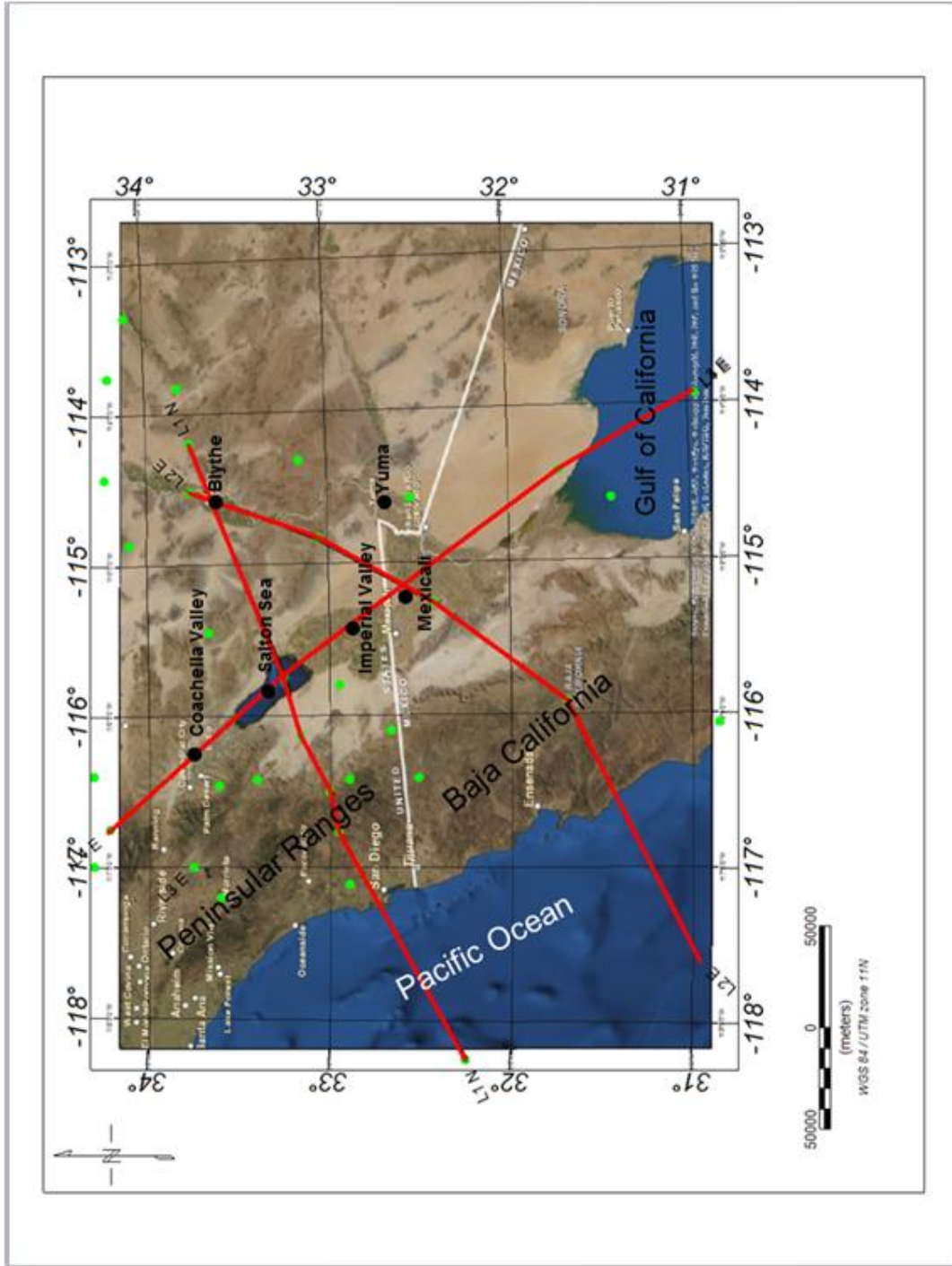


Figure 25: Profile lines (red) for 2-D gravity models across the study area. The green dots are refraction points used to constrain the models.

CHAPTER 5: Two-D models and interpretation

Two-D crustal models were constructed along three profile lines (red lines) across the area as shown in Figure 25. The green dots shown in Figure 25 are locations of refraction stations from which I obtained data on depth to the Moho. The profile lines were selected based on data availability and points of geologic interest. One line runs approximately north-south along the axis of the Trough, and others cut across. The lines tie each other at different points. The models are bound on top by topography and extend to infinity laterally.

5.1 Two-D gravity models

Profile Line 1

Line 1 (Figure 26) is a W-E transect, about 412 kilometers long, running from the continental borderland through the San Diego Trough offshore, across the Peninsular Range and Salton Trough eastward to the southern Basin and Range Province. Moho depth from refraction data along this line varies from 22 km offshore, to about 42 km in the western part of the Peninsular Range. The profile line cuts across numerous faults which are manifested as steep gradients on the gravity and magnetic anomaly curves. Offshore of San Diego in the San Diego Trough, the water depth is about 0.8-1.5 km, and sediment thickness is 3 km as estimated by Shor et al. (1976). Gravity modeling predicts (Figure 26) that the crust here is thin with Moho depth at about 20 km. Onshore, Line 1 crosses the Peninsular Range which forms the western boundary of the Salton Trough. The Range show a moderately high gravity anomaly reading, but two different trends in

the magnetic anomaly on the western and eastern sides of the Range. This difference in magnetic susceptibility of the Peninsular Range batholiths is probably due to a compositional difference between the gabbroic western and granitic eastern parts of the Range (Todd et al., 2003). This compositional difference has been attributed to either the batholith range being a product of two simultaneously occurring Cretaceous magmatic arcs (e.g., Silver and Chappell, 1988), with the older mafic western section being formed in oceanic lithosphere while the younger, more silicic eastern portion developed in continental lithosphere (Gastil, 1993); or a single Cretaceous arc moving eastwards across a pre-Cretaceous lithospheric boundary (Thomson and Girty, 1994).

The model predicts that the Moho depth under the Peninsular Range shallows eastwards with an apparent westward dip of $\sim 20^\circ$. The topographically high eastern end of this range is underlain by thinned crust suggesting extensional tectonics and the Moho topography does not correlate with surface topography. This is an indication of the absence of an Airy crustal root and the need for lateral variation in crustal density for isostatic compensation (Lewis et al., 2001). The gravity model (Figure 26) shows that the crustal density under the batholith changes from 2.75 g/cm^3 to 2.57 g/cm^3 . In the Salton Trough area, sediments fill the Trough from the surface down to depths of 4-7 km (Fuis et al., 1984; Axen and Fletcher, 1998, Dorsey, 2006). These previous estimates of basement depths are confirmed by our models.

Further east, Line 1 crosses a metamorphic block in the Orocopia-Chocolate Mountains area east of the Salton Sea. This is known as the Orocopia schist which

underlies the Chocolate Mountain thrust fault (Irwin, 1990). The model predicted Moho depth is about 27 km here.

Profile Line 2

Line 2 (Figure 27) is 445 kilometers long running in a southwest-northeast direction from offshore of the west of Baja California to the southern Basin and Range Province region. Known Moho depth (from refraction data) along this line varies from 33 km in eastern part of Baja California to 25 km around the western margin of Mexicali valley.

The line starts offshore near the Animal and San Isidro basins, west of Baja California where the water depth is 1.8-1.5 km. Onshore, the line runs across Baja California which shows the same kind of gravity and magnetic anomaly trend as the Peninsular Range north of the US-Mexico border; high Bouguer gravity and magnetic anomaly readings on the western part and lower readings on the eastern part. The gravity models predict that the Moho depth here is ~32 km deep. On Baja California, Line 2 crosses the Angua Blanca and San Miguel Faults both of which show up as steep gradients on the gravity anomaly curve.

Now trending northeast, the line crosses the Laguna Salada Basin. This is a shallow, asymmetric half-graben bound on the east by the west-dipping Laguna Salada fault and Canada David detachment (Figure 1), and on the west side by the main Gulf Escarpment (Axen, 1995; Fletcher and Spelz, 2009). The Laguna Salada Basin is bordered on the west by the Sierra Juarez and on the east by the Sierras Cucapá and El Mayor. The sediment thickness in the Laguna Salada Basin is 5-6 km (Fenby and Gatsil,

1991) thickening eastward (Miele, 1986). Moho depth beneath the Laguna Salada Basin is about 27 km.

Further towards the northeast, Line 2 cuts across the Cerro Prieto fault, a right-lateral strike-slip fault running from the southern part of Mexicali valley into the Gulf of California. In the Mexicali Valley, sediment thickness is 3-5 km (Chávez et al., 1999) and Moho depth from refraction data is about 24 km. Northeast of the Mexicali Valley, there is a sharp drop in gravity anomaly reading over the high elevation of the Black Mountain east of the Imperial Valley.

Profile Line 3

Line 3 is 450 kilometers long running through the central axis of the Salton Trough from the San Geronio Mountain in the north to the Gulf of California. Moho depth obtained from seismic refraction data points along this line varies from 40 km beneath the San Geronio Mountains to 18 km in the Wagner Basin in the Gulf of California.

The San Geronio Mountains is a metamorphic terrane of intermediate to basic composition intruded by Mesozoic quartz monzonite (Allen, 1957). The line crosses through Morongo Valley which consists of alluvium underlain by quartzite, and Palm Springs and Indio in the Coachella Valley where the Moho depth shallows southwards from 33 to 20 km.

The line transects the Salton Sea where refraction data and the gravity models indicate that the crust is approximately 21 km thick. In the Imperial Valley the Moho depth is ~20 km and sediment thickness is 6-7 km (Fuis and Kohler, 1984). South of the Imperial Valley and the US-Mexico border, the line crosses the Mexicali Valley, a valley formed by a combination of rifting, rapid deltaic sedimentation, marine intrusions, and large scale strike-slip faulting (Chávez et al., 1999). Further south, the line crosses the Altar Basin where observed Moho depth is about 24 km and granitic basement is at a depth of 4 km to 5 km (Chávez et al., 1999). The line ends in the Wagner Basin in the Gulf of California.

5.2 Model Results

Different models were created to test all three lines for oceanic, continental, and transitional crustal parameters. The models are bound on top by topography and at depth by the Moho and the Lithosphere-Asthenosphere boundary. Sediment thickness and basement topography under the basins in the area are known and also act to constrain some parts of the models. I used a 3 layer sediment model with sedimentary densities 2.4 g/m^3 , 2.45 kg/m^3 and 2.5 kg/m^3 from top to bottom layer, respectively. Sedimentary layers' densities were kept constant horizontally within one layer in the models, but the densities and shapes of the upper, middle, and lower crustal layers were varied for the different crustal types. The oceanic, mantle, and asthenosphere parameters remained constant in all models.

Oceanic Crust Test

Models were created with oceanic crust underlying the Salton Trough to test whether oceanic crustal densities and thickness would be in agreement with gravity data. Sedimentary layers were modeled with densities 2.4 kg/m^3 , 2.45 kg/m^3 and 2.5 kg/m^3 , the upper crustal layer was modeled with a density of 2.67 kg/m^3 on the west side of the peninsular range and 2.57 kg/m^3 on the east side across the compositional boundary. The middle crustal layer was modeled with a density of 2.8 kg/m^3 and 2.75 kg/m^3 and the lower crust density is $2.85 - 2.9 \text{ kg/m}^3$. Mantle density is 3.2 kg/m^3 , asthenosphere density is 3.16 kg/m^3 and ocean density is 2.45 kg/m^3 .

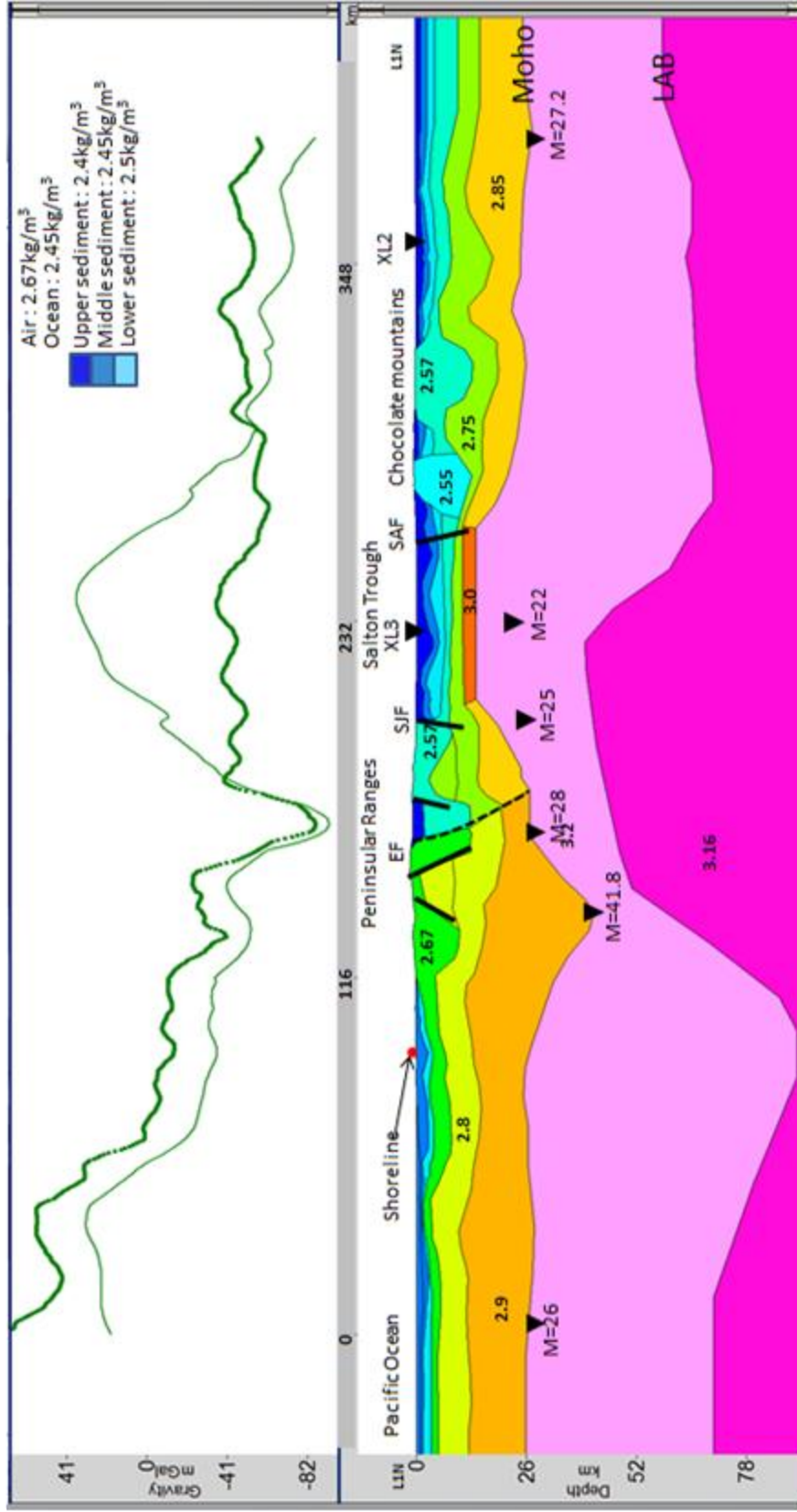


Figure 26: Profile line 1 model for oceanic crust. EF= Elsinore Fault, SJF= San Jacinto Fault, SAF= San Andreas Fault.

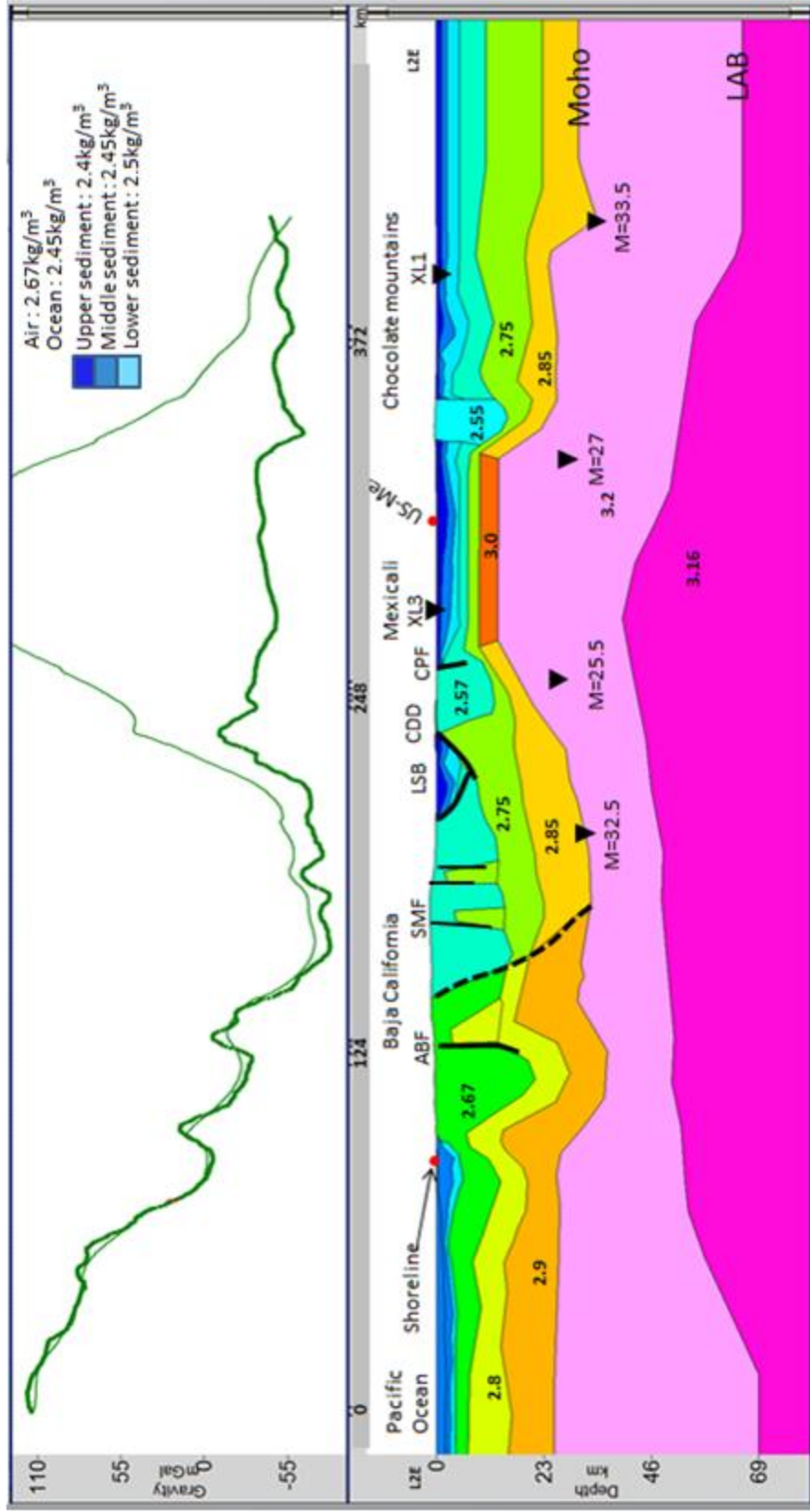


Figure 27: Profile line 2 model for oceanic crust. LSB=Laguna Salada Basin, CDD= Canada David Detachment, and CPF=Cerro Prieto Fault.

On Line 1 (Figure 26), beneath the Peninsular Ranges batholiths, the upper crust density changes from 2.67 kg/m^3 eastwards to 2.57 kg/m^3 . The middle crust density is 2.8 kg/m^3 on the western part and 2.75 kg/m^3 on the eastern part and the lower crust density is $2.85 - 2.9 \text{ kg/m}^3$. Beneath the topographically high Peninsular Range, the crust thins and the Moho shallows eastward across the main gulf escarpment. The lower crustal layer under the Salton Sea and Imperial Valley in the model is intruded and replaced by material of higher density (3.0 kg/m^3). East of the Salton Trough, the granitic basement extends to a depth of 16 km, the middle crust extends to 20 km depth, and the lower crust to 26 km which represents the Moho depth at this location.

On Line 2, (Figure 27), the crustal densities change laterally in the Baja California area from 2.67 kg/m^3 to 2.57 kg/m^3 from west to east. Sediment thickness increases eastwards and the basement layer thins out eastwards beneath the Laguna Salada Basin. Under the Mexicali Valley the crust is modeled again to test for oceanic crust by raising the Moho and replacing the lower crust layer with igneous material of density 3.0 kg/m^3 .

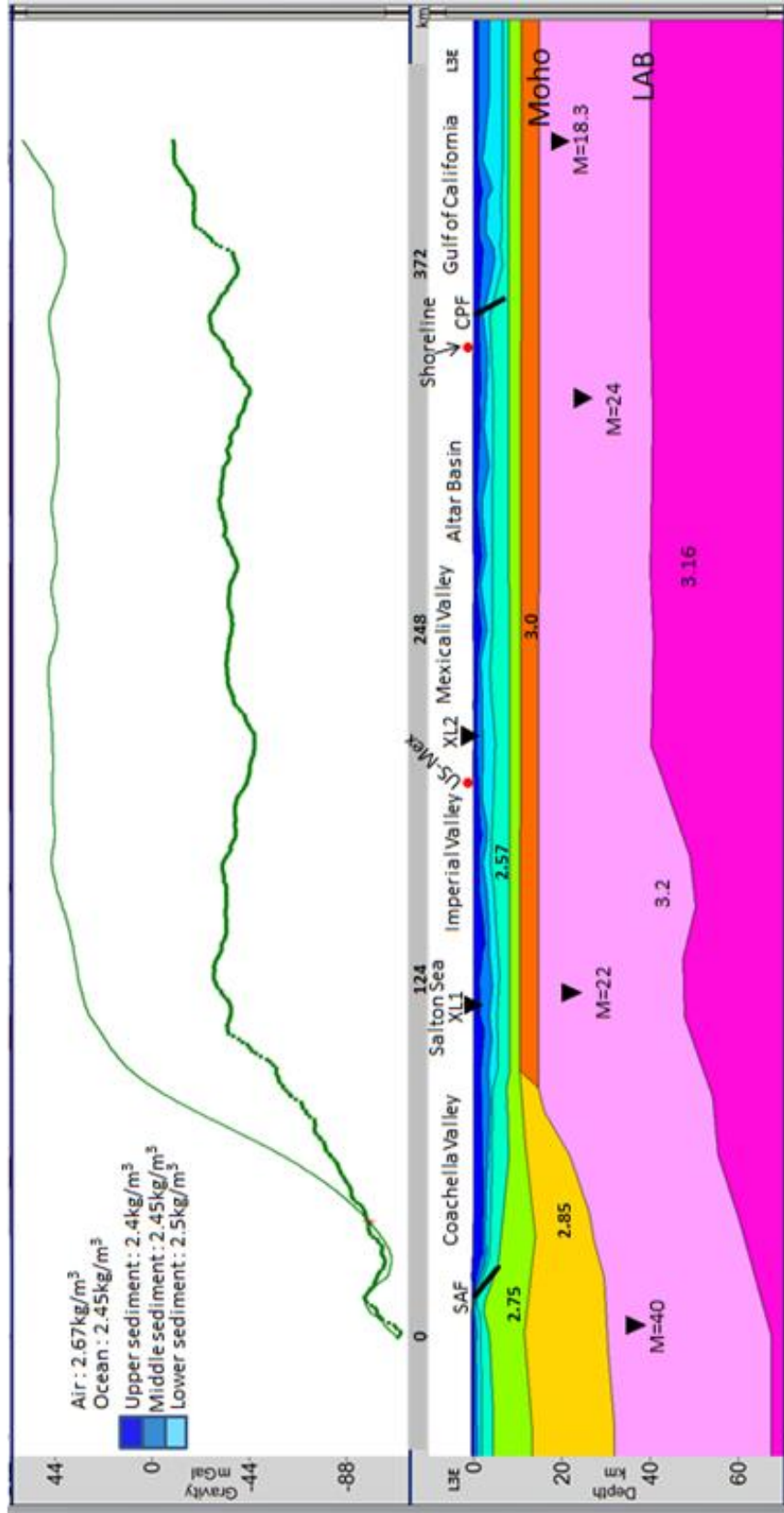


Figure 28: Profile line 3 model for oceanic crust. US-Mex indicates the U.S.A.-Mexico international border.

On line 3 (Figure 28), which runs along the axis of the trough, the lower crust is modeled to be replaced by basaltic material with density 3.0 kg/m^3 and the Moho is raised to a shallow depth along the entire length of the profile from the Salton Sea to the Gulf of California.

The test for oceanic crust involves thinning of the crystalline crustal layers to a thickness of $6.8 \pm 2 \text{ km}$; this requires the Moho layer beneath the Salton Trough to be raised to a shallow depth in conflict with that specified by our refraction control data. The resulting 2-D models do not make a match for the calculated and observed gravity anomaly curves. The oceanic crust scenario was further tested by raising the asthenosphere to a shallow depth (Figures 29, 30 & 31). The implications and results were the same.

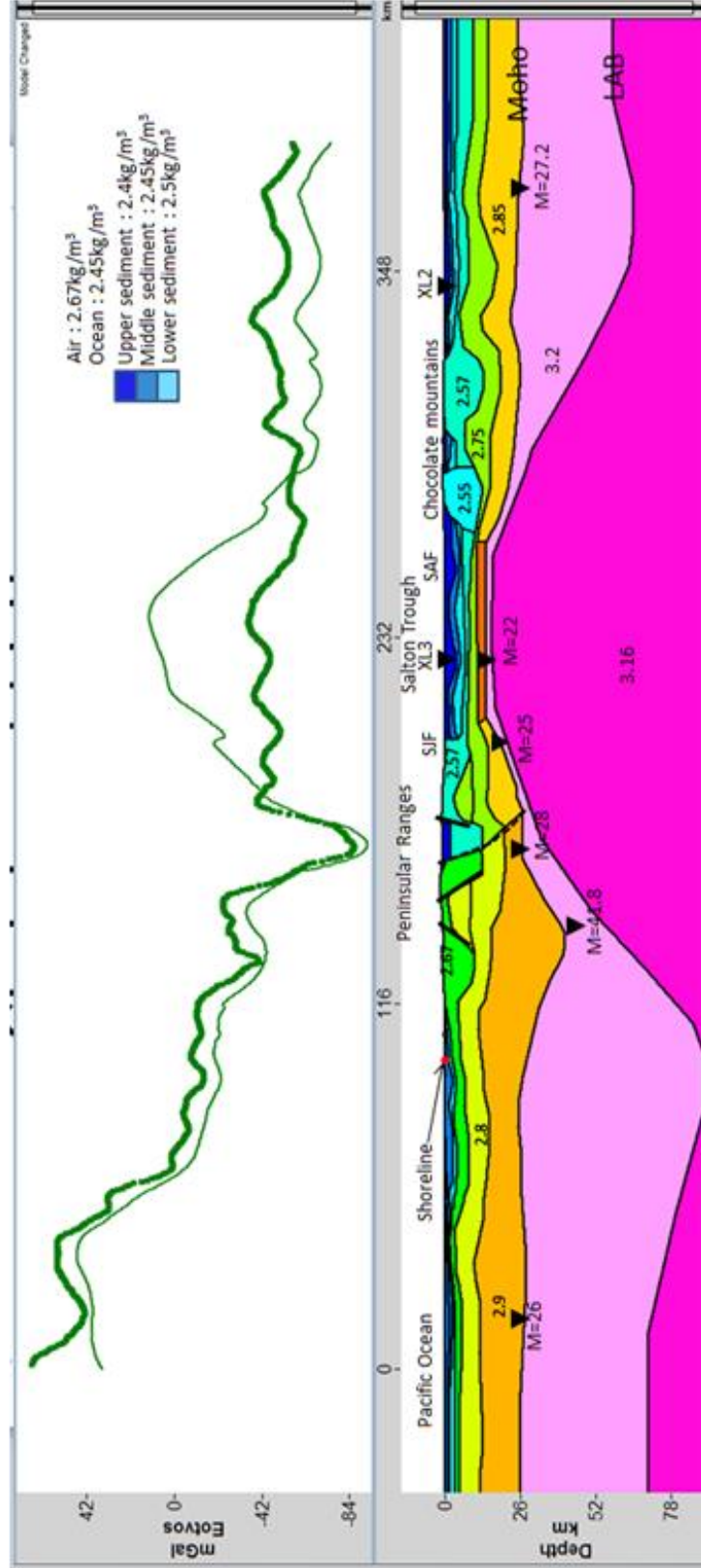


Figure 29: Shallow Asthenosphere test for line 1.

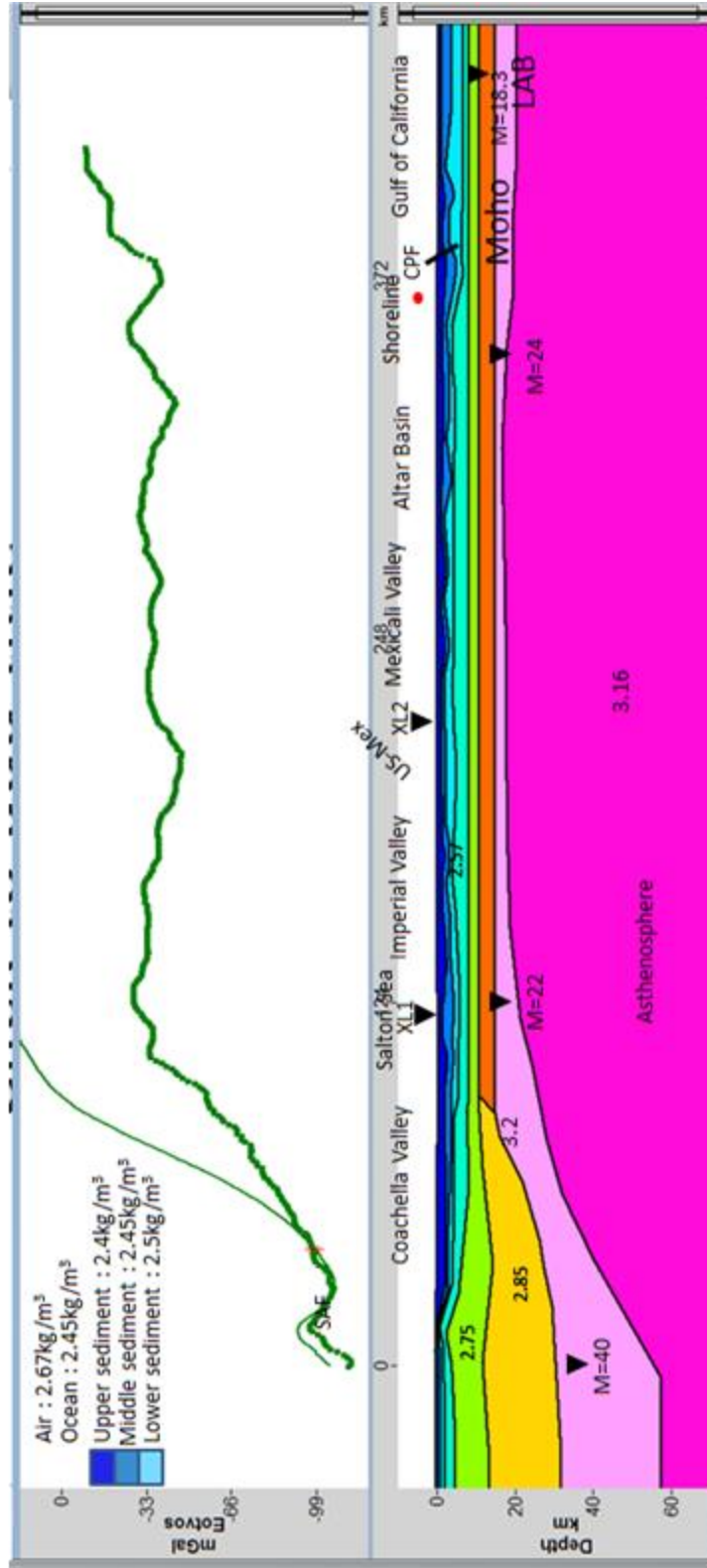


Figure 31: Shallow Asthenosphere test for line 3.

Continental Crust

In the models where the crust was assumed to be of continental composition, sedimentary layers were modeled with the same densities as in the oceanic models: 2.4 kg/m³, 2.45 kg/m³ and 2.5 kg/m³ respectively. The upper crustal layer was modeled with a density of 2.67 kg/m³ on the west side of the Peninsular Range and 2.57 kg/m³ on the east side across the compositional boundary. The middle crustal layer was modeled with a density of 2.75 kg/m³ - 2.8 kg/m³ and 2.85 – 2.9 kg/m³ was chosen for the lower crust. Mantle density is 3.2 kg/m³, asthenosphere density is 3.16 kg/m³ and ocean density remains 2.45kg/m³. Being a purely continental crust model, there are no intrusions included in the models and total crustal thickness is constrained by depth to the Moho.

Under the Peninsular Range batholith, Line 1 (Figure 32), the upper crust changes from 2.67 kg/m³ eastwards to 2.57 kg/m³. East of the Peninsular Range, all 3 crustal layers are thinner from their western thickness. Beneath the Salton Trough, the basement layer below the sediment package is about 2 km, the middle crust is about 3 km thick and the lower crust is 11 km thick. The Moho depth remains constant at 22 km as in previous models.

On line 2, (Figure 33), the crustal densities change laterally in the Baja California area from 2.67 kg/m³ to 2.57 kg/m³ from west to east, similar to the Peninsular Range in the north. The basement layer beneath the Mexicali Valley is extremely thinned to about 5 km. The middle crustal layer is 5.5 km thick and the lower crust thickness is about 12 km.

In Line 3 (Figure 34), the basement layer under the Salton Trough is about 4 km thick, the middle crustal layer is about 5 km thick and the lower crust is about 11 km thick. In the Mexicali Valley region, the basement thickens to 3 km, the middle crust is 4 km thick and the lower crust is 13 km thick. In the Wagner Basin, the basement layer, middle and lower crust all have approximately the same thickness of 4 km in the model.

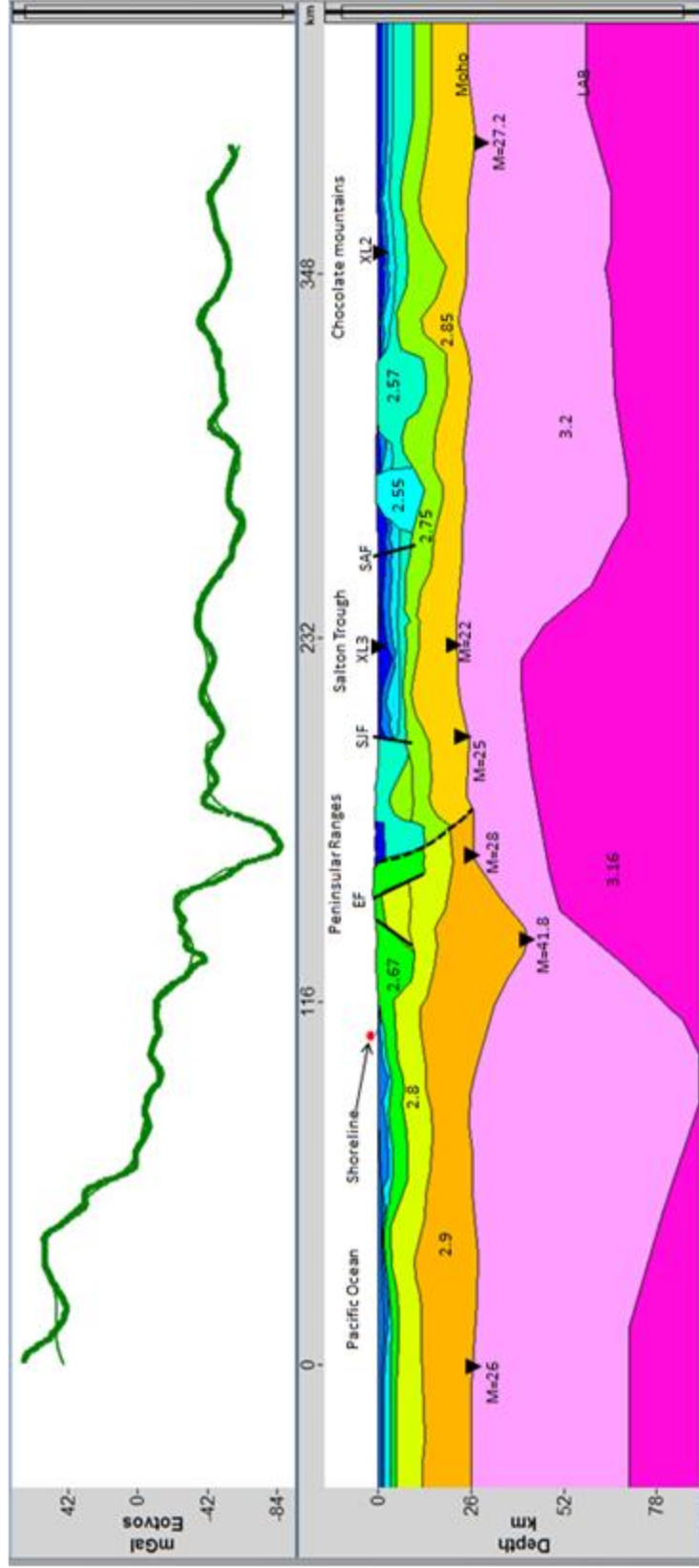


Figure 32: Profile line 1 model for continental crust. Abbreviations: EF= Elsinore Fault, SJF= San Jacinto Fault, SAF=San Andreas Fault, XL3 = Tie point with line 3, XL2 = Tie point with line 2.

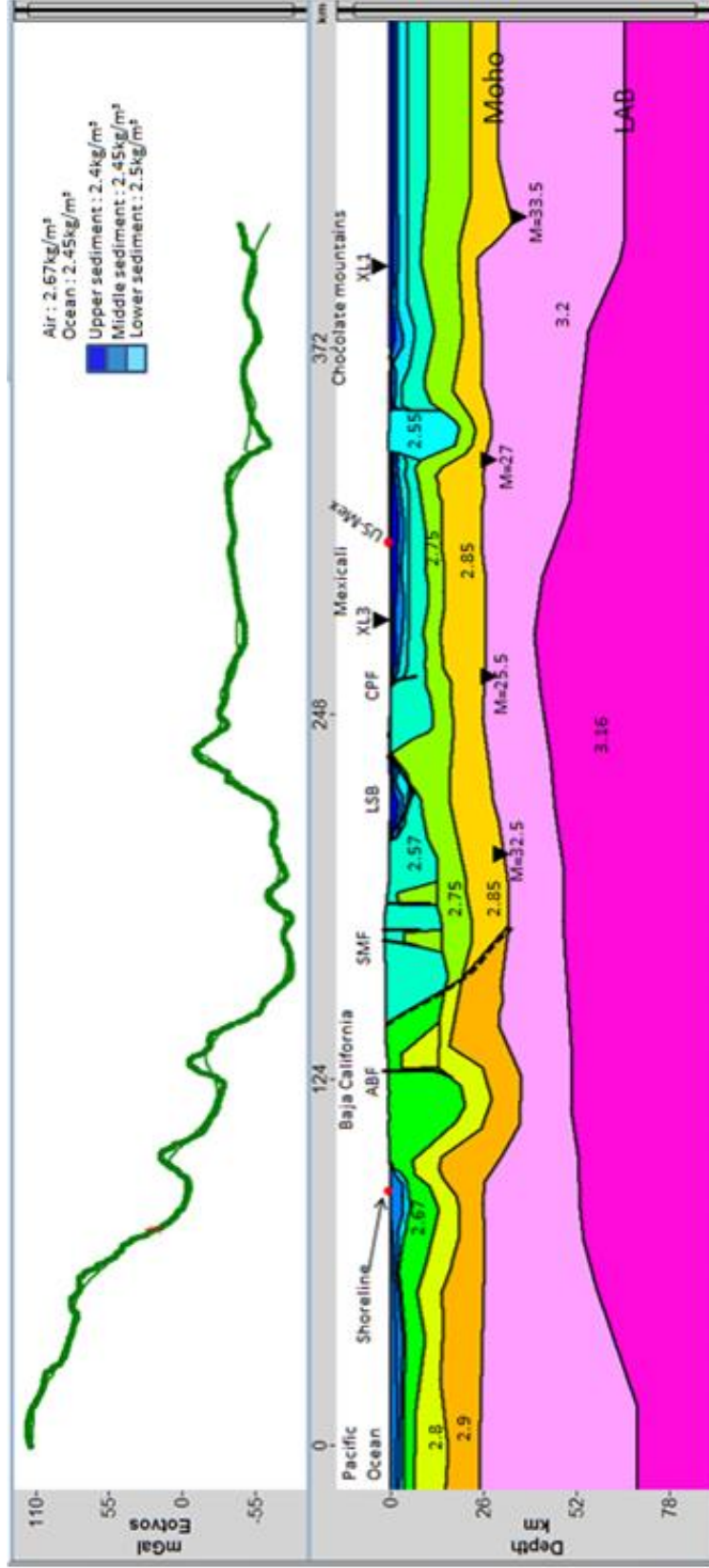


Figure 33: Profile line 2 model for continental crust. Abbreviations: LSB=Laguna Salada Basin, CDD= Canada David Detachment, and CPF=Cerro Prieto Fault, XL1= Tie point with line 1, XL3 = Tie point with line 3.

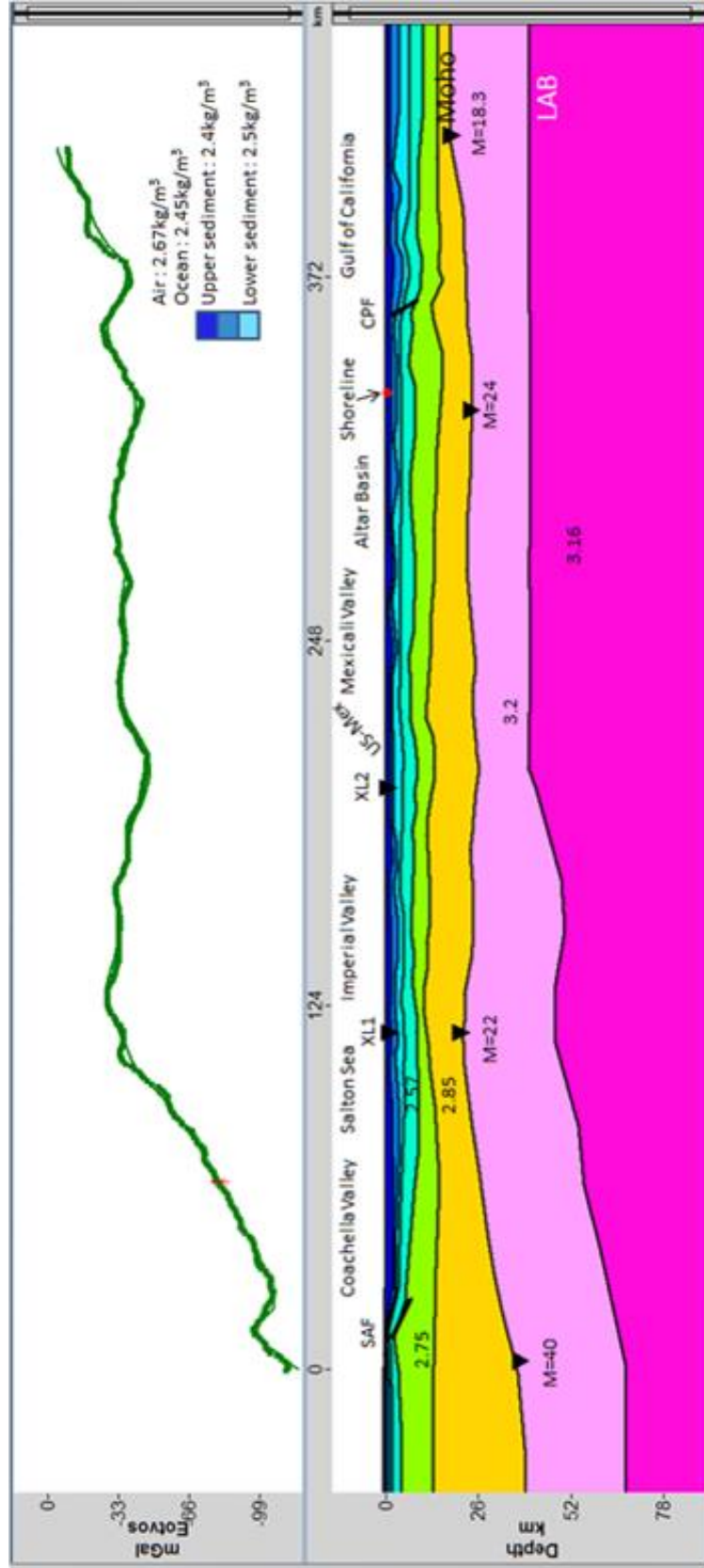


Figure 34: Profile line 3 model for continental crust. US-Mex is U.S.A.-Mexico international border, XL1 = Tie point with line 1 and XL2 = Tie point with line 2.

Intruded Continental Crust

In the models where the crust was assumed to be transitional in nature, the same density values were used to model the sedimentary layers 2.4 kg/m^3 , 2.45 kg/m^3 , and 2.5 kg/m^3 . The upper crustal layer was modeled with densities of 2.67 kg/m^3 and 2.57 kg/m^3 . The density changes laterally from west to east and reflects the change in composition across the Peninsular batholiths Range and Baja California. The middle crustal layer was modeled with a density of 2.8 kg/m^3 on the west and 2.75 kg/m^3 on the east side. The lower crust was modeled with a density of 2.9 kg/m^3 and 2.85 kg/m^3 . Basaltic intrusions were modeled with a density of 3.0 kg/m^3 the mantle density is 3.2 kg/m^3 , asthenosphere density is 3.16 kg/m^3 and ocean density remains 2.45 kg/m^3 .

On line 1 (Figure 35), The Peninsular Range batholith was modeled to contain magmatic dykes of different sizes and the upper crustal layer extends to 8-12 km beneath the Salton Trough with the middle and lower crustal layers being intruded by material of higher density (3.0 kg/m^3). East of the Salton Trough, the Orocochia Schist metamorphic block is modeled with a density of 2.55 kg/m^3 and further east at the end of the profile line, the lower crust is as deep as 26 km which represents the Moho depth at this location.

On line 2 (Figure 36), the crustal densities change laterally in the Baja California area from 2.67 kg/m^3 to 2.57 kg/m^3 from west to east and plutonic rocks of density 2.67 kg/m^3 are modeled to intrude the upper crust under the Sierra Juárez. In the Laguna Salada Basin, sediment thickness increases eastwards and the basement layer thins out at the same location where the middle crust layer lies directly beneath the sedimentary

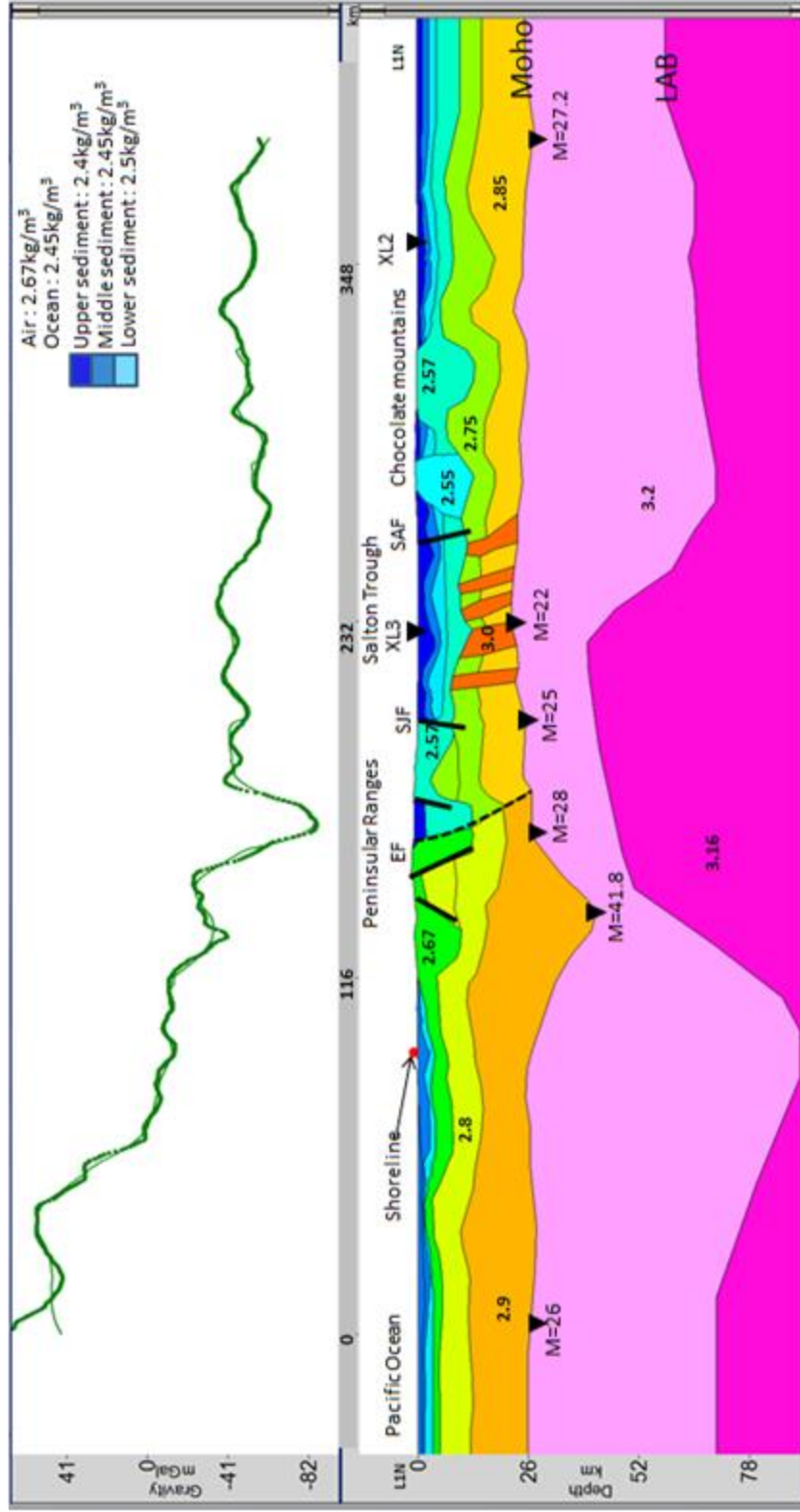


Figure 35: Profile line 1 model for transitional crust. Abbreviations: EF=Elsinore Fault, SJF= San Jacinto Fault, SAF=San Andreas Fault

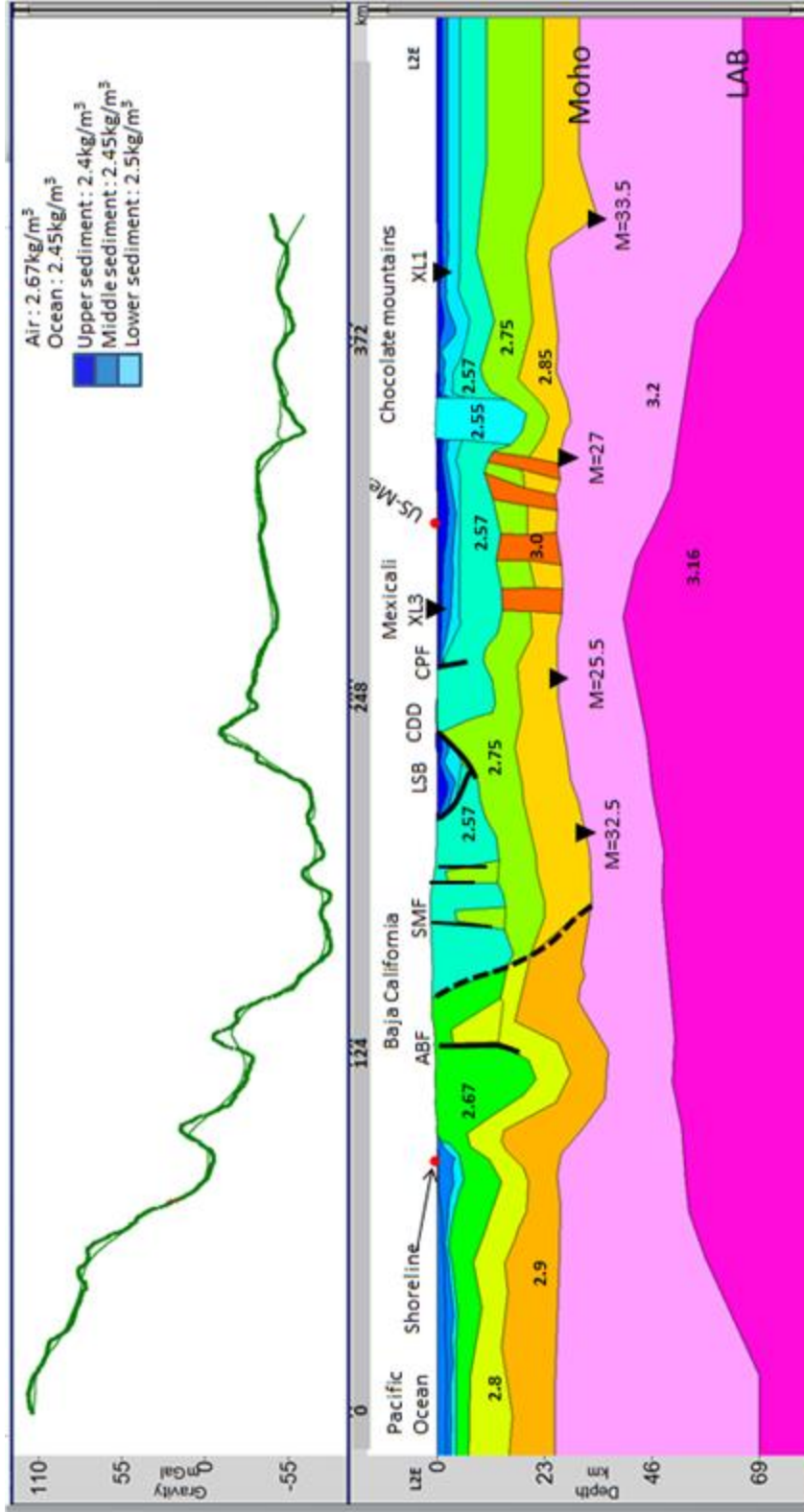


Figure 36: Profile line 2 model for transitional crust. Abbreviations: LSB=Laguna Salada Basin, CDD=Canada David Detachment, CPF=Cerro Prieto Fault.

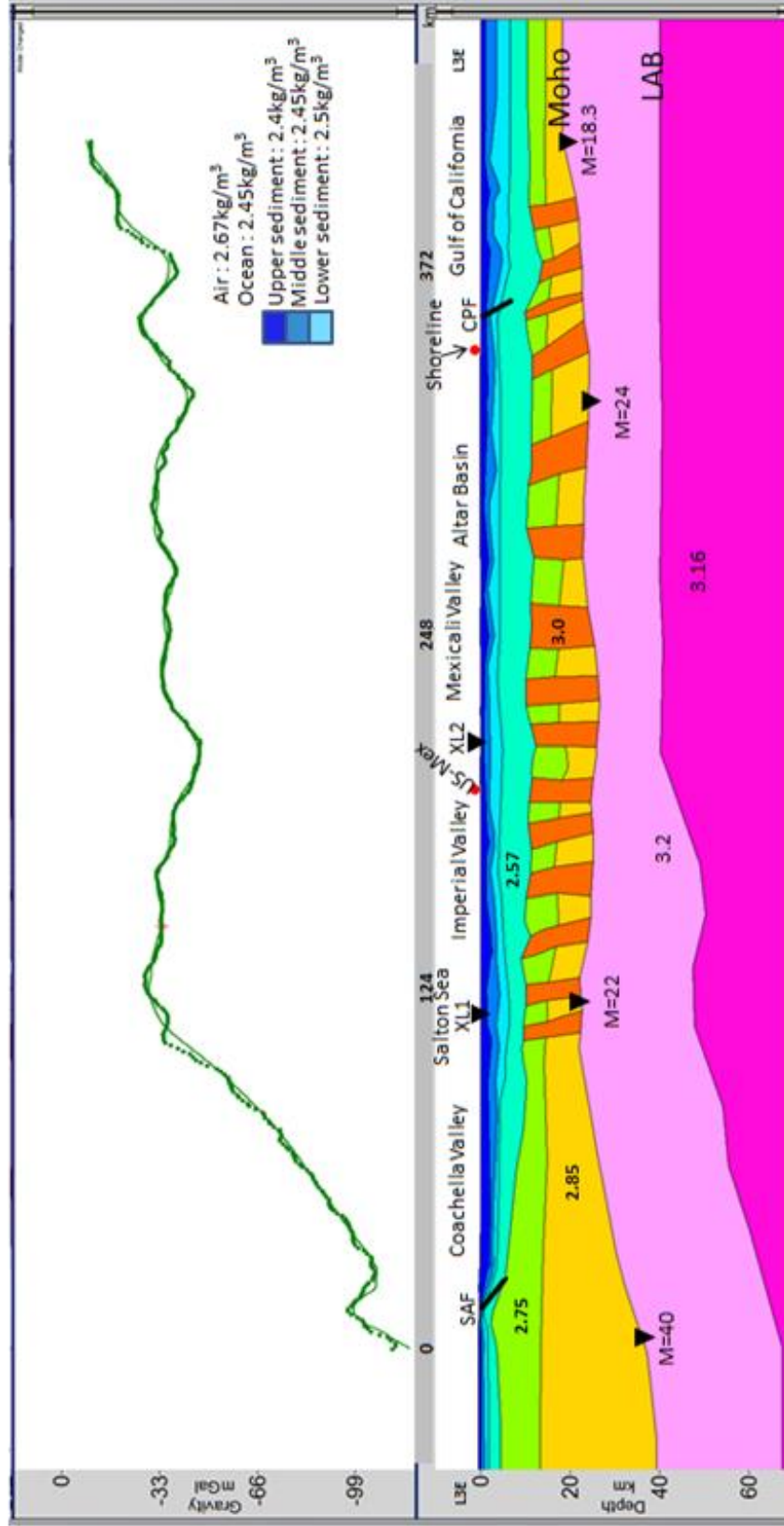


Figure 37: Profile line 3 model for transitional crust.

layer in the Sierra Cucapá region. Under the Mexicali Valley the lower crust is modeled to contain igneous material of density 3.0 kg/m^3 .

On line 3 (Figure 37), there is no west to east variation in density within the layers as the line runs east of the coastal ranges from north to south. The base of the upper crust is about 3 km in the northern tip of the profile, middle crust extends to 13 km and the Moho is at 40 km. The lower and middle crust beneath the Salton Trough and the lower crust in the Mexicali Valley are intruded.

The magmatic material that has intruded the crust beneath the Trough in my models suggests that decompressional melting has occurred in upwelling asthenosphere below the Trough. The magnetic anomaly in the southeastern border of the Salton Sea is positive and spatially correlates with the five volcanic buttes on the southeastern shore of the Salton Sea, reflecting the highly magnetic sills and dykes associated with these volcanoes.

CHAPTER 6: NATURE OF THE CRUST BENEATH THE SALTON TROUGH

Different models for different crustal types (oceanic, continental, and intruded continental) were tested to determine the nature of the crust beneath the Salton Trough region. The gravity anomalies predicted by the oceanic crust models did not fit observed gravity anomalies, while continental crust and intruded continental crust models produced gravity anomalies that closely matched the gravity data.

Earlier gravity modeling studies (Fuis et al. (1984) and Hussein (2007)) only considered oceanic (gabbroic) crust, but this study shows that the gravity anomalies in the region can be explained by a Salton Trough crust that has not developed into an oceanic spreading center. Since the gravity data do not discriminate between the crustal types, other geological data is considered to determine the crustal type below the Trough.

Pull-apart basins go through an evolutionary process with stages (Figure 5) that can be correlated to those in the evolution of continental rifts as they evolve from a stage of lithospheric extension and thinning to when they form incipient ocean basins (Figure 10). The earlier evolutionary stages of pull-apart basin formation (stages 1 and 2, Figure 5) correspond to the immature continental rifting stages (stage 1, Figure 10) where the crust has experienced limited stretching and is still continental crust. The next stage in pull-apart basin formation (stage 3, lazy S or Z, Figure 5) and stage 2 in Figure 10 represents an intermediate stage of crustal extension and stretching; the crust at this stage is still continental crust, with some magmatic activity. For a pull-apart basin in stage 4 (rhomboidal, or stretched rhomboidal, Figure 5) or stage 3 (Figure 10), extension and

stretching is severe and the crust is extremely thinned and weakened. Upwelling of hot asthenosphere results in decompression melting and increased magmatic activity. The crust is heavily intruded, and there is a mixture of igneous intrusions and upper crustal material. The crust at this point is significantly different from oceanic and continental types, and may be called transitional. Such transitional crust has been found for example in the Afar region (Ebinger et al., 2013). Stage 5 (Figure 5) and stage 4 (Figure 10) represent the continental rupture phase. Here, the rifts have evolved into spreading centers and new oceanic crust is being formed with the opening of a new ocean basin.

According to Oskin et al. (2001), the Gulf of California ruptured around 2 to 6.3 Ma and the northern Gulf has opened about 255 ± 10 km since then (Oskin et al., 2001). If the Salton Trough lithosphere which is about 40 km thick represents newly formed oceanic lithosphere and this lithospheric thickness occurs across an area about 150 km wide (Lekic, 2011), then the amount of extension along the current northwest axis of extension (Brothers et al., 2009) is 150 km. This distance does not correspond to the offset amount of 255 ± 10 km evaluated by Oskin et al. (2001) from correlation of late Miocene volcanoclastic strata across the northern Gulf of California. This also suggests that the Salton Trough crust is not actively spreading oceanic crust.

In the Salton Trough, the presence of 5 - 6 km of sediments overlying a basement layer of intermediate compressional wavespeed (v_p) (Fuis et al., 1984) and a deeper layer with higher compressional wavespeed points to a scenario of pre-rift crust replacement by magmatic addition and sediment metamorphism (Fuis et al., 1984; Parsons and McCarthy, 1996). This interpretation is supported by volcanic eruptions in the southern part of the Salton Sea which provides further evidence of magmatic activity. The Salton Trough

region thus is in a mature rifting stage, which suggests that its crust is not normal, thinned continental crust. Although Brothers et al. (2009) suggested that the Salton Trough is an immature rift, its elongate shape lends more credence to the possibility that the Trough is in level 4 (Figure 5) of pull-apart basin formation, or stage 3 (Figure 10), the mature rift stage, which is characterized by extreme crustal thinning and heavy igneous intrusions.

CHAPTER 7: CONCLUSIONS

The Salton Trough is the northward, onshore extension of the Gulf of California. In the southern Gulf of California, there is evidence that the crust has gone from a stage of thinning through initial rifting and finally attained complete rupture with the formation of short oceanic spreading ridges. It is unknown how far north in the Gulf Extensional Province seafloor spreading has progressed because of the thick sediment package covering the basins. Earlier studies have suggested that the Salton Trough crust may be oceanic in nature.

The crust below immature and intermediate age continental rift is thinned and may be the locus of some magmatic activity. In the oceanic spreading stage the continental crust has gone through the stage of thinning and attained eventual rupture and has thus been replaced by oceanic crust. Mature continental rifts that are close to continent rupture are characterized by continental crust which has been heavily intruded, with focused rifting, and basins that are filled with sediments from above and igneous intrusions from below.

In this study, gravity and magnetic modeling, constrained by additional geologic and geophysical datasets, revealed the crustal structure of the Salton Trough and surrounding areas. Three sets of models were tested, with continental, oceanic, and transitional crust underlying the Salton Trough. In the continental crust models, the lower crust underneath the basins is of continental crust density and there is an abrupt change from the lower crust to the mantle below. In the oceanic crust models, the lower crust

underneath the basins has been replaced by gabbroic material with higher density. In the transitional crust models, the lower crust underneath the basins is heavily intruded with basaltic igneous intrusions intermingling with lower continental crustal material.

The gravity anomaly curves for the oceanic crust test do not match for oceanic crust parameters underneath the Trough. The curves for continental crust models fit better with the curves fitting best for models of heavily intruded continental crust. Also, the presence of igneous activity in the Salton Trough, the elongated rhomboidal shape of the Trough, and its thick sediment package all point to a more advanced rifting stage. An active oceanic spreading center under the Salton Trough was excluded based on spatial considerations. The presence and combination of a thick sediment package and basaltic intrusions reveal a situation where the crustal layers are heavily intruded by igneous material.

References

- Aktar, M., Dorbath, C., and Arpat, E., 2004, The seismic velocity and fault structure of the Erzincan basin, Turkey, using local earthquake tomography, *Geophysical Journal International*, v. 156, p. 497-505.
- Albores, A., Reyes, A., Brune, J.N., Gonzalez, J., Garcilazo, F., and Suarez, F., 1980, Seismicity studies in the region of the Cerro Prieto geothermal field, *Geothermics*, v. 9, p. 65-77.
- Allen, P.A., and Allen, J.R., 2005, *Basin Analysis: Principles and Applications*, 2nd ed., Blackwell publishing, 549 pp.
- Allen, C.R., 1957, San Andreas Fault zone in San Geronio Pass, Southern California, *Geological Society of America Bulletin*, v. 68, p. 315-350.
- Atmaoui, N., Kukowski, N., Stöckhert, B., and König, D., 2006, Initiation and development of pull-apart basins with Riedel shear mechanism: insights from scaled clay experiments, *International Journal of Earth Sciences*, v. 25, p. 225-238
- Atwater, T.M., 1998, Plate Tectonic History of Southern California with emphasis on the Western Transverse Ranges and Santa Rosa Island, *American Association of Petroleum Geologists, Miscellaneous Publication 45*, p. 1-8.
- Axen, G.J., and Fletcher, J.M., 1998, Late Miocene-Pleistocene Extensional Faulting, Northern Gulf of California, Mexico and Salton Trough, California, *International Geology Review*, v. 40, p. 217-244.
- Aydin, A., and Nur, A., 1982, Evolution of pull-apart basins and their scale dependence, *Tectonics*, v. 1, no. 1, p. 91-105.
- Basile, C., and Brun, J.P., 1999, Transtensional faulting patterns ranging from pull-apart basins to transform continental margin: an experimental investigation, *Journal of Structural Geology*, v. 21, p. 23-37.
- Bates, R.L., and Jackson, J.A., 1987, 1980, *Glossary of Geology*, 2nd ed., American Geological Institute, Falls Church, 751 pp.
- Bilham, R., and King, G., 1989, The morphology of strike-slip faults : Examples from the San Andreas Fault, California, *Journal of Geophysical Research*, v. 94, no. B8, p. 204-216.
- Bischoff, J.L. and Henyey, T.L., 1974, Tectonic elements of the central part of the Gulf of California. *Geological Society of America Bulletin*, v. 85, p. 1893-1904.

Blakely, R.J., 1995, *Potential Theory in Gravity and Magnetic Applications*. Cambridge University Press, 441 pp.

Blakely, R.J., Jachens, R.C., Calzia, J.P., and Langenheim, V.E, 1999, Cenozoic basins of the Death Valley extended terrane as reflected in regional-scale gravity anomalies, *Geological Society of America Special Paper 333*, p. 1-16.

Bohannon, R. G., and Howell, D. G., 1982, Kinematic evolution of the junction of the San Andreas, Garlock, and Big Pine faults, California, *Geology*, v. 10, p. 358- 363.

Bott, M.H. P., 1995, Continental rifts: Evolution, structure, tectonics, *Developments in Geotectonics*, v. 25, no. 264, p.27-43.

Bowin, C.O., 1968, Geophysical study of the Cayman Trough, *Journal of Geophysical Research*, v. 73, no. 16, p. 5159-5173.

Brew, G., Lupa, J., Barazangi, M., Sawaf, T., Al-Imam., A., and Zaza, T., 2001, Structure and tectonic development of the Ghab Basin and the Dead Sea fault system, Syria. *Journal of the Geological Society of London*, v. 158, p. 665-674.

Brown, R.D., jr., 1990, Quarternary deformation. In: Wallace, R. E., (editor), *The San Andreas Fault System, California : US Geological Survey Professional paper 1515*, p. 82-113.

Brothers, D. S., Driscoll, N.W., Kent, G.M., Harding, A.J., Babcock, J.M., and Baskin, R.L., 2009, Tectonic evolution of the Salton Sea inferred from seismic reflection data. *Nature Geoscience*, v. 2, 581-584.

Buck, R.W., 1991, Modes of continental lithospheric extension, *Journal of Geophysical Research*, v. 96, no. B1, P. 161-178.

Burke, K.C.A. and Dewey, J.F., 1973, An outline of Precambrian plate development. In : D.H. Tarling and S.K. Runcorn (editors), *Implications of Continental Drift to the Earth Sciences*, Academic Press, London, v. 2, p.1035-1045.

Chávez, R.E., Lazaro-Mancilla, O., Campos-Enríquez, J.O., and Flores-Márquez, E.L., 1999, Basement topography of the Mexicali Valley from spectral and ideal body analysis of gravity data, *Journal of South American Earth Sciences*, v. 12, 579-587.

Christie-Blick, N., and Biddle, K.T., 1985, Deformation and basin formation along strike-slip faults. In: Biddle K.T. AND Christie-Blick, N., (editors), *Strike-Slip Deformation, Basin Formation, and Sedimentation*, SEPM Special Publication, v. 37, p. 1-34.

- Clayton, L., 1966, Tectonic depressions along the Hope Fault, a transcurrent fault in north Canterbury, New Zealand, *New Zealand Journal of Geology and Geophysics*, v. 9 , p. 95-104.
- Cochran, J.R., 1983, A model for the development of the Red Sea, *American Association of Petroleum Geologists Bulletin*, v.67, p. 41-69.
- Cowan, H.A., 1990, Late Quaternary displacements on the Hope Fault at Glynn Wye, North Canterbury, *New Zealand Journal of Geology and Geophysics*, v. 33, p. 285-293.
- Crowell, J. C., 1974, Origin of Late Cenozoic basins in southern California, In: Dickinson, W.R (editor) *Tectonics and Sedimentation*, SEPM Special Publication 22, p. 190-204.
- Crowell, J.C., 1974, Sedimentation along the San Andreas Fault, California. In: Dott, R.H. Jr. and Shaver, R.J., (editors), *Modern and Ancient Geosynclinal Sedimentation*, SEPM Special Publication 19, p. 292-303.
- Curry, J.R., 2005, Tectonics and history of the Andaman Sea region, *Journal of Asian Earth Sciences*, v. 25, p. 187-232.
- Cunningham, W.D., and Mann, P., 2007, Tectonics of strike-slip restraining and releasing bends. In: Cunningham, W.D. and Mann, P. (editors), *Tectonics of Strike-Slip Restraining and Releasing Bends*, Geological Society, London, Special Publication, 290, p. 1-12.
- Davis, G.H., Bump, A.P., García, P. E., and Ahlgren, S.G., 2000, Conjugate Riedel deformation band shear zones, *Journal of Structural Geology*, v. 22, 169-190.
- Dickinson, W.R., 1974, *Plate Tectonics and Sedimentation*, SEPM Special Publication 19, p. 1-27.
- Dooley, T., and McClay, K., 1997, Analog Modeling of Pull-Apart Basins, *American Association of Petroleum Geologists Bulletin*, v. 81, no. 11, p. 1804-1826.
- Dorsey, R.J., 2010, Sedimentation and crustal recycling along an active oblique-rift margin: Salton Trough and northern Gulf of California, *Geological Society of America*, v. 38, no. 5, p. 443-446.
- Dorsey, R. J., 2006. Stratigraphy tectonics, and basin evolution in the Anza-Borrego Desert Region. In: Jefferson, G.T., and Lindsay, L.E., (editors) *Fossil Treasures of Anza-Borrego Desert*, Sunbelt Publications, San Diego, CA, p. 89-104.

- Dorsey, R., and Martín-Barajas, A., 1999, Sedimentation and deformation in a Pliocene-Pleistocene transtensional supradetachment basin, Laguna Salada, northwest Mexico, *Basin Research*, v. 11, p. 205-221.
- Dorsey, R.J., and Uhmoefter, P.J., 2011, Influence of sediment input and plate motion obliquity on basin development along an active oblique-divergent plate boundary: Gulf of California and Salton Trough, In: Busby, C., and Azor A., *Tectonics of Sedimentary Basins: Recent Advances*, Blackwell publishing, 664 pp.
- Ebinger, C., van Wijk, J., and Keir, D., 2013, The time scales of continental rifting: implications for global processes. In: Bickford, M., (editor) *Geological Society of America Special Paper 500*, p. 1–26.
- Einsele, G., 2000, *Sedimentary Basins: Evolution, Facies and Sediment Budget*, Springer, Berlin. p. 630-643.
- Elders, W.A., Rex, R.W., Meidav, T., Robinson, P., and Biehler, S., 1972, Crustal spreading in southern California, *Science*, v. 178, pp. 15-24.
- Elders, W.A., and Sass, J.H., 1988, The Salton Sea scientific drilling project, *Journal of Geophysical Research*, v.93, p. 953-968.
- Embley, R.W., and Wilson, D.S., 1992, Morphology of the Blanco transform fault zone – NE Pacific: Implications for its tectonic evolution, *Marine Geophysical Research*, v. 14, p. 25-45.
- Fletcher, J.M., and Spelz, R.M., 2009, Patterns of Quaternary deformation and rupture propagation associated with an active low-angle normal fault, Laguna Salada, Mexico : Evidence of a rolling hinge ? , *Geological Society of America Bulletin*, v. 5, no. 4, p. 385-407.
- Fletcher, J. M., Grove, M., Kimbrough, D. L., Lovera, O., and Gehrels, G. E., 2007, Ridge-trench interactions and the Neogene tectonic evolution of the Magdalena Shelf and southern Gulf of California: Insights from detrital zircon U-Pb Ages from the Magdalena Fan and adjacent areas, *Geological Society of America Bulletin*, v. 119, no. 11-12, p. 1313-1336.
- Frez, J., and González, J.J., 1991, Crustal structure and seismotectonics of northern Baja California. In: Dauphin J. P. and Simoneit B.R.T. (editors) *The Gulf and Peninsular Province of the Californias*, American Association of Petroleum Geologists, Memoir 47, p. 261-283.
- Freund, R., 1971, The Hope Fault, a strike-slip fault in New Zealand, *New Zealand Geological Survey Bulletin*, v. 86, p. 1-49.

- Fuis, G.S, Mooney, W.D, Healy, J.H, McMechan, G.A, and Lutter, W.J, 1984, A seismic refraction survey of the Imperial Valley Region, California. *Journal of Geophysical Research*, v. 89, p. 1165-1189.
- Fuis, G.S., and Kohler, W.M., 1984, Crustal structure and tectonics of the Imperial Valley region, California, *The Imperial Basin Tectonics, Sedimentation and Thermal Aspects*, Pacific section SEPM., p. 1-13.
- García-Abdeslem, J., Espinosa-Cardena, J.M., Munguía-Orzoco, L., Wong-Ortega, V.M., and Ramírez-Hernández, J., 2001, Crustal structure from 2-D gravity and magnetic data modeling, magnetic power spectrum inversion, and seismotectonics in the Laguna Salada basin, northern Baja California, Mexico, *Geofisica Internacional*, v. 40, no. 2, p. 67-85.
- Garfunkel, Z, 1981, Internal structure of the Dead Sea leaky transform in relation to plate kinematics, *Tectonophysics*, v.80, p. 81-108.
- Garfunkel, Z., and Ben-Avraham, Z., 1996, The structure of the Dead Sea basin, *Tectonophysics*, v. 266, p. 155-176.
- Glowacka, E., Gonzalez, J., Fabriol, H., 1999, Recent vertical deformation in Mexicali Valley and its relationship with tectonics, seismicity, and the exploitation of the Cerro Prieto geothermal field, Mexico, *Pure and Applied Geophysics*, v. 156, p. 591-614.
- Goldstein, N.E., Wilt, M.J., and Corrigan, D.J., 1984, Analysis of the Nuevo León magnetic anomaly and its possible relation to the Cerro Prieto magmatic-hydrothermal system: *Geothermics*, v. 13, p. 3-11.
- González-Escobar, M., Aguilar-Campos, C., Suárez-Vidal, F., and Martín-Barajas, A., 2009, Geometry of the Wagner Basin, upper Gulf of California based on seismic reflections, *International Geology Review*, 51. No.12, p. 133-144.
- González-Escobar, M., Pérez-Tinajero, C.I., Suarez-Vidal, F. , and González- Fernández, A., 2013, Structural characteristics of the Altar Basin, Northwest Sonora, Mexico, 2013; *International Geology Review*, v. 55, no. 3, p. 322-336.
- Gürbüz A., 2010, Geometric characteristics of pull-apart basins, *Lithosphere*, v.2, p. 199–206.
- Gürbüz, A., and Gürer, O.F., 2008, Middle Pleistocene extinction process of pull-apart basins along the North Anatolian Fault zone. *Physics of the Earth and Planetary Interiors*, v. 173, p. 177-180.
- Hamilton, R.M., 1970, Time-term analysis of explosion data from the vicinity of the Borrego Mountain, California earthquake of 9 April 1968, *Seismological Society of America Bulletin*, v. 60, no. 2, p. 367-381.

- Hearn, T.M., 1984, Pn travel times in southern California, *Journal of Geophysical Research*, v. 89, no. B3, p. 1843-1855.
- Helgeson, H.C., 1968, Geologic and thermodynamic characteristics of the Salton Sea geothermal system. *American Journal of Science*, v. 266, p. 129-166.
- Hempton, M., and Dunne, L., 1984, Sedimentation in pull-apart basins: active examples in Turkey, *Journal of Geology*, v. 92, p. 513-530.
- Henry, T.L., and Bischoff, J.L., 1973, Tectonic elements of the northern part of the Gulf of California, *Geological Society of America Bulletin*, v. 84, p. 315-330.
- Herzig, C.T., and Jacobs, D.C., 1994, Cenozoic volcanism and two-stage extension in the Salton Trough, southern California and northern Baja California, *Geology*, v. 22, p. 991-994.
- Hill, M.L., and Troxel, B.W., 1966, Tectonics of Death Valley region, California: *Geological Society of America Bulletin*, v.77, p. 435-438.
- Holcombe, T.L., Vogt, P.R., Matthews, J.E., and Murchison, R.R., 1973, Evidence of sea-floor spreading in the Cayman Trough, *Earth and Planetary Science Letters*, v. 20, p. 357-371.
- Hull, A.G., and Nicholson, C., 1992, Seismotectonics of the northern Elsinore fault zone, southern California, *Seismological Society of America*, v.82, no. 2, p. 800-818.
- Hussein M.J, 2007, Integrated geophysical study of the crustal structure of the Salton Trough, PhD Dissertation, University of Texas at El Paso, El Paso, 90 pp.
- Hussein, M., Velasco, A., and Serpa, L., 2011, Crustal structure of the Salton Trough : Incorporation of receiver function, gravity and magnetic data, *International Journal of Geosciences*, v. 2, p. 502-512.
- Irwin, W.P., 1990, Geology and plate tectonic development. In: Wallace, R.E. (editor) *The San Andreas Fault System, California: U.S. Geological Survey Professional Paper 1515*, p.61-80.
- Johnson, C.E., and Hill, D.P., 1982, Seismicity of the Imperial Valley. In: *The Imperial Valley, California, earthquake of October, 15, 1979: US Geological Survey Professional Paper 1254*, p. 59-76.
- Johnson, C.E., and Hadley, D.M., 1976, Tectonic implications of the Brawley earthquake swarm, Imperial Valley, California, *Seismological Society of America*, v. 66, p. 1133-1144.

- Kayal, J.R., 2008, *Microearthquake seismology and seismotectonics of South Asia*, Springer Heidelberg, 503 pp.
- Keener, C., Serpa, L., and Pavlis, T.L., 1993, Faulting at Mormon Point, Death Valley, California: A low-angle normal fault cut by high-angle faults, *Geology*, v. 21, p. 327-330.
- Lachenbruch, A.H., Sass, J.H., and Galanis, S.P., 1985, Heat flow in southernmost California and the origin of the Salton Trough: *Journal of Geophysical Research*, v. 90, p. 6709-6736.
- Larsen, S., and Reilinger, R., 1991, Age constraints for the present fault configuration in the Imperial Valley, California: Evidence for northwest propagation of the Gulf of California rift system, *Journal of Geophysical Research*, v. 96, no. B6, p. 339-346.
- Lekic, V., French, S.W., and Fisher, K.M., 2011, Lithospheric thinning beneath rifted regions of southern California, *Science*, v. 334, p. 783-787.
- Leroy, S., Mauffret, A., Patriat, P., and Mercier de Lepinay, B., 2000, An alternative interpretation of the Cayman trough evolution from a reidentification of magnetic anomalies, *Geophysics Journal International*, v. 141, p.539–557.
- Lewis, J.L., Day, S.M., Magistrale, H., Astiz, C.L., Rebollar, C., Eakins, J., Vernon, F.L., and Brune, J.N., 2001, Crustal thickness of the peninsular ranges and gulf extensional province in the Californias, *Journal of Geophysical Research*, v. 106, no. B7, p. 599-611.
- Lizarralde, D., Axen, G.J., Brown, H.E., Fletcher, J.M., and González-Fernández, A., Harding, A.J., Holbrook, W.S., Kent, G.M., Paramo, P., Sutherland, F., and Umhoefer, P.J., 2007, Variations in styles of rifting in the Gulf of California: *Nature*, v. 448, p. 466–469.
- Lomnitz, C., F., Mooser, C. R., Allen, J. N., Brune, and Thatcher W., 1970, Seismicity and tectonics of the northern Gulf of California region, *Mexico Geophysical International*, v. 10, 37-48.
- Lowman, D.P., 1980, Vertical displacement on the Elsinore fault of southern California: Evidence from orbital photographs, *the Journal of Geology*, v. 88, no. 4, p. 415-432.
- Lowrie, W., 2007, *Fundamentals of Geophysics*, 2nd ed., Cambridge University Press, 415 pp.
- Mammerickx, J., and Klitgord, K.D., 1982, Northern East Pacific Rise: Evolution from 25 m.y. B.P. to the present, *Journal of Geophysical Research*, v. 87, no. B8, P. 6751-6759.

Mann , P., Hempton, P.R, Bradley, D.C., and Burke, K., 1983, Development of pull-apart basins, *Journal of Geology*, v. 91, p. 529-554.

McCarthy, J., Larkin, S.P., Fuis, G.S., Simpson, R.W., and Howard, K.A., 1991, Anatomy of a metamorphic core complex: Seismic refraction/wide-angle reflection profiling in southeastern California and western Arizona, *Journal of Geophysical Research*, v. 96, no. B7, p. 259-291.

McKenzie, 1978, Some remarks on the development of Sedimentary basins, *Earth and Planetary Science Letters*, v. 40, p25-32.

Menard, H.W., and Atwater, T.W., 1968, Changes in direction of sea floor spreading, *Nature*, v. 219, p. 463-467.

Menard, H.W., 1967, Transitional types of crust under small ocean basins, *Journal of geophysical research*, v. 72, no. 12, p.3061-3073.

Merriam, R., and Bandy, O.L., 1965, Source of upper Cenozoic sediments in the Colorado River delta region: *Journal of Sedimentary Petrology*, v. 35, p. 911-916.

Mickus, K. L, Backus and Gilbert., 1989, Inversion of two and one half dimensional gravity and magnetic anomalies and crustal studies in western Arizona and the eastern Mojave desert, California, Ph.D thesis. University of Texas at El Paso, 211 pp.

Miele, M.J., 1986, a magnetotelluric profiling and geophysical investigation of the Laguna Salada basin, Baja California, PhD thesis, San Diego University, 153 pp.

Morgan, P., and Baker, B.H., 1983, Processes of continental rifting, *Tectonophysics*, v. 94, p. 1-10.

Muffler L.J.P., and White, D.E., Active metamorphism of upper Cenozoic sediments in the Salton Sea geothermal field and the Salton Trough, Southeastern California, 1968; *Geological Society of America Bulletin*, v. 80 no. 2 , p. 157-182

Nava, F.A., and Brune, J.N., 1982, An earthquake-explosion reversed refraction line in the Peninsular Ranges of southern California and Baja California Norte, *Bulletin of Seismological Society of America*, v. 72, no. 4, p. 1195- 1206.

Nicholson, C., Sorlien, C.C, Atwater T, Crowell J.C, and Luyendyk, B.P, 1994, Microplate capture, rotation of the western transverse ranges, and initiation of the San Andreas transform as a low-angle fault system. *Geology*, v. 22, p. 491-495.

Olsen, K.H., 1982, The role of seismic refraction data for studies of the origin and evolution of continental rifts, *Tectonophysics*, v. 98, p. 349-370.

- Olsen, K.H., and Morgan, P., 1995, Continental rifts: Evolution, structure, tectonics, *Developments in Geotectonics*, v. 25, no. 264, p.3-26
- Oskin, M.E., and Stock, J.M., 2003, Pacific–North America plate motion and opening of the Upper Delfin basin, northern Gulf of California, Mexico, *Geological Society of America Bulletin*, v. 115, p. 1173–1190.
- Oskin, M., Stock, J., and Martín-Barajas, A., 2001, Rapid localization of Pacific-North America plate motion in the Gulf of California: *Geology*, v. 29, p. 459-462.
- Parons, T., and McCarthy, J., 1996, Crustal and upper mantle velocity structure of the Salton Trough, southeast California, *Tectonics*, v. 15, no. 2, p. 456-471.
- Pacheco-Romero, M.F., Martín-Barajas, A., Elders, W.A., Espinosa-Cardena, J.M., Helenes, J., and Segura, A., 2006, Stratigraphy and structure of the Altar basin of NW Sonora: Implications for the history of the Colorado River delta and the Salton Trough: *Revista Mexicana de Ciencias Geológicas*, v. 23, no. 1, p. 1-22.
- Persaud, P., Pérez-Campos, X., and Clayton, R.W., 2007, Crustal thickness variations in the margins of the Gulf of California, *International Journal of Geophysics*, v. 170, p. 687-699.
- Philips, R.P., 1964, Seismic refraction studies in the Gulf of California, in T.H van Andel and Shor Jr eds *Marine Geology of the Gulf of California*, American Association of Petroleum Geologists, Memoir. no. 3, p. 90.
- Pitman, W.C., and Andrews, J.A., 1985, Subsidence and thermal history of small pull-apart basins. In: Biddle, K.T., and Christie-Blick, N., (editors) *Strike-slip deformation, basin formation and sedimentation*, SEPM Special Publication 37, p. 45–49.
- Prieto, C., 1996, Gravity/Magnetic signatures of various geologic models – an exercise in pattern recognition. Integrated Geophysics Corporation – Footnotes on interpretation.
- Puente, C. I. and De la Pefia L. A., 1979, Geology of the Cerro Prieto geothermal field, *Geothermics*, v. 8, p. 155.
- Rahe, B., Ferrill, D.A., and Morris, A.P., 1998, Physical analog modeling of pull-apart basin evolution, *Tectonophysics*, v. 285, 21-40.
- Rezanov, I.A., 1983, Types of crust, *International Geology Review*, v. 25, no. 5, p. 609-616.
- Rudnick, R.L., and Gao, S., 2003, Composition of the continental crust. In : Rudnick, R.L.(editor) *The Crust Treatise on Geochemistry*, v. 3, Elseiver, Oxford, p. 1-70.

- Schubert, C., 1982, Origin of the Cariaco Basin, Southern Caribbean Sea, *Marine Geology*, v. 47, p. 345-360.
- Segall, P., and Pollard, D.D., 1980, Mechanics of discontinuous faults, *Journal of geophysical research*, v. 85, no. B8, p. 4337-4350.
- Sengör , A.M.C., Görür, N, and Şaroğlu, F., 1985, Strike-slip faulting and related basin formation in zones of tectonic escape: Turkey as a case study. In: Biddle, K., and Christie-Blick, N., (editors), *Strike-Slip Deformation, Basin Formation, and Sedimentation*, SEPM Special Publication 37, p. 227-264.
- Sharp, R.V., 1967, San Jacinto fault zone in the Peninsular Ranges of Southern California, *Geological Society of America Bulletin*, v. 78, p. 705-729.
- Shor, G.G. Jr., Raitt, R.W., and McGowan, D.D., 1976, Seismic refraction studies in the southern California borderland, 1949-1974, *Scripps Institute of Oceanography*, 70 pp.
- Siem, M.E., 1992, The structure and petrology of Sierra El Mayor, northeastern Baja California, Mexico, M. Sc. Thesis, San Diego University, 244 pp.
- Steinhart, J.S., and Meyer, R.P., 1961, Explosion studies of continental structure, *Carnegie Institute of Washington*, no. 622, p. 226-383.
- Sylvester, A.G., 1988, Strike-slip faults, *Geological Society of America Bulletin*, v. 100, p. 1666-1703.
- Sylvester, A.G., and Smith. R.R., 1976, Tectonic transpression and basement-controlled deformation in San Andreas Fault zone, salton trough, California. *American Association of Petroleum Geologists Bulletin*, v. 60, no. 12, p. 2081-2102.
- Tartar, O., Yurtmen, S., Temiz, H., Gürsoy, H., Kocbulut, F., Mesci, B.L., and Guezou, J.C., 2007, Intracontinental Quaternary volcanism in the Niksar pull-apart basin, North Anatolian Fault zone, Turkey, *Turkish Journal of Earth Sciences*, v. 16, pp. 417-440.
- Tchalenko, J.S., 1970, Similarities between shear zones of different magnitudes, *Geological Society of America Bulletin*, v. 81, p. 1625-1640.
- ten Brink, U.S., and Ben-Avraham, Z., 1989, The anatomy of pull-apart basins: seismic reflection observations of the Dead Sea Basin, *Tectonics*, v. 8, p. 333-350.
- ten Brink, U., Coleman, D.F., and Dillon, W.P., 2002, The nature of the crust under the Cayman Trough from gravity, *Marine and Petroleum geology*, v. 19, p. 971-987.
- Thompson, R.N., and Gibson, S.A., 1994, Magmatic expression of lithospheric thinning across continental rifts, *Tectonophysics*, v. 233, p. 41-68.

- Thomson, C.N., and Girty, G.H., 1994, Early Cretaceous intra-arc ductile strain in Triassic-Jurassic and Cretaceous continental margin arc rocks, Peninsular Ranges, California: *Tectonics*, v. 13, p. 1108-1119.
- Turcotte, D.L., and Emerman, S.H., 1983, Mechanisms of active and passive rifting, *Tectonophysics*, v. 94, p. 39 -50.
- Twiss, R.J., and Moores, E. M., 2007, *Structural Geology*, 2nd ed., W.H Freeman, New York, 736 pp.
- Umhoefer, P.J., Why did the Southern Gulf of California rupture so rapidly? - Oblique divergence across hot, weak lithosphere along a tectonically active margin. *Geological Society of America Today*, v. 21, no. 11, November 2011.
- Wallace R.E., 1990, General features. In: Wallace, R.E. (editor) *The San Andreas Fault System, California: U.S. Geological Survey Professional Paper 1515*, p.3-12.
- Whitmarsh, R.B., Manatschal, G., and Minshull, T.A., 2001, Evolution of magma-poor continental margins from rifting to seafloor spreading, *Nature*, v. 413, p.150-154.
- Whitmarsh, R.B., Pinheiro, L.M., Miles, P.R., Recq, M., and Sibuet, J.C., 1993, Thin crust at the western Iberia ocean-continent transition and ophiolites, *Tectonics*, v. 12, no. 5, p. 1230-1239.
- Winker, C.D., 1987, Neogene stratigraphy of the Fish Creek–Vallecito section, southern California: Implications for early history of the northern Gulf of California and the Colorado Delta, Ph.D. thesis, University of Arizona, Tucson, 494 pp.
- Wolfgang, J., and Smilde, P.L., 2009, *Gravity Interpretation: Fundamentals and Application of Gravity Inversion and Geological Interpretation*, Springer Berlin Heidelberg, 395 pp.
- Xie, X., and Heller, P.L., 2009, Plate tectonics and basin subsidence history, *Geological Society of America Bulletin*, v. 121, p. 55-64.
- Younker, L.W., Kasameyer, P.W., and Tewhey, J.D., 1982, Geological, geophysical, and thermal characteristics of the Salton Sea geothermal field, California, *Journal of Volcanology and Geothermal Research*, v.12, p. 221-258.
- Zhu, L., and Kanamori, H., 2000, Moho depth variation in southern California from teleseismic receiver functions, *Journal of Geophysical Research*, v. 105, no. B2, p. 2969-2980.

Web References:

bgi.omp.obs-mip.fr/

<ftp://ftp.birdgeo.com/>

<http://irpsrvgis00.utep.edu/repositorywebsite/>

http://www.gps.caltech.edu/~clay/SC_RFdir/Moho_Depth_Table.html

<http://ngmdb.usgs.gov/gmna/>

igppweb.ucsd.edu/~gabi/3dmodels.html

<http://www.iris.edu/dms/products/emc/velocityTrend.html>